A mathematical analysis of marine size spectra

Samik Datta

Thesis submitted for the degree of Doctor of Philosophy

University of York
Department of Biology

August 2011

Abstract

Aquatic ecosystems are observed to follow regular patterns in abundance. The frequency distribution of all individuals across the spectrum of body mass, irrespective of their taxonomic identity (known as a 'size spectrum'), follows a power law and this has mathematically been explained by the processes of growth and mortality primarily driven by predation. In this theory of the size spectrum, predation is driven by body size: as organisms grow bigger the size of their prey also increases. This process is thought to be particularly important for marine organisms such as fish, where individual body size is an important determinant for what they eat because they are mostly limited by the size of their mouths.

Models need to capture the behaviour of real systems if reliable predictions are to emerge from them. Here, new equations for size-based predation are derived from a stochastic process, allowing variability in organism growth. The new equations are postulated to capture real feeding behaviour better than classical models often used to simulate size spectra. Marine systems are often perturbed by seasonal processes, environmental factors and exploitation. I show how models with diffusive growth stabilise the observed power-law steady state in marine systems, and stability is explicitly linked to parameters involved in feeding.

Seasonal plankton blooms are introduced into the model, along with time-dependent reproduction, both of which are widely observed in aquatic systems. The population dynamics, along with growth and survival rates during blooms are investigated, and preliminary results are reflected in empirical data. The match/mismatch hypothesis is tested, with theoretical findings in agreement with observed seasonal trends. Adding factors such as these will make the behaviour of size-based models more indicative of real ecosystems, and thus well-informed management decisions about exploitation can be made.

Contents

List of Figures

List of Tables

Acknowledgements

To begin with, I would like to extend a huge thank-you to my supervisors, Richard Law, Gustav Delius and Julia Blanchard for all their help and guidance over the course of my Ph.D. It has been a rewarding three and a half years thanks in large part to the interaction I have had with them.

I want to thank the staff and students at the University of York who have helped with my research, including Will Pyman, Jenny Burrow and Mariella Canales. I would also like to thank the members of my thesis advisory panel, Jon Pitchford and Zdzislaw Brzezniak. Gratitude to everyone at Cefas who helped me during my time at York. Chats with Simon Jennings, Carolyn Barnes and Steve Mackinson have helped to shape this thesis into what it is. My trip to the University of Canterbury, New Zealand, was an important part of the development of the last two chapters of my Ph.D; I would like to extend my thanks to Mike Plank and Alex James for their help arranging my visit, and also for their extensive Matlab tutorials. Thanks also to my housemates in Christchurch, Nicky, Sarah, Margot, Eddie, Josh and Simon, who made my stay even more enjoyable.

The support I have been given by friends and family whilst doing my thesis will not be forgotten. An exhaustive list would extend this thesis significantly, but thanks to my sister Soheni and her husband Sean for their hospitality during my trips down to Cefas, and to Iain The-Rockley-s and Ed Doyer-Round for their unwavering positive support during the late-night work sessions. Thanks must also be extended to the other Ph.D students with whom I tackled all the problems along the way: Val Milton, Zeenat Noordally, Jen Lucey, Dan Horsfall, Mark Eslick, Bethan O'Leary, Lucy Goulding and Matthew Beacham all assisted me in driving forwards with my work. Stephen Rablen provided a good example of a diligent Ph.D student for me to live up to, and gave much useful advice during the writing-up stages.

Finally, my mum and dad have provided support from before the start of my thesis until the day I handed in. The home-made food definitely bolstered my spirits! A heartfelt thanks to them for all their support along the way.

Author's Declaration

I hereby declare that this submission is entirely my own work except where due acknowledgement is given.

Chapter 1 has been published in the Bulletin of Mathematical Biology (see Datta et al. (2010a)), and was co-authored by Gustav W. Delius and Richard Law.

Chapter 2 has been published in the Journal of Mathematical Biology (see Datta et al. (2010b)), and was co-authored by Gustav W. Delius, Richard Law and Michael J. Plank.

Chapters 3 and 4 are currently being written into manuscripts for submission.

"And all this science... I don't understand."

- William Shatner, **Rocketman** (1978).

General Introduction

The mathematics of ecology

> *"Ecology: The scientific study of the interrelationships among organisms and between organisms, and between them and all aspects, living and non-living, of their environment."*
>
> - Allaby, **A dictionary of ecology** (2010).

Since the term "ecology" was coined by Haeckel (1866), the subject has undergone radical advances and branched out into numerous subdisciplines; examples include behavioural, community, evolutionary, population and systems ecology (Kot, 2001). In this thesis population and community ecology of aquatic ecosystems are the main foci of my work.

Traditionally, when studying ecosystems scientists used one of three separate approaches: experimental, field or theoretical. Theoretical models originally developed were deemed too simplified to capture the complexity of nature. However, the last hundred years have seen a greater overlap between empirical and mathematical approaches to studying communities (Kingsland, 1995). Models have been expanded and increased in detail to represent the various biotic and abiotic factors that organisms are subject to more accurately. For example, the advent of computer technology has allowed complex food web models with many links between species to be constructed and analysed (e.g. Cohen et al., 2003; Brose et al., 2005b; Woodward et al., 2005a). See Kot (2001) for an overview of mathematical applications to ecosystem processes and dynamics.

Methods for recording empirical data have also become more accurate, with greater spatial and temporal resolution. In marine communities, abundances of different size classes of phytoplankton were originally measured using filtration, Coulter counters and autoanalysis of chlorophyll pigmentation (e.g. Menzel and Ryther, 1960; Sheldon and Parsons, 1967; Strickland, 1968). In more recent studies water samples have been collected and analysed using inverted microscopy to count individuals (e.g. Irigoien

et al., 2005; Cermeño et al., 2006; Wang et al., 2006; Barnes et al., 2011). Environmental factors have been quantified using more advanced sensors to estimate abiotic factors such as sea surface temperature, wind speed, turbulence and chlorophyll *a* concentration (e.g. Cózar and Echevarría, 2005; Reul et al., 2005; Zhou et al., 2010). Satellite data detailing ocean surfaces have become more widely used, increasing the temporal resolution and spatial range of available data (e.g Barnes et al., 2010, 2011).

Rising global populations have increased the harvesting of nature for both food and resources. Excessive fishing has led to collapses of species populations throughout the world; a famous example is that of cod stocks in Newfoundland (Cook et al., 1997; Longhurst, 1998), although there are many more cases (Dulvy et al., 2003). The Food and Agriculture Organization of the United Nations (FAO, 2008) recently announced that, for the first time in history, more than half of fish consumed by humans was set to come from aquaculture rather than fishing. This highlights a trend in declining abundance of fish species in the oceans, as well as increased output from farmed fish stocks. Approximately 20% of assessed fish populations are thought to be overexploited (FAO, 2010), with the majority of stocks of the top ten species either fully exploited or overexploited (hence unable to increase catches further). Thus, much research has been put into the causes of fish stock collapse; most collapses have been attributed to exploitation and habitat loss (e.g. Myers et al., 1997; Pauly et al., 2002), declaring a reduction in fishing pressure needed to aid stock recovery. Subsidiary factors including climate change and disease have also been investigated for other possible mechanisms for reduced stock abundances (Hilton-Taylor, 2000).

As the need to model ecosystems has grown, the mathematics to govern the population dynamics has evolved to meet the needs of ecologists. One of the earliest and most influential models in population ecology is the Lotka integral equation (Lotka, 1939), in which an age-structured population gives birth to new offspring; the model solution has been studied in detail since its conception (e.g. Feller, 1941; Kot, 2001). Another popular approach to age-structured population modelling has been the Leslie matrix (Leslie, 1945); a matrix containing age-dependent survival and fecundity rates is used to model the age distribution of female individuals over time. This approach has been used to model plant and animal populations (Sarukhan and Gadgil, 1974; Horwood and Shepherd, 1981; Law, 1983), and its stability properties analysed (Silva and Hallam, 1993). For biological realism, models have been developed to include spatial structure (Okubo, 1980), to better represent the heterogeneity in the environment of organisms. For single species models, a partial differential equation is generally used, containing a term describing the growth rate of the species and an additional term describing the movement of the individuals in the environment (Levin and Paine, 1974; Hastings, 1990).

Single species do not exist independent of other species, and the various interactions

between species, such as predation and competition, are the basis of community ecology. One of the first examples of a community model, and a major milestone in community ecology, are the Lotka-Volterra equations, derived independently by Lotka (1925) (one of the first books published on the subject of mathematical biology) and Volterra (1926). These equations were the first to model the interactions between a predator species and a prey species, using simple assumptions for the life processes of the two species. Subsequent models have attempted to address flaws of the model, with improved functions for prey growth (logistic growth, see Berryman (1992)) and the feeding behaviour of the predators, namely type II and III functional responses pioneered by Holling (1959, 1965). Subsequent work has analysed the stability of systems using different functional responses (e.g. Holling, 1973). The equations have also been extended to incorporate interactions other than predation, including competition (Gilpin and Ayala, 1973; Butler et al., 1983) and mutualism (Goh, 1979; Delgado et al., 2000).

Community ecology has expanded beyond simple two-species predator-prey systems. In real ecosystems many species interact with each other (for example, predation and competition for resources and space), and the Lotka-Volterra equations have been extended to multiple species (see e.g. Hastings, 1978; Post and Pimm, 1983; Uchida et al., 2007). Food webs are the most familiar and widely studied form of ecological network (Woodward et al., 2005a), where nodes usually represent species (or taxonomically similar groups of species, see Pimm et al. (1991)), and with links between nodes indicating inter-species interactions such as predation and competition. The aggregation of all organisms of a species into an individual data point allows tractable analyses of potentially complex ecosystem dynamics (Berlow et al., 2004), leading to complex food webs with large numbers of nodes and interactions between species (e.g. Woodward et al., 2002; Cohen et al., 2003). However, aggregating all organisms of a single species can oversimplify population dynamics, as there is no intra-species variation. Individuals within a species will differ in behavioural traits, physiology, reproductive output and mortality rates (all of which are often correlated with size or age). Analyses of real food web data have revealed strong correlations between prey size and predator size, irrespective of species (Warren and Lawton, 1987; Cohen et al., 1993; Woodward et al., 2005a). Thus, the importance of variation within populations has become more recognised (Werner and Gilliam, 1984), and age- and size-structured multi-species food web models have been developed to disaggregate individuals within species (e.g. Gurney et al., 1983; Law, 1983; Chase, 1999; Woodward et al., 2005b; Hartvig et al., 2011).

The emergent patterns of communities have often been shown to produce simple and regular trends over large spatial scales; the study of these correlations is known as macroecology, a term coined by Brown and Maurer (1989). Abundance - body mass relationships have been studied in terrestrial systems (Damuth, 1981; Brown and Mau-

rer, 1989; Nee et al., 1991; Gaston and Blackburn, 2000; White et al., 2007), where an average body mass is often used to summarise each species. In aquatic systems a regular power-law relationship between body mass and abundance has often been observed when organisms are only defined by body mass and not taxonomic identity (e.g. Boudreau and Dickie, 1992; Jennings and Mackinson, 2003; Barnes et al., 2011). This form of analysis started when Sheldon et al. (1972) sampled size distributions of plankton in the ocean and found roughly equivalent abundances of biomass in logarithmically increasing weight brackets. The term "size spectrum" was coined (to describe the correlation between abundance and body size), and has been the subject of extensive analysis.

The importance of body size in food webs

Body size influences many life processes in multi-cellular organisms. One of the basic physiological processes of all organisms is metabolism, where a power-law relationship with body mass (or any other parameter parameterising organism body size) has been established from small microbes up to large terrestrial and aquatic organisms (Gillooly et al., 2001; Enquist et al., 2003; Brown et al., 2004). Other size-dependent life processes include movement, food consumption (Ware, 1978), growth (Gillooly et al., 2002), fecundity (Wootton, 1977; Duarte and Alcaraz, 1989), and mortality (Andersen and Ursin, 1977).

Food web models are commonplace in modelling interactions between species within ecosystems (e.g. Paine, 1966; Fry, 1988; Hall and Raffaelli, 1991; Cohen et al., 2003; Brose et al., 2005b). It has been shown in food web data that body size is negatively correlated with numerical abundance, in terrestrial species such as mammals and birds (Damuth, 1981; Nee et al., 1991) and aquatic species (Boudreau and Dickie, 1992; Cohen et al., 2003). Data is often aggregated by taxonomic group (Brown et al., 2004), and average masses are used to produce a node for each species in food webs (e.g. Brose et al., 2006a). It has been shown that predator size tends to increase with prey size (Cohen et al., 1993, 2003; Brose et al., 2006a), and predators are orders of magnitude both larger, and less common, than their prey (Petchey et al., 2004; Reuman and Cohen, 2004).

In aquatic systems, the body size - abundance trend is observed at the community level, where organisms are only defined by body weight and not taxonomic identity (known as the size spectrum, see Sheldon et al. (1972)). A negative power-law relationship between body mass and abundance was established when sampling plankton abundances in different size classes (Sheldon et al., 1972); this pattern has been observed over different size ranges, from phytoplankton (San Martin et al., 2006; Huete-Ortega et al., 2010; Barnes et al., 2011) up to large fish species (Boudreau and Dickie,

1992; Jennings and Mackinson, 2003; Jennings et al., 2007). Transient predator-prey relationships and cannibalism are common in aquatic species, due to the fact that aquatic organisms can grow more than five orders of magnitude over the course of their lives (Cushing, 1975), for example, Atlantic cod (Knijn et al., 1993). Thus trophic level is strongly dependent on size, as opposed to species, for aquatic organisms (Jennings et al., 2001). The body size of an aquatic individual determines its potential predators and prey (Ursin, 1973; Andersen and Ursin, 1977; Cohen et al., 1993), along with the rates of life processes such as mortality (Beyer, 1989; Jennings et al., 1998), reproduction (Wootton, 1977; Duarte and Alcaraz, 1989) and growth (von Bertalanffy, 1957; Kooijman, 1986). A linear relationship has been found between the mass of organisms and their preferred prey mass (i.e. the predator : prey mass ratio), which is approximately constant over the weight range 2-2048g (Jennings et al., 2002b), although a recent study which aggregated data across the whole size spectrum from 21 locations across the world found that body mass and the predator : prey mass ratio had a power-law relationship (Barnes et al., 2010).

The concept of the size spectrum (Sheldon et al., 1972) has led to an entire sub-branch of community ecology dealing with body size - abundance relationships in aquatic ecosystems. The attraction for modelling whole ecosystems using individual body size as the only trait for organisms is that it allows examination of very complex food webs without taking into account species-based interactions. Rather, the emergent patterns of the size distribution can be analysed for possible justifications for the observed power-law shape of body size - abundance relationships.

The existence of a power-law steady state in aquatic ecosystems has led to much theoretical work to explain the dynamics behind the phenomenon, using the size-based feeding strategy observed in aquatic organisms (Ursin, 1973; Andersen and Ursin, 1977). Platt and Denman (1977) first hypothesised a model incorporating weight-dependent growth and metabolism to give a power-law steady state (although predation was not explicitly modelled here). Since then, models incorporating size-dependent feeding have also been shown to produce power-law steady states: using a fixed predator : prey mass ratio (Silvert, 1980), allowing organisms to feed upon all smaller prey (Camacho and Solé, 2001) and, more recently, over a restricted weight range dependent on the predator weight (Benoît and Rochet, 2004; Andersen and Beyer, 2006; Law et al., 2009; Blanchard et al., 2009).

Inspired by the size-based approach, previously obtained population-level food web data sets (e.g. Tuesday Lake, U.S.A. (Carpenter et al., 1987) and Broadstone Stream, U.K. (Woodward et al., 2002)) have more recently been re-examined to draw conclusions about size-based interactions between organisms in the ecosystem, using novel approaches such as a trivariate description of the community incorporating food web structure, body mass and abundance (Cohen et al., 2003; Jonsson et al., 2005) and

metabolic theory (Woodward et al., 2005a). Berlow et al. (2004) state how food webs "provide tractable abstractions of the complexity and interconnectedness of natural communities that potentially transcend system-specific detail"; the paper then goes on to highlight issues with classic food web ecology, in particular differentiating between species-specific dynamics and community-level patterns when interpreting results. More recent work has attempted to incorporate population dynamics into food web models (Uchida et al., 2007), or relaxed the assumptions of interaction strengths between nodes in food webs in favour of optimal foraging strategies which are less dependent on specific species (Petchey et al., 2008); the latter model successfully predicts 65% of links in the studied food webs. Woodward et al. (2010) contrasted size-based models and species-based models to explain trophic links in real ecosystems, with body size accounting for a higher proportion of predator-prey interactions in some systems. Recent work has also developed multi-species size spectrum models, in order to allow both species-based and size-based feeding interactions within communities (Andersen et al., 2009; Andersen and Pedersen, 2010; Hartvig et al., 2011). In conclusion, food web ecology has seen a shift in focus in the last decade, with more emphasis placed on the behaviour of individuals rather than population-level interactions. The abstraction of species-based networks are being reconsidered in light of increasing evidence of size-based processes occurring at the individual level.

Scaling processes from individuals to the population level

The recognition that population level models may be too simplified has led to the development of individual based models (IBMs). The motivation behind IBMs was to relax the assumption that all organisms within a species are identical, by allowing environmental and density-dependent factors to vary depending on the age of organisms (e.g. Lomnicki, 1978). Modelling at the individual level has its advantages: individuals within a species vary in traits such as vital rates and age, and allowing variation allows more detailed conclusions to be drawn from the model than averaging over all organisms for construction of population models (Uchmaski and Grimm, 1996). The rise of IBMs, due to the increasingly recognised importance of local interactions between individuals, and the ability to produce larger scale IBMs thanks to the advances of computer power and software, is discussed in a review by Judson (1994). Working at the individual level allows further detail such as explicit spatial and temporal heterogeneity to be modelled (McCauley et al., 1993). For further examples of IBMs and their use in ecology, see e.g. De Roos et al. (1991); Hinckley et al. (1996); Hermann et al. (2001).

Of course, all ecological models (individual based or otherwise) are abstractions of real ecosystems, constructed to simulate various life processes of organisms. In doing

so, the hope is that emergent phenomena from empirical data may be attributed to biological properties of organisms. Interpreting individual based models is difficult, as the models used are often complex to construct, and difficult to analyse (Grimm et al., 1999). IBMs are often very specific to the ecological problem that they are tackling, and as such, their uses in constructing mathematical models to describe population behaviour can be limited (Uchmaski and Grimm, 1996; Grimm, 1999). Scaling up from individual level processes to population level dynamics is not trivial, with numerous pitfalls (see Lomnicki, 1999). Examples of mathematically rigorous approaches for producing age-structured population models from individual biological rates are not common; for example, see Nisbet and Gurney (1983); Gurney et al. (1983); Nisbet et al. (1989). To summarise, individual level processes have been recognised to be an important part of population behaviour, and subsequently integrated into models by explicitly modelling individuals (commonly in age- or size-structured populations). However, IBMs are limited in their ability to answer questions about population ecology, and a more theoretical groundwork is needed for individual-based modelling to account for emergent community patterns in nature (Grimm, 1999).

A method for deriving deterministic models from basic stochastic processes at the individual level is the master equation approach. The method has often been adopted in physics and chemistry, as a probabilistic approach to the time-evolution of a system (van Kampen, 1992). The system generally occupies one of a discrete number of states, with Markov processes determining the probabilities of moving between states. An example could be a chemical reaction, where reactant molecules are present in a container (the system), and upon collision there is a chance that they will combine to form new molecules. With the exception of simple linear processes, master equations cannot be solved explicitly, and approximations must be derived. One such approximation involves an expansion method around a system parameter, details of which are given in van Kampen (1992). In short, the highest order terms of the expansion give the macroscopic model, which describes the deterministic behaviour of the system. The next-to-highest order terms give the distribution of fluctuations around the macroscopic value. For examples of the uses of master equations see Schnakenberg (1976); Gillespie (2000); McKane and Newman (2005).

In Chapter 1, a similar approach to the example of a chemical reaction is taken to model the predation process: at an individual level, two organisms collide and (by the predator swallowing the prey) produce one larger organism, where the biomass feeding efficiency dictates what portion of the mass is assimilated from the prey organism. This stochastic process can be written as a master equation, but not solved explicitly due to the nonlinearity of the predation process. To make progress, the expansion method of van Kampen (1992) is followed to derive the macroscopic model for the stochastic process (which is labelled the deterministic jump-growth equation). This is with the assumption that the system size is large, which is reasonable in most

aquatic ecosystems, where communities exist in large volumes of water. The next-to-highest order terms of the expansion form a linear Fokker-Planck equation to describe the fluctuations around the deterministic model. The new model, like other size spectrum models, is mostly based on fish or pelagic predators but is also applicable to other marine animals that feed in a size-based way, such as zooplankton.

The power-law steady state, often observed in aquatic ecosystems (e.g. Boudreau and Dickie, 1992; Jennings and Mackinson, 2003; San Martin et al., 2006), is derived analytically for the deterministic jump-growth equation. The jump-growth model is compared to the classical model often used to describe growth via predation in aquatic ecosystems, the McKendrick-von Foerster equation (e.g. Benoît and Rochet, 2004; Andersen and Beyer, 2006; Law et al., 2009; Blanchard et al., 2011). It is found that the McKendrick-von Foerster equation is the first-order approximation to the jump-growth equation, and a suitable approximation when predators feed upon prey significantly smaller than themselves, and the system is close to the power-law steady state. Thus the jump-growth equation is postulated to simulate the feeding process in marine systems more robustly than the classical model. The McKendrick-von Foerster equation has its roots in age-based distributions (McKendrick, 1926; von Foerster, 1959), and has subsequently been adapted into weight-based systems. Its applicability compared to the jump-growth equation is discussed in Chapter 1.

Stability in community models

Ecologists are often interested in the long-term behaviour of communities. Food webs can have many nodes and links (for example, see Cohen et al., 2003; Woodward et al., 2005a), leading to high levels of complexity (i.e. average number of trophic links per species) in food web data. A recent analysis of complex food webs concluded that on average any two species are two links from each other (Williams et al., 2002), meaning community dynamics are extremely complex. Modelling these intricate ecosystems is challenging, and theoretical studies often deal with reduced numbers of species and broad assumptions to reach conclusions (e.g. Brose et al., 2006b). On top of these difficulties, there has been a paradigm shift away from species-specific traits and towards individual behaviour. Montoya et al. (2006) conclude that species are not as separate as once conceived, and interdependent factors of body size, nested diets and connectance strength all affect the dynamics of food webs. Emmerson and Raffaelli (2004) note that calculating the interaction strength for all the links in complex food webs is unfeasible, and Berlow et al. (2004) conclude that interaction strengths alone are not enough to combine food webs and population dynamics successfully, and are "a useful conduit for discussion but not an endpoint".

Stability in food web models is a wide subject with a vast range of published litera-

ture. Much research has been performed since the pivotal works of MacArthur (1955) and May (1972) contested whether increasing complexity (i.e. the number of links between nodes in food webs) made systems more or less stable. Varying definitions of stability are used, as scientists working with food webs come from a range of backgrounds (including theoretical physics, mathematics and the more traditional roots of ecology). The term "stability" most often refers to the tendency for a community of species at equilibrium, when perturbed slightly by altering the number density of one or more species, to return to that equilibrium (Pimm, 1979). This tests *local stability* or Lyapunov stability (e.g. Krabs and Pickl, 2010). That is, a system is defined as stable if, when initiated in a neighbourhood of the fixed point, it remains in the neighbourhood indefinitely. Asymptotic stability requires that as time $t \to \infty$, a system initiated in the neighbourhood of the fixed point tends to the fixed point. A stronger stability condition is *global stability*; a comparison between the two, highlighting limitations of the former approach, is given by Chen and Cohen (2001).

Alternative tests for stability have also been incorporated in models. Species deletion stability (e.g. Paine, 1966; Pimm, 1979; Post and Pimm, 1983) investigates the effect of removing one species from a stable food web on the dynamics of the resulting community. This concept is closer to the type of stability described by MacArthur (1955). On the other hand, studies have modelled adding species to existing stable food webs, to test whether invasion is possible and, if so, the resulting distribution of species (Post and Pimm, 1983; Drake, 1991; Law and Morton, 1996). As well as qualitative tests for stability, theoretical work has investigated the speed at which a perturbed system returns to equilibrium (Pimm, 1977), termed resilience in later studies (Pimm, 1984; Montoya et al., 2006). It has been argued that real communities may not always reach an equilibrium, but rather co-exist in cyclic or chaotic systems; to test for this in models, the concept of "permanence" has been introduced, which only requires biomasses of all species present to be positive and finite, rather than reaching fixed values (Law and Morton, 1996; Petchey et al., 2004). For a summary of different methods used for testing stability in theoretical models, see Pimm (1984).

In this thesis the dynamics of aquatic communities is studied. The power-law steady state in aquatic communities appears to be ubiquitous, repeatedly observed at different scales, seasons and locations globally (see e.g. Sheldon et al., 1972; Boudreau and Dickie, 1992; San Martin et al., 2006; Barnes et al., 2011). The stability and persistence of aquatic communities is of paramount interest from both a scientific and economic viewpoint when considering the impact of fishing on ecosystems; fishing is a global industry, providing livelihoods for 43.5 million people, and producing an estimated per capita supply of 16.7kg (Jennings et al., 1999; Mullon et al., 2005; FAO, 2008). Fishing generally removes the largest organisms in the system, as valuable species are often large, and minimum size limits are frequently used in fisheries management (Rochet and Benoît, 2011). This removal of large individuals causes high variability

in size-truncated populations (Hsieh et al., 2006; Anderson et al., 2008). At the community level, the size spectrum slope and intercept can provide information about the effects of exploitation on the abundance and size distribution of the resulting ecosystem (Bianchi et al., 2000); as a consequence, fishing effects on size spectrum dynamics have been studied numerically (e.g. Blanchard et al., 2005; Rochet and Benoît, 2011).

A deeper mathematical understanding of the stability of the power-law steady state has been limited thus far. A departure from the power-law steady state was observed by Law et al. (2009) in numerical simulations, with waves of abundance forming and moving up the size spectrum; this bifurcation was linked to the feeding behaviour of individuals, with travelling waves appearing as the diet breadth was made narrower. This behaviour is also observed when the jump-growth equation is used to model predation in Chapter 1. One of the only known analyses of the power-law steady state in marine size spectra is by Arino et al. (2004), although in the model dynamics predation and organism growth are not explicitly linked, which misses a vital feedback present in real ecosystems. Recently, Rossberg (2011) derived for the first time an approximate analytic description of the power-law steady state and behaviour of perturbations, using a model which accounted for multiple species.

Chapter 2 of this thesis shows the first local stability analysis performed analytically on the power-law steady state observed in marine ecosystems. Three equations for modelling the predation process are analysed, and with certain parameter constraints the eigenvalue spectrum for the linearised evolution operator is derived. It is shown analytically that the steady state of the McKendrick-von Foerster equation is always unstable, whereas adding a diffusion term can stabilise the steady state, and gives eigenvalue spectra closer to those for the jump-growth equation. Stability of the steady state is shown to be more likely with a low preferred predator : prey mass ratio, large diet breadth and high feeding efficiency. The work has since been expanded upon by Capitan and Delius (2010) by including the effects of metabolism and reproduction on the stability of the steady state, and these are found to be stabilising.

Seasonal trends in aquatic ecosystems

The power-law distribution in size spectra is well-documented. However, many empirical studies involve averaging spatially or temporally (e.g. Li, 2002; Jennings and Mackinson, 2003). Studies with more frequent sampling (Boudreau and Dickie, 1992; Heath, 1995; Huete-Ortega et al., 2010) show the variation that can occur throughout the year due to changing environmental conditions; this detail is lost when aggregating size spectra. Thus, the power-law "steady state" may not exist at any specific time, but only as an emergent phenomenon over large timescales.

Seasonality in aquatic systems causes deviations away from the power-law steady

state. An annual cycle of nutrient upwelling, temperature gradients and sunlight causes phytoplankton blooms in the springtime and, to a lesser extent, the autumn (Kaiser et al., 2005). This extra abundance (normally lasting several weeks or months, see Menzel and Ryther (1960); Navarro and Thompson (1995); Irigoien et al. (2000)) causes a rise in the zooplankton population, the organisms that predate most upon the phytoplankton (Heath, 1995; Zhou et al., 2010), which in turn provides a higher prey abundance for newborn fish larvae. Many fish species spawn only over a specific period of the year (Knijn et al., 1993; Hutchings and Myers, 1994; Mertz and Myers, 1994; Buckley and Durbin, 2006), and so the timing of reproduction in relation to the phyto- and zooplankton peaks can be important for recruitment in fish species.

This has led to the concept of the match/mismatch hypothesis (Hjort, 1914; Cushing, 1969, 1975), which hypothesises a link between the synchrony of the zooplankton abundance peak and the reproductive period of a fish species, and the recruitment success of larvae later in the year. Much theoretical and empirical research has been carried out to test the validity of the hypothesis (e.g. Bradford, 1992; Cushing and Horwood, 1994; Gotceitas et al., 1996; Johnson, 2000; Platt et al., 2003; Durant et al., 2005), while other research has investigated the importance of predation mortality in determining the survival rate of offspring born at different times (Anderson, 1988; Rice et al., 1993). Models have commonly used a predetermined larval prey period before testing the growth success of larvae born at different times relative to this period (e.g. Mertz and Myers, 1994; Pope et al., 1994; Burrow et al., 2011). Empirical data has shown varying levels of agreement with the match/mismatch hypothesis (see Bollens et al., 1992; Buckley and Durbin, 2006). There is still some way to go before the causes of recruitment success/failure are fully understood, probably because of many different processes at play, natural variability and difficulties in sampling in time and space.

This thesis extends knowledge of the behaviour of a size spectrum model under seasonal forcing and the timing and duration of reproduction. In Chapter 3 the dynamics of a community size spectrum are investigated when annual phytoplankton blooms are incorporated into the model. A range of bloom amplitudes, durations and dynamics are simulated to test the resulting dynamics in the consumer spectrum. In Chapter 4 reproduction is then explicitly added to this seasonal environment as a function of time, to examine the consequences of altering both the timing and duration of reproduction. The match/mismatch hypothesis proposed by Cushing (1975) is then tested. It is found that both the growth rate and mortality rate of fish larvae increase during the plankton bloom, and fish species face a trade-off between numbers remaining and body weight of the surviving offspring.

Observed data shows only the end results of many different dynamical processes occurring simultaneously. To understand trends seen in empirical data, it is important

to disaggregate different life processes, so that the consequences of environmental or human changes to an ecosystem may be understood. Throughout the thesis I use analytical methods wherever possible in order to attempt to explain observed patterns in aquatic systems, allowing investigation of the importance of different parameters on the system. Numerical simulations are used to support and extend the knowledge acquired from the mathematical analyses contained in the thesis.

Structure of thesis

In Chapter 1, I derive a new model for predation in marine systems, and perform both analytical and numerical analyses while comparing it to the classical equation used to model predation. In Chapter 2, a stability analysis of the power-law steady state is carried out for three models, and stability is explicitly linked to parameters that govern feeding. In Chapter 3, I add seasonal phytoplankton blooms to a community size spectrum model, in order to investigate the dynamics caused further up the spectrum by increased prey abundance. In Chapter 4, a time-dependent reproduction term is also added, and the match/mismatch hypothesis is tested in the presence of plankton blooms; numerical integrations show that less biomass is conserved by being born away from the bloom. I conclude with a discussion about the methods used within the thesis, the uses and drawbacks of size-based approaches for modelling aquatic systems, limitations of the research I have carried out, and possible future avenues for further study.

Chapter 1

A jump-growth model for predator-prey dynamics: derivation and application to marine ecosystems

Samik Datta, Gustav W. Delius, Richard Law

Departments of Biology and Mathematics,
University of York,
York YO10 5DD, U.K.[1]

[1]emails: sd550, gwd2, rl1 @york.ac.uk

Abstract

This paper investigates the dynamics of biomass in a marine ecosystem. A stochastic process is defined in which organisms undergo jumps in body size as they catch and eat smaller organisms. Using a systematic expansion of the master equation, we derive a deterministic equation for the macroscopic dynamics, which we call the deterministic jump-growth equation, and a linear Fokker-Planck equation for the stochastic fluctuations. The McKendrick–von Foerster equation, used in previous studies, is shown to be a first-order approximation, appropriate in equilibrium systems where predators are much larger than their prey. The model has a power-law steady state consistent with the approximate constancy of mass density in logarithmic intervals of body mass often observed in marine ecosystems. The behaviours of the stochastic process, the deterministic jump-growth equation and the McKendrick–von Foerster equation are compared using numerical methods. The numerical analysis shows two classes of attractors: steady states and travelling waves.

Keywords: growth diffusion; marine ecosystem; master equation; McKendrick–von Foerster equation; predator-prey; size spectrum; stochastic process; systematic expansion

1.1 Introduction

Marine and freshwater ecosystems exhibit a remarkable regularity in the relation between abundance of organisms and their body masses. Treating organisms simply as particles of different size, i.e. ignoring taxonomic identity, the total biomass (abundance $\times$ body mass) in logarithmic intervals of body mass is observed to be approximately constant (Sheldon et al., 1972, 1977; Boudreau and Dickie, 1992; Kerr and Dickie, 2001). Equivalently, the logarithm of abundance expressed as a function of the logarithm of body mass, often referred to as a size spectrum, is approximately linear with a gradient close to -1. Removing the logarithms, this is equivalent to density in mass space being a power function of mass with an exponent -2. This approximate regularity applies over a wide range of body size from micro-organisms to large verte-

brates, and has been the subject of much research and discussion in ecology (Sheldon et al., 1972; Platt and Denman, 1978; Heath, 1995; Marquet et al., 2005).

Understanding of the dynamics of biomass flow that lead to this regularity is important: the biomass of most marine ecosystems supports major fisheries that play a significant role in the economies of maritime countries. The dynamics are often studied by means of a partial differential equation (PDE), in which abundance is taken as a function of both body mass and time. The PDE is motivated by a model of McKendrick (1926) and von Foerster (1959), in which abundance is a function of age and time. We will follow the convention of calling this PDE the McKendrick–von Foerster equation, notwithstanding the change in variable from age to size.

The McKendrick–von Foerster equation was first adopted by Silvert and Platt (1978) in a model allowing growth and mortality to be functions of body mass. Following this, Silvert (1980) coupled growth at one size to death at another, because organisms grow in size spectra by eating smaller organisms. More recently, the approach has been extended, first to allow organisms to eat those at all smaller sizes (Camacho and Solé, 2001), and second, by using a feeding-kernel function, to allow them to eat organisms in a restricted size range (Benoît and Rochet, 2004). PDEs of this kind are now being used quite extensively to understand processes in marine ecosystems (Andersen and Beyer, 2006; Maury et al., 2007a; Andersen et al., 2009). It can, for instance, be shown in numerical analyses that the PDE at steady state gives size spectra with gradients which are similar to those in marine ecosystems (Blanchard et al., 2009).

The McKendrick–von Foerster equation is implicitly assumed to be an appropriate approximation for an underlying stochastic process in which individual organisms grow by eating prey items. A first investigation of the relationship between the PDE and the stochastic process (Law et al., 2009) showed that the PDE could describe the approach to a steady-state size spectrum. However, the stochastic process could also develop travelling-waves; although these were also possible in the PDE, the properties of these waves were somewhat different. The research described in the present paper was motivated by these discrepancies.

A possible source of these discrepancies is that the McKendrick–von Foerster equation was originally conceived of as a model for organisms indexed by age, rather than by weight. Age and weight do not change in quite the same way over time. An organism grows older continuously, whereas its weight grows in jumps each time it finds a prey item to feed upon. As time progresses, organisms which start at the same age clearly remain the same age as each other, whereas organisms which start at the same weight in general do not remain the same weight as each other. Pfister and Stevens (2002) stressed the importance of growth variability in cohorts of organisms. Motivated by this, Gurney and Veitch (2007) considered the consequences of allowing growth to be both a random variable and also size-dependent, in a von Bertalanffy

growth model. However, the emphasis in dynamic size spectra is somewhat different because variation in body weight here emerges from random encounters with prey items of various weights.

In this paper we therefore start from a stochastic process in which organisms undergo jumps in body size as they catch and eat smaller organisms. We introduce this individual-based stochastic process in Section 1.2.1 and describe it as a population-level model in Section 1.2.2. In Section 1.2.3 we use a systematic expansion of the master equation (van Kampen, 1992) to derive an equation for the macroscopic dynamics (which we call the the deterministic jump-growth equation (1.12)) and a Fokker-Planck equation for the stochastic fluctuations. We also provide an appendix with an alternative derivation of a Langevin equation, following Gillespie (2000), to clarify an issue unresolved by the systematic expansion. Section 1.2.5 shows that the McKendrick–von Foerster equation is a first-order approximation of the deterministic jump-growth equation, which applies at steady state when predators are much larger than their prey. In Section 1.2.6 we show that our model has a power-law steady state and we derive an approximate analytic expression for its exponent, thereby showing that the steady state is consistent with the approximate regularity seen in marine ecosystems. However, the steady state is not necessarily an attractor. In Section 1.3 the behaviour of the deterministic models and of the stochastic model are compared using numerical methods. As in the case of the McKendrick–von Foerster equation (Law et al., 2009), certain parts of parameter space allow a travelling-wave solution.

1.2 A dynamical model of size-dependent predation

1.2.1 An individual-based stochastic process

We model predation as a Markov process. The primary stochastic event comprises a predator of weight w_a consuming a prey of weight w_b and, as a result, increasing to become weight w_c (Figure 1.1). Predation is inefficient and, in keeping with ecological convention, we assume that a fixed proportion K of prey mass is assimilated by the predator so that $w_c = w_a + Kw_b$ (the assumption of constant K could be relaxed). We call this model the 'jump-growth model' because the changes in the weight distribution are caused by discrete steps in body size as predators eat prey, and the mortality that comes with this predation.

It would be easy to add additional events to the jump-growth model to account for natural death and for birth (recruitment) but, as we will see, for the purpose of this paper of explaining the observed power law size spectrum these additional events are not required, and we will therefore restrict our attention to the pure predation events.

The next three subsections will be concerned with the derivation of equations de-

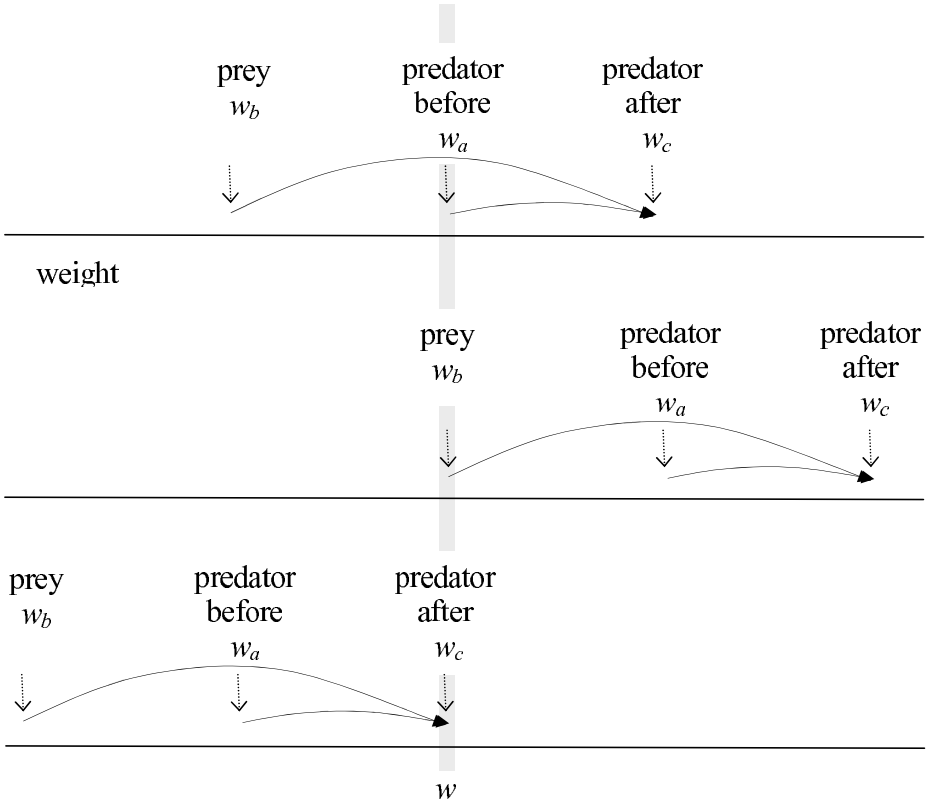

Figure 1.1: The primary predation event replaces an individual predator and prey by a new, larger predator individual. Taking some arbitrary weight w, there are two ways in which an individual can change from this weight: by feeding and thereby increasing in weight, and by being eaten and so disappearing altogether. There is also one way in which an individual can become weight w: by being of smaller weight and feeding on a prey of just the right size to become weight w. These events are reflected in the three terms of the deterministic jump-growth equation (1.12) in Section 1.2.4.

scribing the time evolution of the weight distribution that follows from this stochastic process. The main result from these sections that we will use further in this paper is the deterministic jump-growth equation (1.12) given in Section 1.2.4. That equation has an intuitive explanation in Figure 1.1 and is enough to follow the remainder of the paper.

A mathematically rigorous treatment of the individual-based model may be possible following the techniques developed for stochastic processes on configuration-space, see for example (Finkelshtein et al., 2009). In this paper we will instead pursue a heuristic treatment of a corresponding population-level model.

1.2.2 A population-level master equation

Instead of keeping track of the weight of each individual, we aggregate individuals of similar weights into weight brackets, and follow the the number of individuals in each bracket. We introduce a set of weights w_i and corresponding weight

brackets $[w_i, w_{i+1})$, with $i \in \mathbb{Z}$. In practice, the size of the weight brackets should be chosen small enough so that discretisation errors are small. The weight distribution of organisms in a large fixed volume Ω is described by a sequence of numbers $''[\ldots, n_{-1}, n_0, n_1, \ldots]$, where n_i is the number of organisms in Ω with weights in the i-th weight bracket between w_i and w_{i+1}.

Let k_{ij}/Ω denote the rate constants for the predation events, where the indices of k are ordered: predator before feeding, prey. Then the probability in an infinitesimal time interval dt for any one of n_i organisms in weight bracket i to eat any one of the n_j organisms of weight bracket j is $k_{ij}\Omega^{-1}n_i n_j dt$. The time evolution of the probability $P(\boldsymbol{n}, t)$ that the system is in the state $\boldsymbol{n}$ at time t is then given by the master equation

$$\frac{\partial P(\boldsymbol{n}, t)}{\partial t} = \sum_{i,j} \frac{k_{ij}}{\Omega} \left[(n_i + 1)(n_j + 1) P(\boldsymbol{n} - \boldsymbol{\nu}_{ij}, t) - n_i n_j P(\boldsymbol{n}, t) \right], \tag{1.1}$$

where $\boldsymbol{n} - \boldsymbol{\nu}_{ij} = (\ldots, n_j + 1, \ldots, n_i + 1, \ldots, n_l - 1, \ldots)$, and l is the index of the weight bracket $w_l \leq w_i + Kw_j < w_{l+1}$. The first (positive) term in (1.1) corresponds to having one extra predator in weight bracket (i), one extra prey in (j), and one less predator in (l), so that one predation event will move the system from state $\boldsymbol{n} - \boldsymbol{\nu}_{ij}$ into state $\boldsymbol{n}$. The second (negative) term corresponds to another such predation event that moves the system out of state $\boldsymbol{n}$. Hence the master equation is commonly referred to as a "gain-loss" equation.

1.2.3 Separation of macroscopic behaviour and fluctuations

The master equation (1.1) has non-linear coefficients and is difficult to solve analytically. We therefore make use of the property that, in systems of sufficiently large volume Ω, the fluctuations are relatively small because they are suppressed by a factor of the square root of Ω; the conditions required for this to be true are given in Appendix 1.5. In this section we adopt the approach of van Kampen (1992), carrying out an expansion of (1.1) in Ω, and collecting together the highest-order terms in Ω. To do this, it helps to rewrite the master equation (1.1) using a step-operator notation:

$$\frac{\partial P(\boldsymbol{n}, t)}{\partial t} = \sum_{i,j} \frac{k_{ij}}{\Omega} \left(\mathbb{E}_i \mathbb{E}_j \mathbb{E}_l^{-1} - \mathbb{I} \right) \left(n_i n_j P(\boldsymbol{n}, t) \right). \tag{1.2}$$

Here $\mathbb{E}_i$ is a step operator that acts on a function $f(\boldsymbol{n})$ to give $\mathbb{E}_i f([\ldots, n_i, \ldots]) = f([\ldots, n_i + 1, \ldots])$; similarly $\mathbb{E}_j$ acts on a function $f(\boldsymbol{n})$ to give $\mathbb{E}_j f([\ldots, n_j, \ldots]) = f([\ldots, n_j + 1, \ldots])$; conversely $\mathbb{E}_l^{-1}$ acts on a function $f(\boldsymbol{n})$ to give $\mathbb{E}_l^{-1} f([, \ldots, n_l, \ldots]) = f([\ldots, n_l - 1, \ldots])$. Thus (1.2) is just an alternative notation for (1.1). For further explanation of the step-operator notation, see van Kampen (1992, page 139).

Following the method used by van Kampen (1992), we separate each random variable

n_i into a deterministic component $\phi_i(t)$ which describes the density of individuals in weight bracket i, and a random fluctuation component $\xi_i(t)$ as

$$n_i = \Omega\phi_i(t) + \Omega^{\frac{1}{2}}\xi_i(t). \tag{1.3}$$

On average the number of individuals will be proportional to the system size Ω, by the law of large numbers, and that is the reason for the factor of Ω multiplying $\phi_i(t)$. That the fluctuations are proportional to the square root of the system size should be justified by some sort of central limit theorem. A heuristic justification is given in Appendix 1.5. Thus disaggregating n_i in this way leaves two variables ϕ_i and ξ_i which no longer scale with the system size. We assume that Ω is so large that the discrete nature of $\boldsymbol{n}$ is no longer noticeable at the level of $\boldsymbol{\phi}$ and $\boldsymbol{\xi}$ and we can treat them as continuous variables.

The new random variables ξ_i are described by a probability distribution $\Pi(\boldsymbol{\xi}, t) = \Omega^{1/2}P(\boldsymbol{n}, t)$. An equation for the time evolution of this probability distribution is obtained by substituting the change of variables (1.3) into the master equation (1.2). Care needs to be taken because this change of variables is time-dependent. This has the consequence that

$$\frac{\partial P(\boldsymbol{n}, t)}{\partial t} = \Omega^{-1/2}\frac{\partial \Pi(\boldsymbol{\xi}, t)}{\partial t} - \sum_i \frac{d\phi_i}{dt}\frac{\partial \Pi(\boldsymbol{\xi}, t)}{\partial \xi_i}. \tag{1.4}$$

Here we used the property that $\Omega^{-1/2}d\boldsymbol{\xi}/dt = -d\boldsymbol{\phi}/dt$ when we keep $\boldsymbol{n}$ fixed. The operators $\mathbb{E}_i$ which change n_i to $n_i + 1$ now change ξ_i to $\xi_i + \Omega^{-1/2}$ and can therefore be expanded as

$$\mathbb{E}_i = 1 + \Omega^{-1/2}\frac{\partial}{\partial \xi_i} + \frac{1}{2}\Omega^{-1}\frac{\partial^2}{\partial \xi_i^2} + \cdots. \tag{1.5}$$

Substituting all this into the master equation (1.2) gives an equation with terms containing various different powers of the system size Ω.

The highest order terms are at order Ω^0. They only contain the macroscopic variables ϕ_i and vanish if these satisfy the deterministic equation

$$\frac{d\phi_i}{dt} = \sum_j \left(-k_{ij}\phi_i\phi_j - k_{ji}\phi_j\phi_i + k_{mj}\phi_m\phi_j\right), \tag{1.6}$$

where m is an index for the weight bracket: $w_m \leq w_i - Kw_j < w_{m+1}$. The three terms in (1.6) are in keeping with the intuition given by Figure 1.1. Losses from weight bracket i (the negative terms) occur because individuals in this bracket eat prey and become heavier, and because these individuals are themselves eaten. Gains into weight bracket i (the positive term) occur through smaller predators growing into this bracket by eating prey. Imposing the deterministic equation (1.6) is not the only possible way to make the terms of order Ω^0 vanish, but it is the most natural and is

independently derived in Appendix 1.5.

Terms at the next order, $\Omega^{-1/2}$, give the linear Fokker-Planck equation for the probability distribution $\Pi(\boldsymbol{\xi})$ of the fluctuations,

$$\frac{\partial \Pi}{\partial t} = -\sum_{ij} A_{ij} \frac{\partial}{\partial \xi_i} \left(\xi_j \Pi \right) + \frac{1}{2} \sum_{ij} B_{ij} \frac{\partial^2}{\partial \xi_i \partial \xi_j} \Pi, \tag{1.7}$$

where the coefficients A_{ij} and B_{ij} are independent of the fluctuations $\boldsymbol{\xi}$. If we introduce the objects k_{ijl} and f_{ijk} by

$$k_{ijl} = \begin{cases} k_{ij} & \text{if } w_l \leq w_i + K w_j < w_{l+1} \\ 0 & \text{otherwise} \end{cases}, \tag{1.8}$$

$$f_{ijl} = \frac{1}{2} \left(k_{ijl} + k_{jil} \right) \tag{1.9}$$

then we can give the succinct expressions

$$A_{ii} = \sum_{jl} f_{ijl} \phi_j, \qquad A_{ij} = \sum_{l} \left(f_{ijl} \phi_i - f_{lji} \phi_l \right), \tag{1.10}$$

$$B_{ii} = \sum_{jl} f_{jli} \phi_j \phi_l, \qquad B_{ij} = \sum_{l} \left(f_{ijl} \phi_i \phi_j - f_{ilj} \phi_i \phi_l - f_{lji} \phi_l \phi_j \right). \tag{1.11}$$

Because the fluctuations are damped by a factor of $\Omega^{1/2}$, in the remainder of this paper we concentrate on studying the deterministic equation (1.6).

1.2.4 The deterministic jump-growth equation

For analytical calculations and also for conceptual considerations it is convenient to work with the continuum limit of the macroscopic equations (1.6). This limit is obtained by writing the size of the weight brackets as $\Delta_i = w_{i+1} - w_i = \mu_i \Delta$ and taking the limit $\Delta \to 0$. The discrete set of variables ϕ_i is replaced by a continuous density function $\phi(w)$ satisfying $\phi(w_i) = \phi_i / \Delta_i$. This function $\phi(w)$ describes the density per unit mass per unit volume as a function of mass w at time t; it therefore has dimensions $\mathrm{M}^{-1}\,\mathrm{L}^{-3}$. The sum over weights in (1.6) is replaced by an integral, $\sum_i \Delta_i \to \int dw$. The rate constants k_{ij} are replaced by a feeding rate $k(w, w')$ satisfying $k(w_i, w_j) = k_{ij}$. The macroscopic equation (1.6) becomes

$$\begin{aligned} \frac{\partial \phi(w)}{\partial t} = \int (& - k(w, w') \phi(w) \phi(w') \\ & - k(w', w) \phi(w') \phi(w) \\ & + k(w - Kw', w') \phi(w - Kw') \phi(w')) dw'. \end{aligned} \tag{1.12}$$

We call this equation the 'deterministic jump-growth' equation. The three terms in (1.12) are equivalent to those in (1.6), and correspond to the idea in Figure (1.1) that there are two ways to leave weight w and one way to enter it. The terms represent, in order: feeding on prey to become larger than weight w, being fed upon and removed from the system entirely, and feeding on prey of exactly the right size to become weight w.

Following Benoît and Rochet (2004) we assume that the feeding rate takes the form

$$k(w, w') = Aw^{\alpha} s\left(w/w'\right). \tag{1.13}$$

This states that the rate at which a particular predator of weight w eats a particular prey of weight w' is a product of the volume searched per unit time and a dimensionless feeding preference function s. The volume searched per unit time Aw^{α} depends on the predator's body weight w, raised to the constant power α. A is a constant volume searched per unit time per unit mass$^{\alpha}$. The feeding preference function s depends only on the ratio w/w' between predator weight and prey weight. In practice this feeding preference function will be peaked around a preferred predator:prey weight ratio B.

When the parameter K, that describes which proportion of the prey mass is assimilated by the predator, is equal to 1, the deterministic jump-growth equation (1.12) reduces to the Smoluchowski coagulation equation (Smoluchowski, 1916), that is used to describe the clumping together of particles, for example in aerosols. However the rate kernels used to describe coagulation differ greatly from our localised feeding rate kernel (1.13). Typical choices in the coagulation equation are $k(x, y) = x + y$ or xy or other homogeneous expressions and these lead to very different behaviour such as the formation of one giant cluster (gelation); see for example Aldous (1999).

1.2.5 Relation to the McKendrick–von Foerster equation

The deterministic jump growth equation (1.12) is not the same as the McKendrick–von Foerster equation which has been widely used to describe the dynamics of size spectra (Silvert and Platt, 1978; Silvert, 1980; Benoît and Rochet, 2004; Maury et al., 2007a; Blanchard et al., 2009; Law et al., 2009) and which reads

$$\frac{\partial \phi}{\partial t} = -\phi D - \frac{\partial}{\partial w}(\phi G), \tag{1.14}$$

where D is the per capita death rate at weight w from predation by larger organisms,

$$D(w) = \int k(w', w)\phi(w')dw', \tag{1.15}$$

and G is the growth rate at weight w from feeding on smaller organisms,

$$G(w) = \int Kw'k(w,w')\phi(w')dw'. \tag{1.16}$$

Here we show that (1.14) emerges as an approximation to (1.12) in the case where the typical prey is small in size compared with the predator. Such an assumption is reasonable in many cases, because predators tend to be of an order 10^2 to 10^3 times the body mass of their prey (Cohen et al., 1993; Jennings and Mackinson, 2003). So the feeding kernel is strongly peaked around $w' = w/B$ with B large. Taking into account further the inefficiency with which prey mass is assimilated ($K \approx 10^{-1}$) (Paloheimo and Dickie, 1966), there is some justification for treating $Kw' << w$ in the last term of (1.12). This motivates a Taylor expansion of this term around w,

$$\begin{aligned} k(w-Kw',w')\phi(w-Kw') = k(w,w')\phi(w) \\ + (-Kw')\frac{\partial}{\partial w}\left(k(w,w')\phi(w)\right) \\ + \frac{(-Kw')^2}{2!}\frac{\partial^2}{\partial w^2}\left(k(w,w')\phi(w)\right) + \cdots \end{aligned} \tag{1.17}$$

Substituting this back into (1.12) gives

$$\begin{aligned} \frac{\partial\phi(w)}{\partial t} = &-\int k(w',w)\phi(w)\phi(w')dw' \\ &-\frac{\partial}{\partial w}\int Kw'k(w,w')\phi(w)\phi(w')dw' \\ &+\frac{1}{2}\frac{\partial^2}{\partial w^2}\int (Kw')^2k(w,w')\phi(w)\phi(w')dw' \\ &+R, \end{aligned} \tag{1.18}$$

where the remainder term R is given by

$$R = \sum_{n=3}^{\infty}\frac{(-1)^n}{n!}\frac{\partial^n}{\partial w^n}\int (Kw')^n k(w,w')\phi(w)\phi(w')dw'. \tag{1.19}$$

The first two terms in (1.18) correspond to those in the McKendrick–von Foerster equation (1.14). For ecosystems near to steady state, where $\phi(w)$ is close to a power law (as we will see in the next section), the higher order terms are suppressed by factors of K/B and are therefore small. Thus the McKendrick–von Foerster equation is a good approximation for (1.12) near the steady state and when prey are typically much smaller than their predators. But the higher order terms are not necessarily small in non-equilibrium ecosystems. In particular, the McKendrick–von Foerster equation is a less good approximation if there is a travelling wave attractor, see Section 1.3.2.

One way to understand the difference between (1.12) and (1.14) is that (1.12) mod-

els the discrete, variously-sized jumps in predator mass as predators feed and grow. This captures the property of the stochastic model that individuals, starting at a given weight, are able to develop a range of weights over the course of time. In contrast to this, the McKendrick–von Foerster equation (1.14) assumes smooth growth along the weight axis. Spreading of body size can be incorporated in (1.14) by introducing the diffusion term, the third term in (1.18). The source of such diffusion is the deterministic jump-growth equation (i.e. terms of order Ω^0), so diffusion is attributable to the deterministic, as opposed to the stochastic, component of the full process.

1.2.6 Steady-state solution

In marine ecosystems, abundance of organisms within body mass classes averaged over space and seasons often changes rather little, suggesting that they may be close to a steady state. In such circumstances and when abundance and mass are both expressed as logarithms (i.e. as a power spectrum) the relationship is approximately linear with a gradient often close to -1, which implies a power-law with an exponent -2 in the untransformed variables. This leads to the important regularity of marine ecosystems that the total biomass is approximately constant when expressed in logarithmic intervals of body mass.

Benoît and Rochet (2004) found that the McKendrick–von Foerster equation has steady state solutions of the power-law form $\hat{\phi}(w) \propto w^{-\gamma}$ (see also Platt and Denman, 1978; Camacho and Solé, 2001), and we will show that the same is true for the deterministic jump-growth equation (1.12). Of course in the real world such a power-law will have to break down for very small weights (where otherwise the power-law would predict an infinite number of very small individuals) and for very large weights (where the power-law would predict a non-zero density of arbitrarily large individuals). Indeed, in a real system with a finite number of individuals, a model just having predation events could not have a non-trivial steady state because the number of individuals would continue to decrease. A non-zero steady state is possible only if there is an inexhaustible reservoir of small individuals. In our model the power-law spectrum provides this reservoir automatically, with $\phi(w) \to \infty$ as $w \to 0$. In a more realistic model one would need to model the plankton as well as recruitment.

A steady state solution $\hat{\phi}(w)$ of (1.12) has to satisfy the equation

$$\begin{aligned} 0 = & - \int k(w,w')\hat{\phi}(w)\hat{\phi}(w')dw' \\ & - \int k(w',w)\hat{\phi}(w')\hat{\phi}(w)dw' \\ & + \int k(w-Kw',w')\hat{\phi}(w-Kw')\hat{\phi}(w')dw', \end{aligned} \tag{1.20}$$

If we substitute the power law Ansatz $\hat{\phi}(w) \propto w^{-\gamma}$ into this equation, use the form

(1.13) for the feeding rate, change to a new integration variable $r = w_{predator}/w_{prey}$ and cancel some overall factors, we obtain an equation for the exponent γ,

$$0 = f(\gamma) = \int s(r)\left(-r^{\gamma-2} - r^{\alpha-\gamma} + r^{\alpha-\gamma}(r+K)^{-\alpha+2\gamma-2} \right) dr. \tag{1.21}$$

The existence of a power law steady state can now be proven using the same argument as that given by Benoît and Rochet (2004) in the case of the McKendrick–von Foerster equation[2]. The argument goes as follows. If we assume that predators are bigger than their prey, then for $\gamma < 1 + \alpha/2$, $f(\gamma)$ is less than zero. Also, $f(\gamma)$ increases monotonically for $\gamma > 1 + \alpha/2$, and is positive for large positive γ. Therefore there will always be a unique γ for which $f(\gamma)$ is zero and thus a unique steady state of the form $\hat{\phi}(w) \propto w^{-\gamma}$. If we allow predators to be smaller than their prey, situations with no power law steady state or multiple power law steady states can be found.

The numerical value of the power law exponent γ is of particular interest because γ is known to have a value close to 2 in marine ecosystems (see Section 1.1). In the special case that $K = 1$, and $\alpha = 1$, a value $\gamma = 2$ does in fact satisfy (1.21). A value of α close to 1 is biologically reasonable as this means that the volume searched by a predator is proportional to its body weight (see Equation (1.13)), although the limited information available suggests a value slightly lower than $\alpha = 1$ (Ware, 1978). More generally, $\gamma = (3 + \alpha)/2$ will satisfy (1.21) for any α, with $K = 1$.

A value of K close to 1 is unrealistic: $K \approx 0.1$ would be more appropriate (Paloheimo and Dickie, 1966) because only a small proportion of food ingested is assimilated into extra body weight. To treat this case analytically we make the assumption that predators feed only on prey of their preferred size, i.e., we set the feeding preference function in (1.21) to the delta function $s(r) = \delta(r - B)$. In that case (1.21) reduces to

$$0 = -B^{\gamma-2} - B^{\alpha-\gamma} + B^{\alpha-\gamma}(B+K)^{-\alpha+2\gamma-2}. \tag{1.22}$$

A Taylor expansion in K/B gives

$$0 \approx (2\gamma - \alpha - 2)\frac{K}{B} - B^{-2\gamma+\alpha+2}, \tag{1.23}$$

and the Lambert W function can be used to express γ explicitly as a function of the other variables

$$\gamma \approx \frac{1}{2}\left(2 + \alpha + \frac{W\left(\frac{B}{K}\log B\right)}{\log B} \right). \tag{1.24}$$

At $K = 1$ and $\alpha = 1$, (1.24) produces $\gamma = 2$ because $W(B \log B) = \log B$. For $K < 1$, the exponent γ increases as either K or B decrease, because in either case less mass is

[2]We thank one of the referees for pointing this out.

transferred to larger organisms. Notice however that the dependence of γ on K and B is weak; for instance, if $K = 0.1$ and $B = 100$ (still with $\alpha = 1$), the exponent only increases to $\gamma = 2.21$. Thus if K and B are given biologically reasonable values the steady-state of the model is broadly consistent with the empirical property of marine ecosystems that γ is close to 2.

The ecological literature contains a relationship between the parameter γ, and K and B based on a quite different premise, that the metabolic rate of organisms scales with body weight as $w^{3/4}$. It can be shown from this scaling that

$$\gamma = 1 + \frac{3}{4} - \frac{\log K}{\log B} \tag{1.25}$$

in the absence of any consideration of dynamics (Brown et al., 2004). There is some resemblance between this equation and (1.24), which becomes evident from taking the asymptotic approximation for the Lambert W function

$$W(z) = \log z - \log\log z + \cdots \tag{1.26}$$

in (1.24), giving an expansion in which the leading terms are

$$\gamma \approx \frac{1}{2}\left(3 + \alpha - \frac{\log K}{\log B} - \frac{\log\log\left(\frac{B}{K}\log B\right)}{\log B} + \frac{\log\log B}{\log B} + \cdots\right). \tag{1.27}$$

Both (1.25) and (1.27) contain the term $(\log K)/(\log B)$, but are not the same. From a biological standpoint the equations have the important difference that the relationship in (1.27) follows simply from dynamical bookkeeping of biomass, without any assumption about metabolic rates being made (see also Law et al. (2009)).

We stress that, although some properties of the steady state have been described here, we have not investigated analytically the region of parameter space in which the steady state is an attractor. The next Section (1.3) shows by means of numerical methods two classes of attractor: a steady state of the kind described above and a travelling wave.

1.3 Numerical results

Here we use numerical methods to compare some properties of the stochastic jump-growth model (1.2), the deterministic jump-growth equation (1.12) and the McKendrick–von Foerster equation (1.14).

Body sizes can span at least ten orders of magnitude in real ecosystems, and it is helpful in computations to discretise weight into logarithmic bins, such that the weight

bracket $[w_i, w_{i+1})$ is the range $[w_i, (1+\Delta)w_i)$. We adopt a notation: $x = \log(w/w_0)$, for some arbitrary weight w_0, and use the function $u(x) = \Omega w \phi(w)$. Thus, integrating $u(x)$ over the range $[x_i, x_i + \Delta)$, returns the total number of individuals in this size range.

Some further biological details have to be specified to do the numerical analysis; Table 1.1 summarises the information, and Section 1.3.1 describes this in more detail. We have chosen the parameters not for biological realism but in order to highlight the differences between the stochastic jump-growth model and the McKendrick–von Foerster equation. In particular we have chosen a smaller predator:prey mass ratio than is realistic.

term	meaning	value		
		Fig 1.2	Fig 1.3	Fig 1.4
$\underline{x}$	min wt of phytoplankton	0	0	0
x_b	min wt of consumers	2	2	2
x_d	max wt of newborn consumers	2.1	2.1	2.1
x_s	wt at start of senescent death	5	7	8
$\overline{x}$	max wt of consumers	7.5	9	10
K	mass conversion efficiency	0.2	0.2	0.2
B	preferred pred:prey mass ratio	e^1	e^1	e^1
A	volume searched mass$^{-\alpha}$	50	50	50
α	search volume exponent	1	1	1
σ	width of feeding kernel	0.3	0.35	variable
μ	intrinsic mortality rate	0.1	0.1	0.1
ρ	growth of senescent death	5	5	5
	stochastic realisation			
N_p	number of phytoplankton	25000	50000	-
N_0	initial number of consumers	2000	4000	-
x_0	initial upper bd of consumers	4	7	-
$\gamma^* - 1$	exponent for fixed spectra	1.3	1.3	-
Δ'	weight bracket for stochastic bins	0.1	0.1	-
	numerical integration			
Δ	wt bracket for integration	0.01	0.01	0.01
δt	time increment for integration	0.0001	0.0001	0.0001

Table 1.1: Parameter meanings and values used in computations for figures.

1.3.1 Model specification for numerics

The numerical results describe an ecosystem with two types of organism: phytoplankton which do not feed on other organisms, and consumers which feed on each other and on phytoplankton. In more detail, the full range of body weights $[\underline{x}, \overline{x})$ is subdivided into the following regions with different ecological properties.

- $[\underline{x}, x_b)$ is reserved for phytoplankton. These organisms are self-supporting; they

do not change in mass, and do not form part of the dynamics. Their densities are held constant, which is equivalent to assuming that, as soon as they are eaten, they are replaced. Such organisms have to be present to provide a supply of food for small consumers.

- $[x_b, x_d)$ is a range reserved for renewal of consumers, i.e. a range over which consumers are born. Renewal is essential: without this, consumers would gradually die out. Biological realism requires this range to be distinguished from $[\underline{x}, x_b)$, because newborn consumers may grow in size. When consumers leave this range (by growth or by death), they are immediately replaced, which amounts to an assumption of perfect density-dependent compensation in the nursery.

- $[x_d, x_s)$ is the range in which consumers experience the standard predation, growth and death processes described in Section 1.2. We include in this range intrinsic mortality at a per-capita rate μ, which takes into account the fact that organisms can die for reasons other than being eaten.

- $[x_s, \overline{x})$ is a range in which the per-capita mortality rate of consumers increases according to the function

$$d(x) = \begin{cases} \mu \exp\left(\rho(x - x_s)\right) & \text{if } x \geq x_s \\ \mu & \text{otherwise} \end{cases} \tag{1.28}$$

  where ρ scales how fast mortality increases beyond size x_s. The purpose of this is to ensure that consumers cannot continue to grow indefinitely, in keeping with biological constraints on body size. The upper bound $\overline{x}$ is set such that the density of organisms at this size is very close to zero.

For numerical studies, the predation-rate function $k(x, x')$ needs to be made explicit. In keeping with (1.13), this function is taken to consist of a volume searched per unit time by predators, together with a feeding preference function, which is assumed to have a Gaussian shape. In logarithmic variables, the function is:

$$k(x, x') = \begin{cases} \frac{Ae^{\alpha x}}{\sigma\sqrt{2\pi}} \exp\left(-\frac{1}{2\sigma^2}(x - x' - \log B)^2\right) & \text{if } x > x' \\ 0 & \text{otherwise} \end{cases} \tag{1.29}$$

where parameters A, α, B remain as defined in Section 1.2.6, and σ measures the range of prey sizes likely to be eaten relative to the size of the predator. We have introduced the assumption here that predators must be larger than their prey.

In stochastic realisations, the fixed phytoplankton population was initialised with N_p individuals taken from an exponential distribution with parameter $\gamma^* - 1$ over the range $[\underline{x}, x_b)$. The consumer spectrum was initialised with N_0 individuals taken from an exponential distribution with parameter $\gamma^* - 1$ over a range $[x_b, x_0)$. N_0 was chosen to make the discontinuity between the two spectra small, the upper weight limit being

initially x_0 in the consumers. After the start, consumers dying or growing out of the renewal range were replaced with newborn individuals, using the same exponential distribution so that the number of consumers in this range would remain constant. We carried out realisations of the individual-based stochastic process (Subsection 1.2.1) using the Gillespie algorithm (Gillespie, 1976). Body sizes were aggregated into bins of width Δ' only for visualisation of the size spectra.

Numerical integrations of the deterministic models were carried out using the explicit Euler method, with a bin width Δ and a time step δt; consumer spectra were held at their initial values in the renewal range. Integrations were initialised with assumptions equivalent to those of the corresponding stochastic realisations. For graphical comparison with stochastic results, $u(x)$ was scaled such that $\int u(x,0)dx$ was N_p and N_0 for the phytoplankton and consumers respectively, and displayed as the number $n(x) = u(x)\Delta'$ over size intervals Δ'.

1.3.2 Travelling waves

Figure 1.2 compares time series from the deterministic jump-growth equation (1.12) and from the McKendrick–von Foerster equation (1.14) against a realisation of the stochastic process. Parameter values are the same for all three time series, and were chosen to contrast the two deterministic models, by making the difference between predator and prey body sizes relatively small, and by ensuring the steady state would not be an attractor. Initial conditions were chosen well away from the steady state, to induce large oscillations in the size spectra from the start.

Large sustained waves in density develop over time in all three models. These waves move along the size spectra from small to large body size as organisms grow. Peaks of the waves are associated with slow growth (prey relatively rare) and low mortality (predators relatively rare). As expected, the deterministic jump-growth time series gives a better match to the stochastic series than the McKendrick–von Foerster one, in terms of the period and shape of the waves (although they are not identical).

1.3.3 Variable growth

The jump-growth model and the McKendrick–von Foerster equation differ in that the former describes a process in which organisms, starting at the same weight, develop different weights over the course of time. In so doing, the jump-growth model captures an important feature of growth: when two organisms of the same weight eat prey items of different weights, the two organisms must subsequently have different weights.

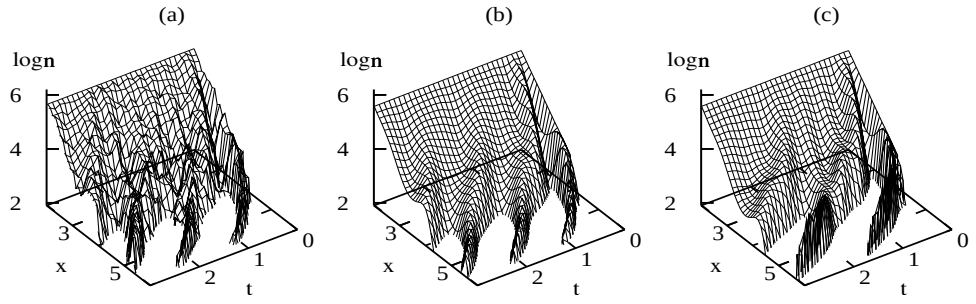

Figure 1.2: Size spectra expressed as logarithm of numbers $\log n(x)$ with logarithm of weights x over time t, constructed from (a) the stochastic jump-growth process, (b) the deterministic jump-growth equation, (c) the McKendrick–von Foerster equation. Parameter values given in Table 1.1.

Figure 1.3 illustrates this feature of the models, using parameter values that highlight the differences between them. The results show the fate of a set of organisms that all start with very similar weights in the range $[x_d, x_d + \Delta')$; the set can be thought of as a cohort which grows older without renewal. In the stochastic jump-growth model, organisms were tagged individually, and the size distribution of the cohort over time was monitored. In the deterministic jump-growth model we assumed a tagged cohort $u^*(x)$ at a density low enough relative to $u(x)$ for changes in $u^*(x)$ to come just from feeding on and being fed upon by $u(x)$, without any reciprocal effect of $u^*(x)$ on $u(x)$. In the McKendrick–von Foerster simulation, differential equations for survival and growth in weight in the cohort were solved using the growth and death rates (1.15) and (1.16) respectively, as described in Law et al. (2009).

The stochastic realisation (Figure 1.3a) shows the number of tagged individuals declining as time goes on (they are being eaten by larger organisms); it also shows the distribution of body weights spreading out. The behaviour of the deterministic jump-growth equation matches the stochastic cohort closely (Figure 1.3b). However, the McKendrick–von Foerster equation (Figure 1.3c) retains its initial spike-like distribution, because the growth trajectory from any size is fixed.

The average growth trajectories of all three models are close together (Figure 1.3d). As time goes on and the number of individuals in the stochastic cohort becomes small, fluctuations in the stochastic growth trajectory can be seen. Also, growth according to the McKendrick–von Foerster equation is slightly slower than in the deterministic jump-growth equation. However, these differences are small, and it is only when the second moments of growth are considered that the spreading in body sizes, missing from the McKendrick–von Foerster equation, becomes evident.

Adding the second-order diffusion term of (1.18) to the McKendrick–von Foerster equation (1.14) would recover the tendency for body size to spread. However, this still leaves out higher order terms of the Taylor expansion (1.18) which do not necessarily become small unless the steady state is an attractor.

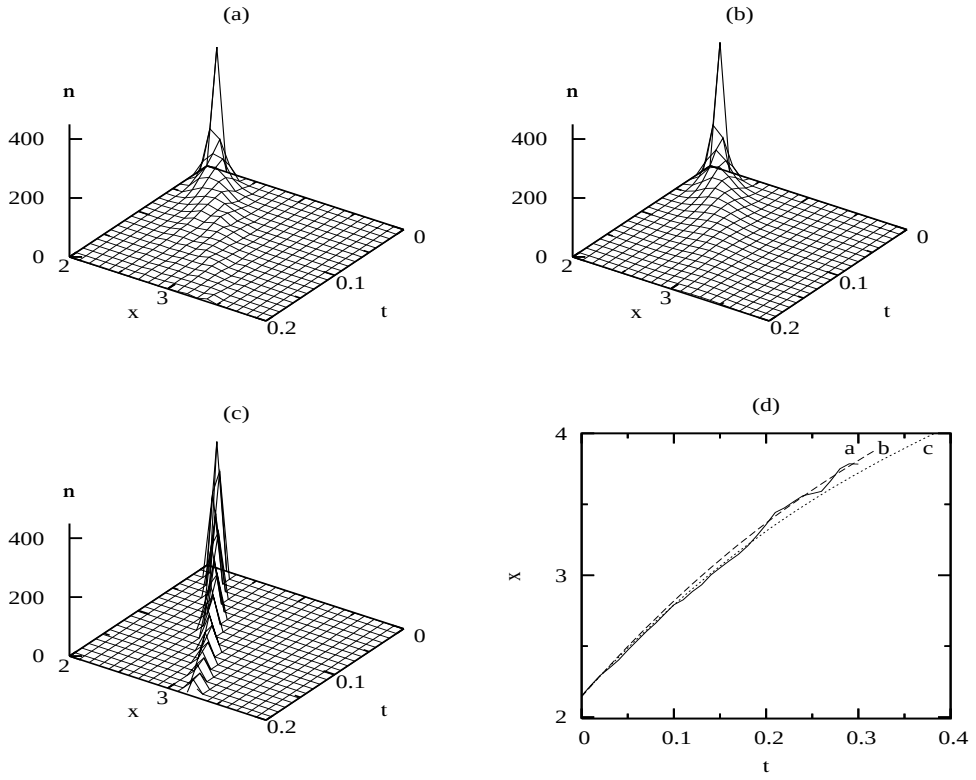

Figure 1.3: Number $n(x)$ of organisms with log weight x over time t in tagged cohorts embedded in size spectra. Cohorts start in a weight range $2.1 \leq x < 2.2$ at $t = 0$. (a) Stochastic jump-growth process; (b) deterministic jump-growth equation; (c) McKendrick–von Foerster equation; (d) mean weights over time computed for the cohorts shown in (a), (b), (c), and labelled correspondingly. Parameter values given in Table 1.1.

1.3.4 Dynamical stability

Figure 1.4 gives examples of the steady states and stability properties of the jump-growth and McKendrick–von Foerster models. The breadth of diet σ decreases from top to bottom in the figure.

At steady-state, the size spectra have similar shapes in the two models, and diet breadth has little effect on them. For the most part the steady states are close to linear under the log transformation of both axes. This linearity applies until near $x = 8$, where the extra size-dependent mortality starts to take effect. In the region $2.1 \leq x < 7$ which is close to linear, the slopes are approximately -1.42 in the deterministic jump-growth equation and -1.47 in the McKendrick–von Foerster equation, equivalent to exponents $\gamma = 2.42$ and $\gamma = 2.47$ respectively. These values are close to the value 2.47 predicted from analysis of the delta-function version of the feeding preference equation (1.24).

Figure 1.4 shows the existence of a bifurcation point at which the system flips from one dynamical regime to another as σ changes. For large enough σ the steady state is an attractor, i.e. the Jacobian matrix evaluated at the steady state has $\max(Re(\lambda)) < 0$:

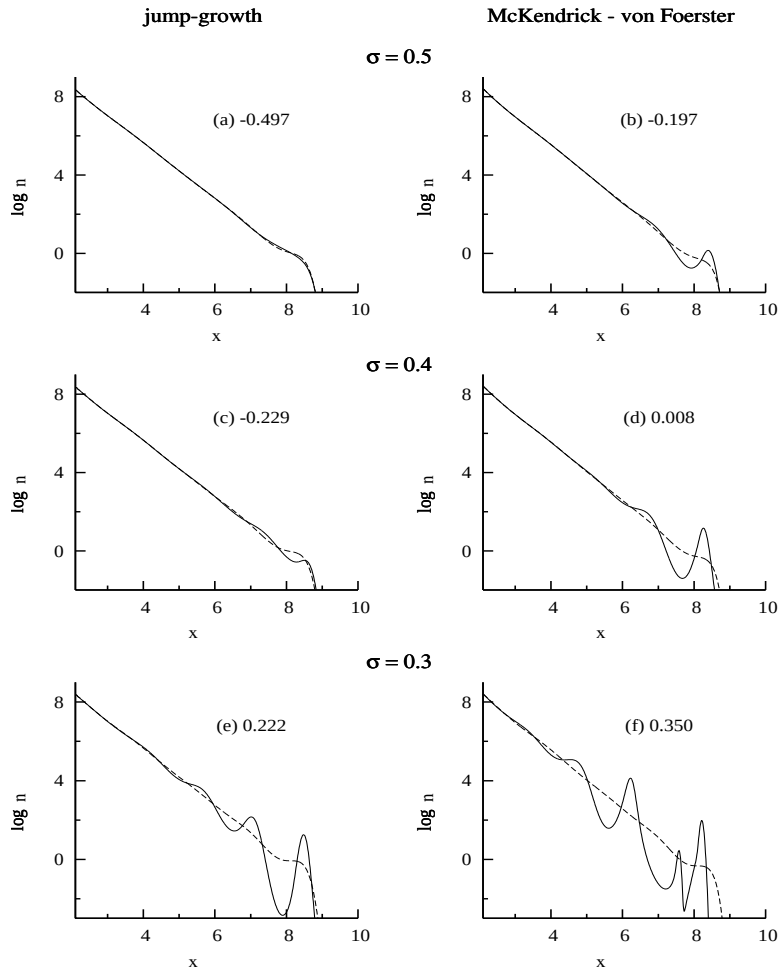

Figure 1.4: Steady-state size spectra (dashed lines), and transient size spectra (continuous lines) after a period of 5 time units has elapsed starting from the same initial function. Column 1 (a, c, e) obtained from the deterministic jump-growth equation; column 2 (b, d, f) obtained from the McKendrick–von Foerster equation. Diet breadths σ: 0.5 (a, b), 0.4 (c, d), 0.3 (e, f); other parameters given in Table 1.1. Steady states obtained by Newton-Raphson iteration, which also gives the Jacobian matrix at steady state (Press et al., 1992); numbers given for each graph are $\max(Re(\lambda))$ where λ is an eigenvalue of the Jacobian.

size spectra initialised away from the steady state move towards it. For small enough σ this ceases to be the case, i.e. $\max(Re(\lambda)) > 0$; instead, the size spectra develop travelling waves like those seen in Figure 1.2. Importantly, the bifurcation point occurs at a smaller value of σ in the jump-growth equation. This may be because of the lack of spreading in body size in the McKendrick–von Foerster equation: such spreading would tend to dampen oscillations. A consequence of the difference is that a stability analysis of the McKendrick–von Foerster equation could be misleading; see for instance Law et al. (2009). Although not shown here, the bifurcation to a travelling wave can also be induced by increasing the preferred ratio B of the predator:prey body mass (Law et al., 2009).

1.4 Discussion

The starting point for our analysis was a simple, mechanistic, stochastic process in which a larger organism feeds on a smaller one, thereby causing the death of the prey and increment in its own weight. From the master equation of the process, a macroscopic model for the dynamics of size spectra was derived, which we call the deterministic jump-growth model. The equation is related to the Smoluchowski coagulation equation (Smoluchowski, 1916), which describes how the size-distribution of inanimate coagulating particles changes over time. However, the jump-growth equation has to deal with special features of living organisms, such as their ability to choose the size of their prey, and their inefficiency in turning these prey into their own body mass. To cope with the vagaries of the animate world, the deterministic jump-growth equation is necessarily more general.

The expression for the steady state derived from the deterministic jump-growth equation is consistent with the approximate constancy of biomass in logarithmic intervals of body mass often observed in marine ecosystems. So the basic empirical regularity evidently follows from the bookkeeping of biomass, as it passes through the ecosystem. However, the steady state may or may not be an attractor. As one might anticipate from the general oscillatory nature of predator-prey systems, another non-equilibrium attractor exists, here comprising waves of abundance that travel from small to large body size. These waves have practical as well as theoretical interest in view of the large, often unexplained, fluctuations in exploited marine fish stocks (Hsieh et al., 2006; Anderson et al., 2008; Blanchard et al., 2009, personal communication).

The jump-growth model is not the same as the McKendrick–von Foerster equation widely used in the study of dynamic size spectra. This is because it allows organisms, starting at the same size, to become different through eating prey of different sizes. The McKendrick–von Foerster equation, with its roots in age distributions

(McKendrick, 1926; von Foerster, 1959) does not allow this: organisms which start at the same age must always remain the same age. An age-dependent McKendrick–von Foerster equation has been extended to allow for variable size at age (Gurney and Veitch, 2007), but this was by adding variability to a specified model of growth, the von Bertalanffy equation. Growth of organisms in dynamic size spectra comes about in a quite different way, because it emerges directly from the action of predators feeding on prey. This is not to suggest that variation in prey size is the only cause of variation in predator size; in reality, a variety of extrinsic and intrinsic factors are most likely involved.

Although the deterministic jump-growth model is different from the McKendrick–von Foerster equation, the latter can be derived from it using the lowest-order terms in a Taylor approximation. The approximation requires that prey size is small relative to that of the predator, which will often apply in practice. Thus for many purposes the McKendrick–von Foerster equation should work well, notwithstanding the numerical examples used in Section 1.3 (deliberately chosen to contrast the two models). This is with the caveat that higher-order terms in the Taylor expansion are not necessarily small when the attractor is a travelling-wave rather than a steady state, or when looking at spiky perturbations away from the steady state, even if prey are much smaller than their predators. To describe such non-equilibrium solutions accurately, the jump-growth model is needed.

When solving the jump-growth equation numerically, some care is needed in the discretisation of $\log w$. Unlike the McKendrick–von Foerster equation, there is no guarantee that feeding will generate non-zero rate terms for growth. If the multiplicative weight brackets Δ are too large relative to prey size, weight increments from feeding do not register, and an erroneous solution is obtained. For a Gaussian feeding preference function (1.29), a rule of thumb is that Δ needs to be of an order $K/(Be^{2\sigma})$ to capture properly the rate term due to growth of organisms. Values of the order $B = 10^2$, $\sigma = 0.5 \log B$ and $K = 0.1$ are realistic (Paloheimo and Dickie, 1966; Cohen et al., 1993; Jennings and Mackinson, 2003), requiring Δ to be of an order 10^{-5}. With marine size spectra encompassing ten orders of magnitude, numerical analyses clearly become demanding. A small value of B was used for the illustrations in Section 1.3, but it would be much harder to do the computations in a more realistic setting.

Faced with this difficulty, a halfway house would be to use the McKendrick–von Foerster equation with the diffusion term from the expansion in (1.18). We are not aware of a previous derivation of the diffusion term for growth in body size, although diffusion in physical space has been considered in the context of the McKendrick–von Foerster equation (Okubo and Levin, 2001). Nor have we seen the use of a diffusion term in the McKendrick–von Foerster equation applied to size spectra, although the effects of introducing variability into Gompertz and von Bertalanffy growth models

have been described (Bardos, 2005; Gurney and Veitch, 2007). It would be instructive to know how much the McKendrick–von Foerster approximation could be improved by introducing this extra term.

Several further features of real-world ecosystems, not dealt with in this paper, will modify our results. First, some feedback between the abundance of phytoplankton and consumers is to be expected. Second, perfect compensation in renewal of consumers is unlikely, especially when travelling waves affect the abundance of reproducing individuals. Such processes generate long, potentially destabilizing, feedback loops. Third, consumers do not all start life with the same potential for growth and reproduction. They comprise a number of different species with different life histories (Andersen and Beyer, 2006; Blanchard et al., 2009). They are born at different sizes, they grow to different sizes, and they allocate different proportions of their limited resources to growth, maintenance and reproduction along the way (Maury et al., 2007a). Such processes loosen the dynamical coupling between a feeding organism and its prey.

There is much to learn about the intricacies of biology that can stabilize and destabilize marine ecosystems. It is important to obtain this knowledge because the biomass in such ecosystems is typically of major economic importance, heavily exploited, and with dynamics that are not well understood. The deterministic jump-growth equation derived here should place this programme of research on a more rigorous footing.

Acknowledgements: We thank Julia Blanchard, Jennifer Burrow, Alex James, Jon Pitchford and Michael Plank and the referees of the paper for many helpful insights, and Kai Wirtz for pointing out the relation to the Smoluchowski coagulation equation. The research was supported by a studentship to SD from the Natural Environment Research Council UK, with the Centre for Environment Fisheries and Aquaculture Science UK as the CASE partner. RL was supported by the Royal Society of New Zealand Marsden Fund, grant 08-UOC-034.

1.5 Appendix: Derivation of Langevin equation

Our treatment of the jump-growth model using the van Kampen expansion in Section 1.2.3 did not provide a justification for assuming that the fluctuations $\boldsymbol{\xi}$ around the solution $\boldsymbol{\phi}$ of the deterministic equation (1.6) are damped by a factor of $\Omega^{1/2}$. In this appendix we derive an approximate stochastic differential equation for the jump-growth model, adapting an approximation procedure used by Gillespie (2000) for stochastic models of chemical reactions. We will find that the deterministic part of the equation coincides with our deterministic jump-growth equation (1.6) and that the stochastic noise term is indeed suppressed by a factor of $\Omega^{1/2}$.

Because of the stochastic nature of the jump-growth model, the vector of numbers $[\dots, n_{-1}, n_0, n_1, \dots]$ in each weight bracket introduced in subsection (1.2.2) is described by a stochastic process $\boldsymbol{n}(t)$. In a time interval $[t, t+\tau]$ a number of predation events will take place, each of which changes the numbers. This is expressed by the equation

$$\boldsymbol{n}(t+\tau) = \boldsymbol{n}(t) + \sum_{i,j} R_{ij}(\boldsymbol{n}(t), \tau)\boldsymbol{\nu}_{ij}, \tag{1.30}$$

where the $R_{ij}(\boldsymbol{n}, \tau)$ are random variables giving the number of predation events taking place in the time interval $[t, t+\tau]$ that involve a predator from weight bracket i and a prey from weight bracket j. The $\boldsymbol{\nu}_{ij}$ are the vectors that give the change in numbers caused by such a predation process, as described in Subsection (1.2.2). We now will argue that the random variables $R_{ij}(\boldsymbol{n}(t), \tau)$ can be approximated by normally distributed variables.

The rate a_{ij} of each individual predation event depends on the numbers of individuals

$$a_{ij}(\boldsymbol{n}) = \Omega^{-1} k_{ij} n_i n_j. \tag{1.31}$$

As the numbers change after each event, the events are unfortunately not independent. However, because the numbers change only by ± 1 in each event, the change to the rates is very small if the numbers are large. So, if we choose the time span τ small enough so that not too many predation events take place, the rates can be approximated as remaining constant throughout the time interval,

$$a_{ij}(\boldsymbol{n}(t')) \approx a_{ij}(\boldsymbol{n}(t)) \quad \forall t' \in [t, t+\tau]. \tag{1.32}$$

In that case the predation events can be treated as independent and therefore the number $R_{ij}(\boldsymbol{n}(t), \tau)$ of event taking place in the time interval follows the Poisson distribution with parameter $\tau a_{ij}(\boldsymbol{n}(t))$.

Next we assume that the parameter $\tau a_{ij}(\boldsymbol{n}(t))$ is either zero or large enough so that the Poisson distribution is well approximated by the normal distribution with mean

and variance both equal to $\tau a_{ij}(\boldsymbol{n}(t))$. Again this is easy to justify when the numbers are large and provided the feeding kernel k_{ij} is bounded away from zero. In our case, where the feeding kernel contains a Gaussian, we need to neglect the rare events in the tails of the Gaussian.

Note that we are placing two opposing conditions on the size of the time interval τ: it needs to be both small enough so that the rates don't change much but also large enough so that the number of events can be taken to be normally distributed. Such an intermediate range for τ will exist, provided the numbers of individuals in the weight brackets are large enough. In our application, where the overall number of individuals involved is truly huge, our approximations will be very good except for very large weights where the density is very small and where the approximations will break down.

Now that we have argued that the R_{ij} are well approximated by normal random variables with mean and variance both equal to $\tau a_{ij}(\boldsymbol{n}(t))$, we express them as

$$R_{ij}(\boldsymbol{n}(t),\tau) = a_{ij}(\boldsymbol{n}(t))\tau + \sqrt{a_{ij}(\boldsymbol{n}(t))\tau}\, r_{ij} \tag{1.33}$$

where the r_{ij} are normal random variables with mean 0 and variance 1. Substituting this into (1.30), rearranging terms and dividing by τ gives

$$\frac{\boldsymbol{n}(t+\tau)-\boldsymbol{n}(t)}{\tau} = \sum_{ij} a_{ij}(\boldsymbol{n}(t))\boldsymbol{\nu}_{ij} + \sum_{ij}\sqrt{a_{ij}(\boldsymbol{n}(t))}\boldsymbol{\nu}_{ij}\tau^{-1/2}r_{ij}. \tag{1.34}$$

We now approximate this equation, which is valid for small but finite τ, by the stochastic differential equation obtained by taking the limit $\tau \to 0$,

$$\frac{d\boldsymbol{n}(t)}{dt} = \sum_{ij} a_{ij}(\boldsymbol{n}(t))\boldsymbol{\nu}_{ij} + \sum_{ij}\sqrt{a_{ij}(\boldsymbol{n}(t))}\boldsymbol{\nu}_{ij}\eta_{ij}(t), \tag{1.35}$$

where $\eta_{ij}(t)$ are independent white noise processes. This type of equation is known as a Langevin equation, see for example van Kampen (1992).

Substituting the explicit expressions (1.31) for the rates into the Langevin equation (1.35) gives

$$\begin{aligned}\frac{dn_i}{dt} =& \Omega^{-1}\sum_j \left(-k_{ij}n_in_j - k_{ji}n_jn_i + k_{mj}n_mn_j\right) \\ &+ \Omega^{-1/2}\sum_j\left(-\sqrt{k_{ij}n_in_j}\eta_{ij} - \sqrt{k_{ji}n_jn_i}\eta_{ji} + \sqrt{k_{mj}n_mn_j}\eta_{mj}\right).\end{aligned} \tag{1.36}$$

When we write the equation in terms of the population densities $\Phi_i = \Omega^{-1}n_i$ we see

that the fluctuation terms are suppressed by a factor of $\Omega^{-1/2}$.

$$\begin{aligned}\frac{d\Phi_i}{dt} = &\sum_j \left(-k_{ij}\Phi_i\Phi_j - k_{ji}\Phi_j\Phi_i + k_{mj}\Phi_m\Phi_j\right) \\ &+ \Omega^{-1/2}\sum_j \left(-\sqrt{k_{ij}\Phi_i\Phi_j}\eta_{ij} - \sqrt{k_{ji}\Phi_j\Phi_i}\eta_{ji} + \sqrt{k_{mj}\Phi_m\Phi_j}\eta_{mj}\right).\end{aligned}$$

For large system size Ω the fluctuation terms can be neglected and we end up with our equation (1.6).

Chapter 2

A stability analysis of the power-law steady state of marine size spectra

Samik Datta*, Gustav W. Delius*, Richard Law*, Michael J. Plank**

** Departments of Biology and Mathematics,*
University of York, York YO10 5DD, U.K.

*** Department of Mathematics and Statistics, University of Canterbury,*
Christchurch, New Zealand [1]

[1]emails: sd550, gwd2, rl1 @york.ac.uk, ** M.Plank@math.canterbury.ac.nz

Abstract

This paper investigates the stability of the power-law steady state often observed in marine ecosystems. Three dynamical systems are considered, describing the abundance of organisms as a function of body mass and time: a "jump-growth" equation, a first order approximation which is the widely used McKendrick-von Foerster equation, and a second order approximation which is the McKendrick-von Foerster equation with a diffusion term. All of these yield a power-law steady state. We derive, for the first time, the eigenvalue spectrum for the linearised evolution operator, under certain constraints on the parameters. This provides new knowledge of the stability properties of the power-law steady state. It is shown analytically that the steady state of the McKendrick-von Foerster equation without the diffusion term is always unstable. Furthermore, numerical plots show that eigenvalue spectra of the McKendrick-von Foerster equation with diffusion give a good approximation to those of the jump-growth equation. The steady state is more likely to be stable with a low preferred predator:prey mass ratio, a large diet breadth and a high feeding efficiency. The effects of demographic stochasticity are also investigated and it is concluded that these are likely to be small in real systems.

Keywords: marine ecosystem; stability; size-spectrum; McKendrick-von Foerster equation; predator-prey; growth diffusion; eigenvalues

2.1 Introduction

It is well established that marine ecosystems often show roughly equal abundances of biomass in logarithmically increasing weight intervals, when organisms are identified by body mass rather than by species identity (Sheldon et al., 1972; Boudreau and Dickie, 1992). This is equivalent to a power-law for the abundance density as a function of body mass with exponent of approximately -2. Alternatively, plotting log(abundance) against log(mass) gives a "size spectrum" (Sheldon and Parsons, 1967; Platt and Denman, 1978) which is approximately linear with gradient near to -1.

This empirical pattern has motivated a programme of theoretical research. Silvert

and Platt (1978; 1980) developed a size-dependent partial differential equation modelling growth and death in a size spectrum, and established the existence of a power-law steady state. The power-law steady state has also been shown in systems where predators are allowed to eat any prey smaller than themselves (Camacho and Solé, 2001). When predators are assumed to be more selective (i.e. eating only a certain range of prey), the existence of a power-law steady state has also been proven, using an integro-differential equation for the model instead of a partial differential equation; the exponent generally depends on assimilation efficiency, external mortality and predator-prey interaction rates (Benoît and Rochet, 2004). In these and other studies (e.g. Andersen and Beyer, 2006; Blanchard et al., 2009; Law et al., 2009), the McKendrick-von Foerster equation is commonly used. However, a derivation from a stochastic model of predation leads to a more general equation (Datta et al., 2010a), which we will refer to as the "jump-growth" equation in the following analysis. The McKendrick-von Foerster equation is the first order approximation (in an infinite series) to the jump-growth equation when prey are typically much smaller than predators. The second order approximation brings a diffusion term into the McKendrick-von Foerster equation (Datta et al., 2010a), the effects of which have not previously been studied.

Marine biologists need to understand the resilience of the power-law steady state to perturbations caused by fishing and natural phenomena, such as springtime plankton blooms. For instance, it has been shown that fishing increases the temporal variability in abundance of marine species (Hsieh et al., 2006; Anderson et al., 2008). Fundamental to this understanding are the stability properties of the power-law steady state, about which very little is known. We do know from recent numerical studies on the jump-growth equation and the McKendrick-von Foerster equation that there is a bifurcation from a stable power-law steady state to a travelling-wave attractor under certain parameter conditions (Law et al., 2009; Datta et al., 2010a). However, the only stability analysis we are aware of assumed growth to be independent of prey density (Arino et al., 2004), thereby excluding a key predator-prey interaction at the heart of the dynamics. The power-law steady state plays a pivotal role in marine ecosystems, and it is essential to understand the factors that contribute to its stability and instability.

This paper provides the first detailed stability analysis on the jump-growth equation and its low order approximations, the McKendrick-von Foerster equation and the McKendrick-von Foerster equation with diffusion. It is also the first analysis of the effects of including the second order diffusion term in the McKendrick-von Foerster equation, and of the effects of demographic noise on the stable power-law steady state. The results shows that the first order approximation is unstable, whereas the second order approximation can be stable, and gives a much better approximation to the jump-growth equation. The steady state is shown to be more likely to be stable

when the preferred predator:prey mass ratio is reduced and the diet breadth and the feeding efficiency are increased.

For readers interested in the mathematical derivation of the perturbation equations and eigenvalue spectra, Section 2.2 shows the necessary steps taken. However, for those more interested in the results of the stability analyses, Section 2.3 shows the behaviour of the three models, and reading Section 2.2.1 should provide sufficient background reading to understand the different models used.

2.2 Analysis of the power-law steady state

2.2.1 Three models of predation

The analysis focuses on perturbations around the power-law steady state of three equations: the jump-growth equation (2.1), the McKendrick-von Foerster equation (1.14) and the McKendrick-von Foerster equation with diffusion (2.3). These equations describe the rate of change in the density of organisms of weight w, which we call $\phi(w)$, with dimensions $\mathrm{M}^{-1}\mathrm{L}^{-3}$, where M is the mass dimension and L is the length dimension. This density is with respect to both mass and volume, so the number of organisms in a volume V with weight between w and $w + dw$ is $V\phi(w)dw$. The first equation is based on the jump-growth equation of Datta et al. (2010a),

$$\begin{aligned}\frac{\partial\phi(w)}{\partial t} &= \int \big(-T(w,w')\phi(w)\phi(w') - T(w',w)\phi(w')\phi(w) \\ &\qquad +T(w-Kw',w')\phi(w-Kw')\phi(w')\big)\ dw' - \mu\phi(w). \end{aligned} \tag{2.1}$$

$T(w,w')$ is proportional to the feeding rate of individuals of weight w on individuals of weight w', and $0 < K < 1$ is the conversion efficiency of biomass from prey to predator (Law et al., 2009). There are three ways in which a feeding event can result in a change in the density of individuals at a given weight w, corresponding to the three terms in the integrand. The first term represents the loss of individuals of weight w due to growth to a larger size (predation of w upon w'), the second term the loss of individuals of weight w due to death (predation of w' upon w), and the third term the gain of individuals of weight w due to growth from from a smaller size (predation of $w - Kw'$ on w'). Here we have also included a linear natural death rate μ (with the dimension of inverse time) to allow for other sources of mortality.

A Taylor expansion of the third term in the jump-growth equation in powers of K gives an infinite series of approximations to the full jump-growth equation (Datta et al., 2010a). Expanding up to and including terms linear in K gives our second

model, the McKendrick-von Foerster equation,

$$\begin{aligned}\frac{\partial \phi(w)}{\partial t} &= -\int T(w', w)\phi(w)\phi(w')\, dw' \\ &\quad -\frac{\partial}{\partial w}\int Kw'\, T(w, w')\phi(w)\phi(w')\, dw' - \mu\phi(w)\end{aligned} \tag{2.2}$$

and including terms quadratic in K gives our third model,

$$\begin{aligned}\frac{\partial \phi(w)}{\partial t} &= -\int T(w', w)\phi(w)\phi(w')\, dw' \\ &\quad -\frac{\partial}{\partial w}\int Kw'\, T(w, w')\phi(w)\phi(w')\, dw' \\ &\quad +\frac{1}{2}\frac{\partial^2}{\partial w^2}\int (Kw')^2\, T(w, w')\phi(w)\phi(w')\, dw' - \mu\phi(w),\end{aligned} \tag{2.3}$$

which we will refer to as the McKendrick-von Foerster equation with diffusion. Note that, as in equation (2.1), a linear death rate μ has been included in these two approximations.

We assume a feeding kernel of the form

$$T(w, w') = Aw^{\alpha} s\left(\frac{w}{w'}\right) \tag{2.4}$$

where A is the predator search volume per unit mass$^{-\alpha}$ per unit time, α is the predator search exponent, calculated to have a value of approximately 0.8 (see Ware, 1978), and $s(w/w')$ is the feeding preference function, centred around some preferred predator:prey mass ratio B. To make analytical progress in this paper we assume that $\alpha = \gamma - 1$, where γ is the exponent of the power-law steady state (≈ 2). This assumption then has the consequence that the steady state is a power-law (see below). In addition, the eigenvalue spectrum can then be written as a closed form expression and its properties analysed. Although probably not realistic from a biological point of view (discussed in Section 2.4), the assumption places stability analyses of size spectra on a firm mathematical foundation and provides a basis from which exploration of a broader class of systems can begin.

Section 2.2.2 defines the power-law steady state for the jump-growth equation (2.1) and its two approximations (2.2) and (2.3). Section 2.2.3 develops equations for the dynamics of small perturbations to this steady state and Section 2.2.4 gives explicit equations for the eigenvalue spectra. In Section 2.2.5, the effect of demographic noise on the system at steady state is investigated. Finally, Section 2.2.6 incorporates a Gaussian feeding preference for predators.

2.2.2 The power law steady state

The steady state for equations (2.1), (2.2) and (2.3) is given by

$$\hat{\phi}(w) = \phi_0 w^{-\gamma} \tag{2.5}$$

where ϕ_0 is a constant. Below, it helps to transform the variable w to a dimensionless log weight variable $x = \ln(w/w_0)$ (for some arbitrary weight w_0). For analysing the steady state of the jump-growth equation (2.1) it is convenient to change the integration variable of each of the three terms to the predator:prey mass ratio, which leads to the transformed equation

$$\begin{aligned}\frac{\partial v(x)}{\partial t} &= \hat{A}\int s(e^r)\Big(-e^{\alpha r}v(x)v(x-r) - v(x)v(x+r) \\ &\qquad + e^{\alpha(r+\psi(r))}v(x-\psi(r))v(x-r-\psi(r))\Big)\,dr - \mu v(x), \end{aligned}\tag{2.6}$$

where we have used equation (2.4) for the feeding kernel with $\alpha = \gamma - 1$. Here $v(x)$ has the property that $e^{-(\alpha+1)x}v(x)\,dx = \phi(w)\,dw$ and has dimensions L^{-3}, $\hat{A} = A{w_0}^{\alpha}$, and r is the log of the predator:prey mass ratio with $\psi(r) = \ln(1 + Ke^{-r})$. In the transformed jump-growth equation (2.6), the steady state is simply given by

$$v(x) = v_0, \tag{2.7}$$

where $v_0 = \phi_0 {w_0}^{-\alpha}$ is a constant. Substituting this into equation (2.6) we get the steady state condition,

$$\int s(e^r)\left(-e^{\alpha r} - 1 + e^{\alpha(r+\psi(r))}\right)\,dr - \eta = 0 \tag{2.8}$$

where $\eta = \mu/(\hat{A}v_0)$ is dimensionless. This equation implicitly determines the value of the search volume exponent α (and thus the steady state exponent γ) for a given choice of the parameters K and η and the feeding kernel $s(e^r)$. If we impose the conditions that predators can only feed upon prey smaller than themselves and $K \neq 0$, we can prove analytically that there always exists a unique value for α that solves the steady state condition. Without these conditions we verify its existence and uniqueness numerically. Setting η determines the abundance of fish at the steady state, as it contains the constant v_0.

For the McKendrick-von Foerster equation with diffusion (2.3), the steady state condition is

$$\int s(e^r)\left(-1 + \alpha K e^{(\alpha-1)r} + \alpha(\alpha-1)\frac{K^2}{2}e^{(\alpha-2)r}\right)\,dr - \eta = 0, \tag{2.9}$$

and for the McKendrick-von Foerster equation without diffusion (1.14), terms of order

K^2 in equation (2.9) are ignored.

2.2.3 Perturbations around the steady state of the jump-growth equation

We now add a small perturbation to the steady state of the jump-growth equation and observe its evolution over time. If the perturbation grows over time, then the steady state is not stable, and the system will not stay at the equilibrium; if the perturbation decays, then the steady state is locally asymptotically stable. We call the perturbation $v_0\epsilon(x,t)$ and obtain its evolution equation by substituting

$$v(x,t) = v_0(1+\epsilon(x,t)) \tag{2.10}$$

into equation (2.6). We now assume that we can neglect terms of order ϵ^2 because ϵ is taken to be very small. For a finite-dimensional dynamical system this can be justified rigorously using the Hartman-Grobman theorem (see e.g. Kirchgraber and Palmer (1990)), however in an infinite-dimensional system this can be more subtle, see for example Aulbach and Garay (1993), and we proceed formally in analogy with the finite-dimensional case. We then use condition (2.8) to eliminate terms of order ϵ^0, so that only terms of ϵ^1 remain. This leads to the linearised perturbation equation

$$\begin{aligned}\frac{\partial\epsilon(x)}{\partial t} &= \hat{A}v_0\int s(e^r)\Big(-e^{\alpha r}(\epsilon(x)+\epsilon(x-r)) \\ &\qquad -(\epsilon(x)+\epsilon(x+r)) \\ &\qquad +e^{\alpha(r+\psi(r))}(\epsilon(x-\psi(r))+\epsilon(x-r-\psi(r)))\Big)\,dr-\mu\epsilon(x).\end{aligned} \tag{2.11}$$

We can change integration variables appropriately so that the right hand side of equation (2.11) is in the form of an integral operator acting on ϵ,

$$\frac{\partial\epsilon(x)}{\partial t} = \hat{A}v_0\int \epsilon(m)G(x,m)\,dm \tag{2.12}$$

where

$$\begin{aligned}G(x,m) &= -\delta(r)\left(\int s(e^z)(e^{\alpha z}+1)dz+\mu\right)-s(e^r)e^{\alpha r}-s(e^{-r}) \\ &\quad +s(e^{z_1})K^{-1}e^{(\alpha+1)(z_1+r)}+s(e^{z_2})e^{(\alpha+1)r-z_2}.\end{aligned} \tag{2.13}$$

Here $r = x-m$, $z_1 = \ln(K/(e^r-1))$, $z_2 = \ln(e^r-K)$ and δ represents the Dirac delta function. The integral kernel $G(x,m)$ can be thought of as an infinite-dimensional version of a matrix with indices x and m and the task of solving equation (2.12) thus reduces to finding the 'eigenvectors' and 'eigenvalues' of this 'matrix'. To define the operator rigorously in the infinite-dimensional case we must first restrict the pertur-

bations to the space of square-integrable periodic functions with some period L. On this space the operator is compact and thus it is meaningful to speak of its spectrum of eigenvalues. In the end we can then take the period L to infinity.

2.2.4 Eigenvalue spectra

We observe that the integral kernel $G(x, m)$ depends on $x - m$ only, i.e. it is a convolution kernel. Its 'eigenvectors' are given by plane waves, $\epsilon_k(x) = e^{ikx}$, for any $k \in \mathbb{R}$. We refer to k as the wavenumber of the plane wave $\epsilon_k(x)$ and denote the corresponding eigenvalue as $\lambda(k)$.

The eigenvalues are

$$\lambda(k) = \int s(e^r) \left(-e^{\alpha r} - e^{ikr} + e^{\alpha r + (\alpha - ik)\psi(r)}\right) \left(1 + e^{-ikr}\right) \, dr - \eta. \tag{2.14}$$

We refer to the values taken by $\lambda(k)$ as the eigenvalue spectrum.

A general perturbation can then be expanded in terms of these plane waves and its time evolution is

$$\epsilon(x, t) = \int C(k) e^{ikx + \hat{A} v_0 \lambda(k) t} \, dk. \tag{2.15}$$

The expansion coefficient function $C(k)$ is an even function because $\epsilon(x, t)$ is real. Notice that if any $\lambda(k)$ has a positive real part then perturbations grow exponentially with time (the factors $\hat{A}$ and v_0 are positive constants and thus do not affect the coefficient of t), which means that the steady state is unstable.

To derive the eigenvalue spectrum for the McKendrick-von Foerster equation with diffusion from equation (2.14), $\psi(r)$ is expanded in powers of K. Taking terms up to and including K^2 yields

$$\begin{aligned} \lambda(k) = \int s(e^r) \left(-e^{ikr} + K(\alpha - ik)e^{(\alpha-1)r} + \frac{K^2}{2}(\alpha - ik)(\alpha - 1 - ik)e^{(\alpha-2)r}\right) \times \\ \left(1 + e^{-ikr}\right) \, dr - \eta. \end{aligned} \tag{2.16}$$

As in equation (2.9), neglecting K^2 terms gives the corresponding eigenvalue spectrum for the McKendrick-von Foerster equation.

It is the real part of the eigenvalue that we are interested in, as it is the sign of this that determines whether the perturbations grow or die out over time. If, for some wavenumber k $\mathrm{Re}(\lambda(k))$ is positive, then any perturbation containing a component with this wavenumber will grow over time and thus the steady state will be unstable. If $\mathrm{Re}(\lambda(k))$ is negative for all k then all perturbations die out over time, and the steady state is stable.

2.2.5 Stochastic fluctuations

The analysis above is concerned with the deterministic jump-growth equation (2.1) and its low-order approximations (2.2) and (2.3). In fact, equation (2.1) is the mean-field equation for a stochastic model of pairwise encounters between predator and prey (Datta et al., 2010a). The magnitude of the fluctuations due to the demographic noise in the stochastic model is a factor of $\Omega^{\frac{1}{2}}$ smaller than the mean-field solution, where Ω is the number of individuals in the system (van Kampen, 1992). For marine ecosystems Ω tends to be very large, so the fluctuations will be relatively small, but they can nonetheless have important effects (McKane and Newman, 2005), and may significantly impact the patterns observed in empirical data.

In this section we describe how the magnitude of the stochastic fluctuations, and the correlations between the fluctuations at different body sizes, can be predicted in the case where the steady state of the mean-field system is stable. In order to make the following statements rigorous, one would work in terms of discrete body size intervals, but we work in the continuum formally for convenience, which gives the same results. We let $n(x,t)$ be a random variable corresponding to the density of individuals of size $w = w_0 e^x$ at time t. The random variable is described by the stochastic process given in previous work (Datta et al., 2010a). Following the method used by van Kampen (1992), we separate $n(x,t)$ into a deterministic component $v(x,t)$, which satisfies the mean-field equations studied above, and a random fluctuation component $\xi(x,t)$:

$$n(x,t) = Ve^{-\alpha x}\left(v(x,t) + \Omega^{-\frac{1}{2}} v_0 \xi(x,t)\right). \tag{2.17}$$

Assuming that the deterministic component is at steady-state, the stochastic fluctuations $\xi(x,t)$ can be described by a Langevin-type equation (for details of the derivation of this equation from the individual-based model see Datta et al., 2010a)

$$\frac{\partial}{\partial t}\xi(x,t) = \hat{A} v_0 \left(\int G(x,y)\xi(y,t)dy + \rho(x,t)\right), \tag{2.18}$$

where the kernel G is given by equation (2.13) and $\rho(x,t)$ is a null-mean noise process. The covariance of noise at two different body sizes is described by a covariance kernel $B(x,y) = \langle \rho(x,t)\rho(y,t)\rangle$, which is given by (see Datta et al., 2010a):

$$\begin{aligned} B(x,y) = e^{\alpha(x+y)} \int \Bigg(& f(x,y,z) - f(x,z,y) - f(z,y,x) \\ & + \delta(x-y) \int \left(f(x,z,z') + \frac{f(z,z',x)}{2} \right) dz' \Bigg) dz, \end{aligned} \tag{2.19}$$

where

$$f(x,y,z) = e^{-\alpha(x+y)} \left(k(x,y,z) + k(y,x,z)\right) \tag{2.20}$$

and

$$k(x,y,z) = e^{\alpha x} s\left(e^{x-y}\right) \delta(z - x - \psi(x-y)). \tag{2.21}$$

The covariance $\langle \xi(x,t)\xi(y,t)\rangle$ of the fluctuations at logarithmic body sizes x and y satisfies

$$\frac{\partial}{\partial t}\langle \xi(x,t)\xi(y,t)\rangle = \hat{A} v_0 \left(\int \left(G(x,z)\langle \xi(z,t)\xi(y,t)\rangle + G(y,z)\langle \xi(z,t)\xi(x,t)\rangle\right) dz + B(x,y) \right). \tag{2.22}$$

In the steady state, the time derivative on the left-hand side vanishes and thus the correlation function $\langle \xi(x,t)\xi(y,t)\rangle$ can be calculated by setting the right-hand side to zero which results in a linear equation to be solved. We present the numeric results in section 2.3.7.

The quantity $\langle \xi(x,t)\xi(y,t)\rangle$ measures the correlation in the stochastic fluctuations at two different body sizes at the same time. Fluctuations may also be correlated across different times, but an investigation of this is beyond the scope of this paper. Although resonance between the natural frequency of the system and the white noise inherent in the stochastic model could cause these correlations to be significant (McKane and Newman, 2005), this phenomenon was not observed in previous simulations of the individual-based model, even with a relatively small system size Ω (Law et al., 2009).

2.2.6 Gaussian feeding preference

Organisms do not eat indiscriminately; here we assume that they feed at some preferred prey size (in relation to their own size), and a range of sizes around this preferred size. To reflect this, a suitable preference function is a Gaussian feeding preference, with peak at β and width proportional to σ (Andersen and Beyer, 2006; Law et al., 2009). This can be represented by the following form for $s(e^r)$,

$$s(e^r) = \frac{1}{\sqrt{2\pi}\sigma} \cdot e^{\frac{-(r-\beta)^2}{2\sigma^2}}. \tag{2.23}$$

In theory this function allows predators to eat prey larger than themselves (i.e. is non-zero for $r < 0$), although for realistic sets of parameter values $s(e^r)$ is typically negligible for $r < 0$.

The eigenvalue spectrum for the jump-growth equation (2.14) with the Gaussian preference function (2.23) unfortunately does not have a closed form. In contrast, the eigenvalue spectra for the McKendrick-von Foerster equation without and with diffusion can be determined analytically. Defining

$$R_n = (\alpha - n)\left(\beta + \frac{1}{2}\sigma^2(\alpha - n)\right) \tag{2.24}$$

$$I_n = k\left(\beta + \sigma^2(\alpha - n)\right), \tag{2.25}$$

and taking the steady state condition (2.9) into account, the eigenvalue spectrum for the equation with diffusion is

$$\begin{aligned}\mathrm{Re}(\lambda(k)) =& e^{-\frac{1}{2}\sigma^2 k^2}\Bigg[-\cos(k\beta) + Ke^{R_1}\left(\alpha\cos(I_1) - k\sin(I_1)\right) \\ &+ \frac{K^2}{2}e^{R_2}\left((\alpha(\alpha-1)-k^2)\cos(I_2) - k(2\alpha-1)\sin(I_2)\right)\Bigg] \\ &- \frac{K^2}{2}e^{R_2}k^2.\end{aligned} \tag{2.26}$$

The diffusion term is removed by excluding terms of order K^2 in equation (2.26). An important difference between the two approximations is that there must always exist values of k for which $\mathrm{Re}(\lambda(k))$ is positive in the eigenvalue function for the McKendrick-von Foerster equation. Consequentially the McKendrick-von Foerster equation will never give a stable spectrum. In contrast, the McKendrick-von Foerster equation with diffusion contains a non-oscillatory term in k which is negative and increases in magnitude as k increases. This has the effect of making the real parts of the eigenvalues more negative for higher values of k. For both approximations the oscillatory terms are damped exponentially by a $e^{-\frac{1}{2}\sigma^2 k^2}$ term. Equation (2.26) is analysed in greater detail in Section 2.3 to explain observed patterns in the behaviour of eigenvalue spectra when altering parameters.

Using the steady state condition (2.8), it can be shown for the jump-growth equation that $\mathrm{Re}(\lambda(0)) = \eta$. This result also applies to both of the approximations. Thus, for any positive η, $\mathrm{Re}(\lambda(k))$ must be positive at $k = 0$, and as $\lambda(k)$ given in equation (2.14) is continuous, there exists a neighbourhood around $k = 0$ where $\mathrm{Re}(\lambda(k)) > 0$. Therefore there will be a range of wavenumbers k for which perturbations e^{ikx} will destabilise the steady state. However, we only expect our model to be realistic for a range of body weights spanning around 12 orders of magnitude (Cohen et al., 2003) and therefore should ignore perturbations with a wavelength longer than this, i.e. those with wavenumbers smaller than about $k \approx 0.2$.

2.3 Results

2.3.1 Eigenvalue spectra of the three models

To evaluate the eigenvalue spectra, we use the Gaussian feeding preference (2.23), for given values for the parameters K, β, σ, η. Where possible we keep these parameters biologically reasonable and close to values from previous studies (Andersen and Beyer, 2006). We use values of $K = 0.2$, $\beta = 5$ and $\sigma = 1.5$ as a base parameter set, and investigate the effects of changing these parameters. For this base parameter set, the

steady state exponent γ is equal to 2.27 when $\eta = 0$ (i.e. no external mortality) and the value of γ increases with η. The values of γ used in the numerical plots mostly lie in the empirical range of 2.2 to 3.25 reported by Blanchard et al. (2009). Values of the wavenumber k are taken over a range from 0 to 30, as the interesting behaviour of the eigenvalue spectra is seen in this frequency range. Note that the expressions for $\mathrm{Re}(\lambda(k))$ are even in k for the three models, so the plotting of negative values of k is unnecessary. We often plot the eigenvalue spectra over a logarithmic k-axis to make it easier to see the details at small k.

Examples of the eigenvalue spectra of the jump-growth equation and its two approximations (all computed numerically using the preference function (2.23)) are compared in Figure 2.1.

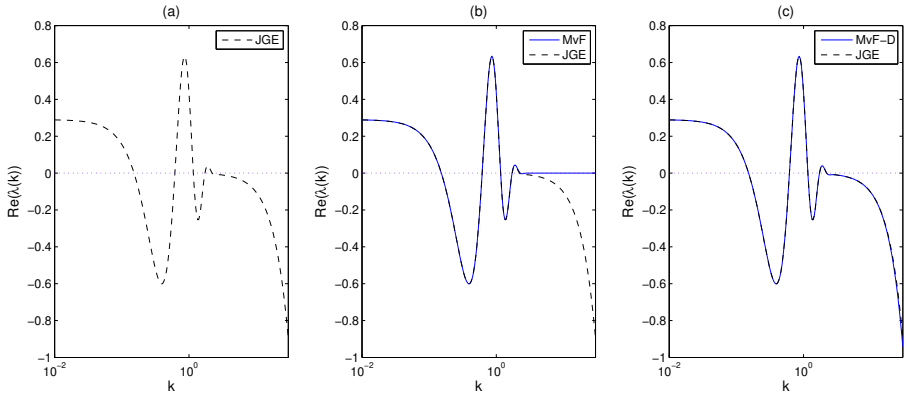

Figure 2.1: The eigenvalue spectra for the (a) jump-growth equation (JGE), (b) McKendrick-von Foerster equation (MvF) and (c) McKendrick-von Foerster equation with diffusion (MvF-D) when using a Gaussian feeding preference. Note that η has been set to give a steady state exponent of roughly 2.3 for all three spectra. Parameter values $K = 0.2$, $\beta = 5$, $\sigma = 1.5$, $\eta = 0.290$, $\gamma = 2.30$.

All three spectra are close to η for small k, as expected from Section 2.2.6. Both approximations are close to the jump-growth equation for low values of k, but as k gets larger only the McKendrick-von Foerster equation with diffusion follows the jump-growth equation closely. This is expected from equation (2.26) because the diffusion term is needed to make the eigenvalue spectrum more negative with increasing k. Adding the diffusion term gives a better approximation to the full jump-growth model. Thus the properties of equation (2.26) will be used to gain insight into the behaviour of the eigenvalue spectra of the jump-growth equation in the subsequent sections.

The power-law steady state is unstable for all three models in this example, because all three spectra contain eigenvalues with a positive real part (the maximum occurring at $k \approx 0.861$). The tendency for unstable steady states to emerge in our analysis will be discussed in Section 2.4.

The different behaviours of the two approximations are not just limited to a Gaussian

feeding preference; similar results have also been obtained when using a step function for the feeding preference. This has the form

$$s(e^r) = \begin{cases} \frac{1}{2\sigma} & \text{if } \beta - \sigma \leq r \leq \beta + \sigma \\ 0 & \text{otherwise} \end{cases} \tag{2.27}$$

and is a rectangular kernel, with midpoint β, width 2σ and height $1/(2\sigma)$. It is worth noting that although behaviour similar to Figure 2.1 is observed, the oscillations are not damped exponentially, and oscillations are observed at all values of k.

2.3.2 Stable and unstable steady states

For some sets of parameter values, the steady state is stable. Figure 2.2 gives an example, obtained by allowing a low preferred predator:prey mass ratio β, a high efficiency K and a relatively large diet breadth σ.

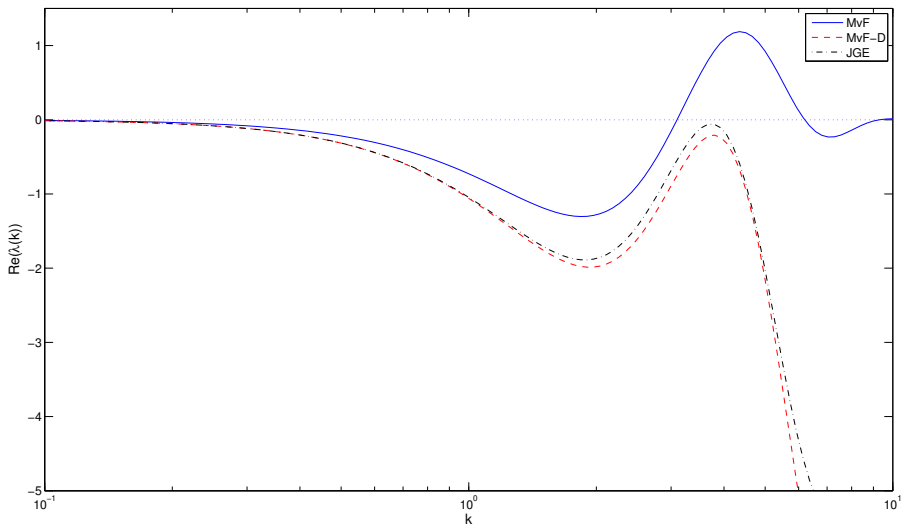

Figure 2.2: Eigenvalue spectra for the McKendrick-von Foerster equation and McKendrick-von Foerster equation with diffusion, compared to that of the jump-growth equation. Parameter values $K = 0.8$, $\beta = 1$, $\sigma = 0.35$, $\eta = 0$, $\gamma = 2.11$.

This example is chosen to illustrate the point that the eigenvalue spectrum for the McKendrick-von Foerster equation can be misleading; the spectrum for the McKendrick-von Foerster equation without diffusion peaks at 1.19, whereas for the equation with diffusion and the jump-growth equation $\mathrm{Re}(\lambda(k)) < 0$ for all k. The spectrum is stabilised by the non-oscillatory term introduced by the inclusion of terms of order K^2. The diffusion term contributes to stability and the effect of this is great enough to make a qualitative difference to the calculated stability of the steady state. As predicted in Section 2.2.6, the McKendrick-von Foerster equation gives an unstable spectrum for

any choice of parameter values.

2.3.3 Time evolution of perturbations

To show the consequences of stable and unstable steady states on the dynamics, we can examine the behaviour of a local perturbation to the size spectrum, and observe its time evolution. Assume a Gaussian perturbation with initial form

$$\epsilon(x,0) = \nu e^{-\frac{x^2}{2\varsigma^2}}, \tag{2.28}$$

where ν is a small constant and ς dictates what range of body sizes in the size spectrum are effected by the initial perturbation. This can be expanded in plane waves, rewriting $\epsilon(x,0)$ as

$$\epsilon(x,0) = \bar{\nu} \int_{-\infty}^{\infty} e^{-\frac{1}{2}\varsigma^2 k^2} e^{ikx}\, dk. \tag{2.29}$$

where $\bar{\nu} = (\nu\varsigma)/\sqrt{2\pi}$. The time dependence of this perturbation then has the following form:

$$\epsilon(x,t) = \bar{\nu} \int_{-\infty}^{\infty} e^{-\frac{1}{2}\varsigma^2 k^2} e^{ikx + \hat{A}v_0\lambda(k)t}\, dk. \tag{2.30}$$

We set ς so that the perturbation covers about one size unit on the x-scale, and choose units so that $\hat{A}v_0 = 1$. We choose to centre our perturbation around $x = 0$ without loss of generality. Plotting the time evolution both for a stable spectrum (Figure 2.2) and an unstable spectrum (Figure 2.1) using the jump-growth equation gives the two behaviours shown in Figure 2.3.

For both plots, the initial perturbation moves along the x-axis over time, as the organisms it contains feed on smaller organisms and grow. In the case of a stable spectrum, the perturbation gives rise to smaller peaks either side of the initial perturbation, and these all die out over time, tending to zero across the whole range of x. In the case of an unstable spectrum, the peaks grow over time. They develop into waves with wavenumber $\hat{k}$, where $\hat{k}$ is the most unstable node of the eigenvalue spectrum. Thus, in the case of Figure 2.3b, where $\hat{k} = 0.861$, the wavelength of the peaks is seen to be around $(2\pi)/\hat{k}$. Over time the peaks grow in magnitude but maintain their wavelength. The speed at which the perturbation moves through the size spectrum is determined by $\mathrm{Im}(\lambda(\hat{k}))$.

2.3.4 Changing the preferred predator:prey mass ratio

Figure 2.4 shows the effect of increasing the logarithm of the preferred predator:prey mass ratio β on the stability of the jump-growth equation.

The maximum real part of the eigenvalues increases as β increases, the steady state

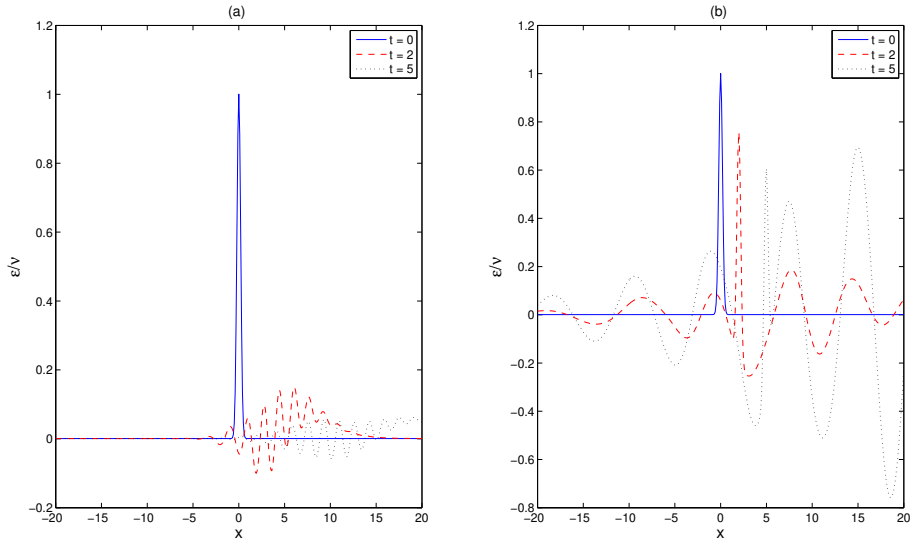

Figure 2.3: The time evolution of a Gaussian perturbation, $\varsigma = 0.2$, when using (a) a stable eigenvalue spectrum (parameter values $K = 0.8$, $\beta = 1$, $\sigma = 0.35$, $\eta = 0$, $\gamma = 2.11$), and (b) an unstable eigenvalue spectrum (parameter values $K = 0.2$, $\beta = 5$, $\sigma = 1.5$, $\eta = 0.290$, $\gamma = 2.30$).

going from stability when $\beta = 1$ (i.e. $\mathrm{Re}(\lambda(k)) < 0$ for all k), to instability for the larger values of β. This is in keeping with previous numerical results, where increasing β led to a bifurcation from the power-law steady state to a travelling wave attractor (Law et al., 2009), although the two results should not be directly compared because in earlier work the assumption $\alpha = \gamma - 1$ was not imposed. The changes seen in Figure 2.4 as β is increased can be understood in terms of equation (2.26), where β occurs both in the R_n exponential terms and in the I_n cosine and sine terms. In R_n, β acts to dampen the waves more as it increases, and in I_n, β acts to reduce the period of the waves as it increases. Both these changes are visible in the figure. Some decrease in the exponent of the power-law steady state is also evident with increasing β in Figure 2.4. We interpret this in biological terms as an outcome of less biomass being lost from the size spectrum as β increases, because biomass is inefficiently consumed fewer times during its passage along the spectrum. Note that σ has been held constant this figure, so that as β is increased, the mean of the predator : prey feeding distribution increases but the variance remains constant.

2.3.5 Changing the feeding efficiency

Figure 2.5 shows the effect of changing the feeding efficiency K on the eigenvalue spectrum.

To understand Figure 2.5, it helps to consider the limiting case of $K \to 0$. Although unrealistic, because it implies no growth of organisms, the eigenvalue spectrum in

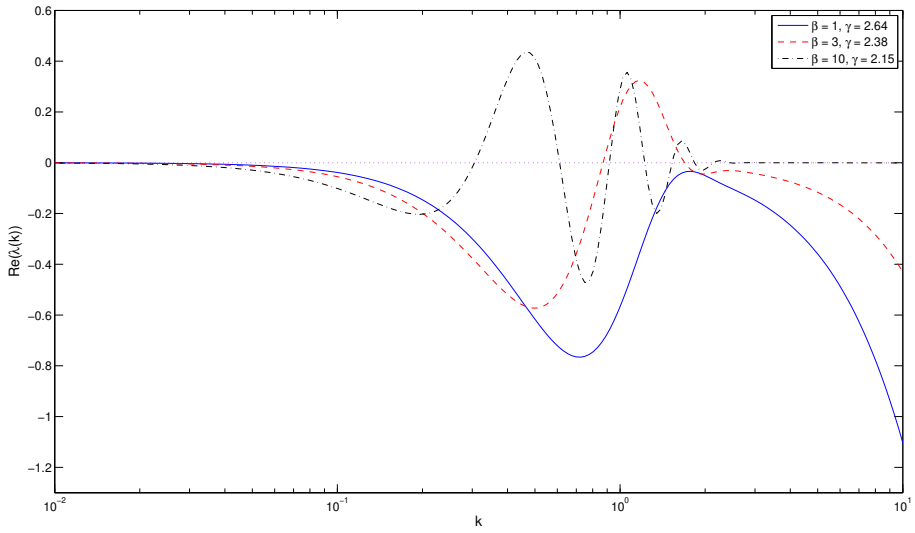

Figure 2.4: The eigenvalue equations for the jump-growth equation with varying logarithm of the preferred predator:prey mass ratio β. Parameter values $\sigma = 1.5$, $K = 0.2$, $\eta = 0$.

equation (2.26) is then simply a damped cosine wave: $\mathrm{Re}(\lambda(k)) = e^{-\frac{1}{2}\sigma^2 k^2}\cos(k\beta)$. Consequently, the most unstable node $\hat{k}$ must be the first peak of this wave, which occurs at $\hat{k} = \pi/\beta$, equivalent to $\hat{k} = 0.628$ with the parameter values in Figure 2.5. We observe in Figure 2.5 that, for small K (1×10^{-5}), the value of $\hat{k}$ (0.655) is close to this limiting value.

Corresponding to the node at $\hat{k} = \pi/\beta$, there is a dominant eigenfunction with a wavelength 2β. This can be understood in biological terms as a straightforward consequence of the predator-prey interaction. A pulse perturbation from steady state that increases the density of predators at some size lowers the density of prey e^{β} times smaller than themselves. This in turn reduces the mortality rate on the prey's prey $e^{2\beta}$ times smaller than the predators, allowing their density to increase. This leads to the wavelength 2β.

Figure 2.5 also shows that, as K increases, $\hat{k}$ grows and $\mathrm{Re}(\lambda(\hat{k}))$ gets smaller. In other words, perturbations from the steady state grow more slowly and have wavelengths less than 2β as K increases. In this case, a pulse increase in predator density at some body size does not remain at the same position in the size spectrum as time goes on. The predators grow as they eat, and their preferred prey body size moves along with them. This mitigates to some extent the destabilizing feedback of slow (or absent) predator growth that would continue to reduce the density of prey approximately e^{β} times smaller than the predator. These results help explain the observation of Law et al. (2009) that perturbations tend to have a wavelength less than 2β. Notice also that the exponent of the power-law steady state becomes substantially smaller as K increases, because more biomass passes along the size spectrum to large organisms.

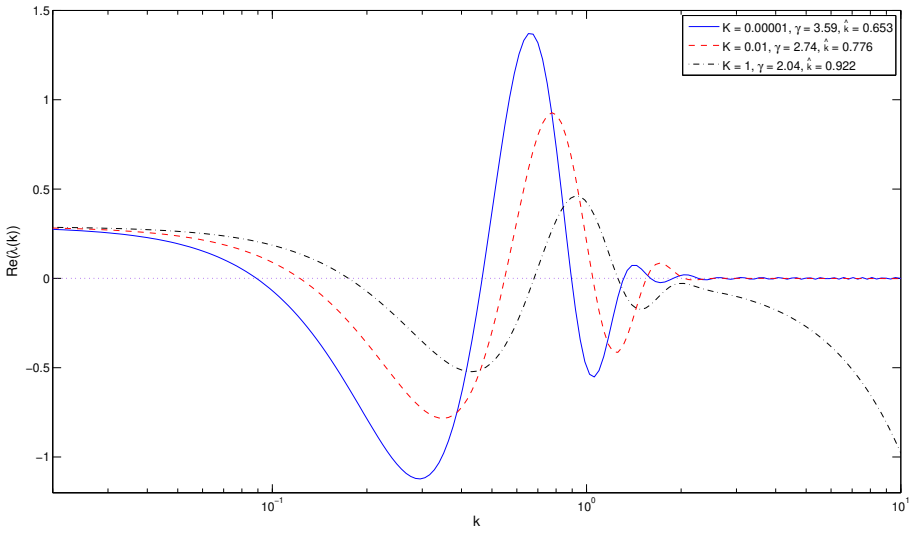

Figure 2.5: The eigenvalue equations for the jump-growth equation, with varying feeding efficiency K; $\hat{k}$ denotes the location of the most unstable node of the spectrum. Parameter values $\beta = 5$, $\sigma = 1.5, \eta = 0.290$.

2.3.6 Changing diet breadth

It has been shown in earlier numerical studies that, by making the diet breadth more narrow (i.e. decreasing σ), the power-law steady state can become unstable, leading to travelling waves of abundance that move along the spectrum with time (Law et al., 2009; Datta et al., 2010a). In the extreme case of a feeding kernel where predators only eat prey of the exact preferred mass ratio, and of no other weight (using a Dirac delta function of the form $s(e^r) = \delta(r - \beta)$ as the feeding preference), the steady state can be shown always to be unstable (proof not given here).

In Figure 2.6 we investigate the effect of increasing the diet breath σ.

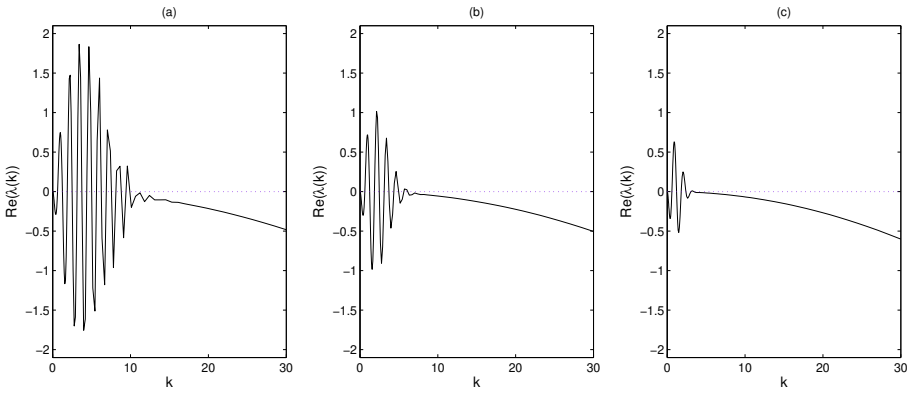

Figure 2.6: The eigenvalue spectra for the jump-growth equation with varying diet breadth: (a) $\sigma = 0.25$ (k^* = 9.60), (b) $\sigma = 0.5$ (k^* = 6.02), and (c) $\sigma = 1$ (k^* = 3.41), where k^* denotes the largest value of k for which $\mathrm{Re}(\lambda(k)) > 0$. Parameter values $K = 0.2$, $\beta = 5$, $\eta = 0$, $\gamma = 2.27$.

As σ increases, the amplitude of oscillations at low values of k decreases, and the range for which $\mathrm{Re}(\lambda(k))$ has positive values becomes narrower; the largest value of k for which $\mathrm{Re}(\lambda(k)) > 0$ k^* is seen to decrease as σ increases. This is consistent with equation (2.26), because increasing σ will cause the oscillations to be damped sooner by the $e^{-\frac{1}{2}\sigma^2 k^2}$ term. Note that it is the change in σ which is causing the change in the spectrum and not the steady state exponent; γ remains at a value of approximately 2.27 in each case.

2.3.7 The effects of demographic noise

As explained in Section 2.2.5, we can calculate the equal-time correlation function $\langle \xi(x,t)\xi(y,t)\rangle$ for the fluctuations in the steady state. This function describes how the fluctuations due to demographic stochasticity are correlated at different weights at steady state. It is obtained by solving the linear integral equation obtained by setting the time derivative to zero in equation (2.22). To perform the calculation we used discrete weight brackets, so that the integral equation becomes a matrix equation, which we solved numerically. Using the same parameter values as in Figure 2.2, the result is plotted in Figure 2.7. The graph has the feature of an exponential decay with increasing distance, typical of correlation functions. Superimposed on the decay is an oscillation with a wavelength of approximately 2β, generated by the non-local predator-prey interaction. The reason for the oscillation is that a positive fluctuation at $x = 0$ gives more food, faster growth and a negative fluctuation near β, which in turn gives less food, slower growth and a positive fluctuation near 2β. The wavelength is slightly greater than 2β because the mean distance in log-weight between a predator and its prey is slightly greater than β (i.e. $\beta + (\gamma - 1)\sigma^2$) since the prey are themselves distributed as $e^{-(\gamma-1)x}$.

2.4 Discussion

We have presented a local stability analysis of the power-law steady state of marine size spectra. The approach has some resemblance to the local stability analyses of steady-state food webs widely applied in ecology (Murray, 2002; Rooney et al., 2006). However, instead of having nodes representing a finite number of species, the analysis here uses a continuous weight range corresponding to an infinite number of "nodes", and this gives a continuous spectrum of eigenvalues. Characterization of the eigenvalue spectrum has been carried out before (Arino et al., 2004); the difference here is that we explicitly link growth of the organisms to predation, which we think is a useful step towards reality.

To do the analysis, the predator search exponent α and steady state exponent γ have

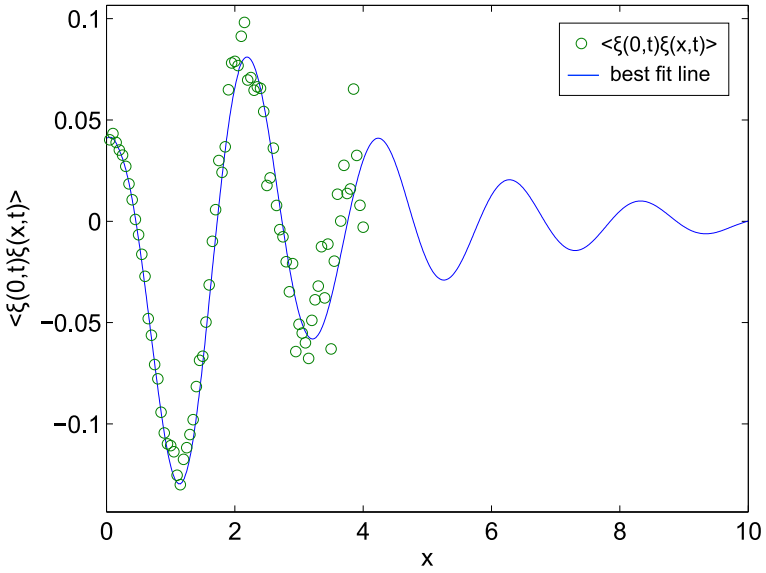

Figure 2.7: The correlation function $\langle \xi(0,t)\xi(x,t)\rangle$ for the fluctuations around a stable steady state due to demographic stochasticity. This measures the correlation between stochastic fluctuations at log body sizes 0 and x; the correlation between fluctuations at log body sizes x and y, $\langle \xi(x,t)\xi(y,t)\rangle$, is equal to $e^{\alpha x}\langle \xi(0,t)\xi(x-y,t)\rangle$. Parameter values $K = 0.8$, $\beta = 1$, $\sigma = 0.35$, $\eta = 0$, $\gamma = 2.11$.

been set so that $\alpha = \gamma - 1$. In addition, we assume that the rate for predation-independent death is independent of body weight. These assumptions imply that the dynamics of small perturbations are described by the convolution operator given in equation (2.12), leading to a simple time dependence of the perturbations in terms of an expansion in plane waves, given in equation (2.15). In general these assumptions would not be appropriate in ecological communities. The reason for using them here is that we believe it is valuable to have analytical results for this special case before beginning numerical explorations of conditions closer to those in nature.

The benchmark for the analysis is a jump-growth equation, obtained as the large-system limit of an underlying stochastic predation-growth process (Datta et al., 2010a). Importantly, the eigenvalue spectrum of the well-known, first-order approximation, the McKendrick-von Foerster equation (Andersen and Beyer, 2006; Law et al., 2009; Blanchard et al., 2009), exhibits a systematic departure from that of the jump-growth equation: the real parts of the eigenvalues of the former tend to zero as wavenumber increases, whereas those of the latter become increasingly negative. Therefore in our analysis the eigenvalue spectrum of the McKendrick-von Foerster equation must always contain eigenvalues with positive real parts, and must always have an unstable steady state.

In contrast to the first-order approximation, the eigenvalue spectrum of the second-order approximation, obtained by adding a diffusion term to the McKendrick-von Foerster equation, contains a negative term that is quadratic in the wavenumber, which

makes the real parts of the eigenvalues much closer to those of the jump-growth equation. The diffusion term is potentially important. One consequence of it is that there can be eigenvalue spectra for which $\mathrm{Re}(\lambda(k)) < 0$ for all wavenumbers $k > 0$, implying local stability of the steady state. This is with the caveat that the eigenvalue spectrum tends to the natural death rate η as the wavenumber tends to zero, so perturbations with sufficiently low wavenumbers (long wavelengths) could still destabilize the steady state.

The second-order approximation with diffusion has not previously been used, but would be worth considering in the future when the full jump-growth equation cannot be used. Interestingly, Benoît and Rochet (2004) found they had to include a diffusion term in numerical integrations of the McKendrick-von Foerster equation to obtain a solution in the absence of natural mortality, although they stated that they did not understand why this should be so. How serious the omission of the diffusion term is in practice depends on the wavenumber k at which the eigenvalue spectrum peaks, because it is this wavenumber that dominates the solution in the long term. If the peak occurs at sufficiently small k, the effect of the negative second-order term in equation (2.26) is small, and the standard McKendrick-von Foerster equation is reliable (Figure 2.1). If the peak occurs at large k, the negative second-order term in equation (2.26) becomes significant, and inferences about stability from McKendrick-von Foerster equation may not be reliable (Figure 2.2). The second-order equation with diffusion itself becomes a poor approximation if the feeding preference function is set such that predators are often smaller than their prey, because the Taylor expansion of the jump-growth equation on which it is based is no longer convergent (Datta et al., 2010a). However, in reality predators are almost always larger than prey, so this is not likely to be an issue.

Key parameters for locating the peak of the eigenvalue spectrum with respect to k are the logarithm of the preferred predator:prey mass ratio β, the efficiency of mass transfer from prey to predator K and the diet breadth σ. The results in Section 2.3.5 suggest that predator-prey interactions would typically restrict the wavenumber k at the peak to be greater than π/β. Overall, to get the peak of the eigenvalue spectrum at a low wavenumber where the McKendrick-von Foerster equation works best, $Ke^{-\beta}$ must be small, i.e. growth increments of predators must be small. As β is made smaller and K is made larger, the McKendrick-von Foerster approximation works less well, because it misses the stabilizing effect of the diffusion term. The diet breadth σ, also affects the shape of the eigenvalue spectrum, the main effect in equation (2.26) being to dampen the oscillations in the real parts of the eigenvalues (Figure 2.6). In so doing σ has the potential to shift positive peaks below $\mathrm{Re}(\lambda(k)) = 0$, and hence to change an unstable steady state into a stable one. This is consistent with the results of earlier studies which have shown the stabilizing effects of broad diets (Law et al., 2009; Datta et al., 2010a).

A feature of the stability analysis here is that the parameter values required to achieve stability are outside the range likely to apply in marine systems (e.g. $K = 0.8$ in Figure 2.2). As stated above, earlier numerical integrations using the McKendrick-von Foerster equation have led to stable steady states using realistic sets of parameter values. There are, however, some important differences between the present analysis and previous work. First, real size spectra span a finite range of body sizes, about twelve orders of magnitude being realistic (Cohen et al., 2003). This means that perturbations with very long wavelengths cannot occur, and corresponding to this, the wavenumber k cannot be less than about 0.2. Second, the finite range calls for lower and upper bounds which are not used here. Imposing such bounds removes the exact power-law steady state, and the boundary conditions themselves influence the stability of the steady state. Third, the constraint on parameter values needed to achieve $\alpha = \gamma - 1$ may exclude those values likely to lead to stability. The present study is best thought of as throwing light on the role that mortality, predation and growth play in determining stability of the power-law steady state. We expect other processes to also leave their own footprint, and some of these could increase the parameter space in which stable steady states arise (Capitan and Delius, 2010).

Nonetheless, at a qualitative level, the results here are consistent with earlier observations that the steady state of marine size spectra undergoes a bifurcation from stability to instability as predator:prey mass ratio is increased and as diet breadth is decreased. The results here indicate that this is a Hopf bifurcation as a complex conjugate pair of eigenvalues cross the imaginary axis. Even without taking other major life processes into account, the analysis makes clearer what kinds of ecosystems are more vulnerable to external disturbances such as those caused by fishing and climate change. Further research should expand upon this, to better understand marine ecosystem dynamics, and better predict the potential consequences of perturbing seemingly robust ecosystems.

Acknowledgements: The research was supported by a studentship to SD from the Natural Environment Research Council UK, with the Centre for Environment Fisheries and Aquaculture Science UK as the CASE partner. RL and MJP acknowledge support from the Royal Society of New Zealand Marsden fund, grant number 08-UOC-034. The research was facilitated by a Research Network Programme of the European Science Foundation on body size and ecosystem dynamics (SIZEMIC). We thank Julia Blanchard, Jennifer Burrow, Alex James, Jon Pitchford, Richard Rhodes, and David Wall for their help and insights.

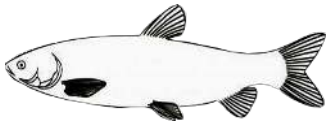

Chapter 3

The effects of seasonality on size spectra

Samik Datta

Department of Biology,
University of York,
York YO10 5DD, U.K.[1]

[1]email: sd550@york.ac.uk

Abstract

In this chapter the dynamics of size spectra are investigated under seasonal "bottom-up" forcing of the system by plankton blooms. A biomass spectrum model is first constructed using the McKendrick-von Foerster equation with diffusion to govern predation of smaller organisms by larger organisms. The lower portion of the spectrum is dominated by small primary producers and is subjected to time-dependent population growth, corresponding to springtime phytoplankton blooms which are widely observed in marine systems. The behaviour of the dynamic consumer spectrum is then investigated using numerical integrations. It is observed that for all the simulated blooms, the time-averaged size spectrum is always close to a power-law distribution, keeping with empirical observations. The match/mismatch hypothesis is studied in detail by monitoring the consequences of the timing of offspring emergence relative to the peak bloom on growth and survival. The growth rate of cohorts is found to be highest prior to the peak of the bloom, although survival is also lowest here. The most abundant cohort stays on the peak of the wave of abundance that passes through the consumer spectrum; thus similar results to an earlier non-dynamic model by Pope et al. (1994) are observed, although quantitative differences arise.

Keywords: marine ecosystem; seasonality; size-spectrum; McKendrick-von Foerster equation; growth diffusion; steady state; phytoplankton bloom

3.1 Introduction

The concept of the size spectrum, established in the pioneering work of Sheldon and Parsons (1967), has initiated a whole branch of research in marine ecology. For example, it has been shown that, in aquatic systems, ignoring taxonomy and looking only at organisms' weights, the abundance of organisms is a negative power-law distribution of the biomass (or equivalently size), and plotting log(abundance) against log(mass) gives a roughly linear fit with gradient -1 (Sheldon et al., 1972; Platt and Denman, 1978). This regular pattern appears to be robust, independent of the size scale which is investigated, and the linear relationship has been observed for phytoplankton spec-

tra (San Martin et al., 2006; Huete-Ortega et al., 2010), zooplankton spectra (Heath, 1995; Zhou et al., 2009) and for fish spectra (Boudreau and Dickie, 1992; Jennings and Mackinson, 2003).

Within this broad pattern there is important seasonal variation caused by changes in temperature, nutrient levels and turbulence. Such environmental factors can alter abundances of plankton and/or larger organisms, influencing the intercepts and slopes of size spectra over the year (Navarro and Thompson, 1995; Mari and Burd, 1998; Cózar and Echevarría, 2005). The single biggest seasonal driver of variation in size spectra is the phytoplankton bloom that occurs at some stage during the year (Barnes et al., 2011), usually in the spring, although smaller blooms can also occur in the autumn (see Truscott, 1995; Findlay et al., 2006). The bloom is characterized by an increase in the phytoplankton from 5 to 10 times its usual abundance (Gasol et al., 1992; Huete-Ortega et al., 2010), depending upon the latitude and surrounding environment, before returning to a fairly constant abundance for the rest of the year. This process can take place over several days or over the course of weeks, and is followed by an increase in abundance of zooplankton further along the size spectrum (Heath, 1995), which in turn provides a larger food source for fish larvae (Cushing and Horwood, 1994; Mertz and Myers, 1994).

Sampling size spectra with high enough temporal resolution to observe these seasonal patterns from plankton to fish is demanding due to the difficulty and cost of efficiently sampling different parts of the community (Jennings et al., 2002b). Nonetheless, variation within plankton spectra has been recorded over the course of a year (Heath, 1995; Huete-Ortega et al., 2010), and recent empirical work with regular sampling has shown intra-annual changes in both phyto- and zooplankton spectra (Zarauz et al., 2009; Zhou et al., 2010). Seasonal plankton models can achieve a qualitative match with the data, with the caveat that the predicted increase in zooplankton abundance can be much greater than that observed (Zhou et al., 2010).

The time of spawning of fish species relative to the timing of plankton blooms is of special interest for understanding the early-life survival of fish and the consequences for fisheries (Hjort, 1914). The match/mismatch hypothesis, a term coined by Cushing (1975), predicts that fish larval recruitment is linked to the timing between the reproductive period of mature fish and the peak of plankton abundance which are the main prey source of fish larvae. The closer that larvae are born to the plankton peak, the greater their food source, leading to a lower rate of starvation and faster growth rate, meaning less opportunity for predators to feed upon the larval population. The idea has been the subject of much study, and has some empirical support (Cushing, 1990; Mertz and Myers, 1994; Platt et al., 2003; Buckley and Durbin, 2006).

It is not just the availability of smaller prey that matters in a seasonal size spectrum. The organisms feeding on smaller prey also run the risk of being eaten themselves;

hence both ”bottom-up” and ”top-down” forces are at play (e.g. Frank et al., 2005). Pope et al. (1994) conjectured that as the biomass is transferred up the size spectrum through time, the wave of biomass becomes dampened at large sizes. Using a fixed von Mises probability distribution as a simple caricature for the seasonal size spectrum, they investigated the consequences of dropping individuals onto the surface to analyse their life history trajectories and simultaneously account for the growth and predation that would be inflicted from the backdrop of this fixed biomass size-time spectrum. They found that the success of cohorts depended upon high prey availability for fast growth and low predator abundance for reduced mortality; cohorts born earlier in the year had faster growth rates and higher amounts of biomass remaining over the course of a year. However, they did not explicitly model the predation process or the dynamics of the size spectrum.

This chapter builds on the approach of Pope et al. (1994) by considering the consequences of a seasonal wave of primary production when the dynamics and predation process of the consumer spectrum are included. There are two reasons for doing this. First, the von Mises shape of the pulse of abundance is affected by the nonlinear dynamics of size-based predation, and may change as the pulse moves through the size spectrum. Second, the speed at which the pulse moves along the size spectrum should depend on the growth rate of consumers, rather than being set externally. The shape of the consumer spectrum subject to a phytoplankton bloom over the course of a year are studied. Time-averaged distributions are found to be close to power-laws for a range of plankton blooms. The growth, survival and biomass of cohorts born at different times of the year are investigated in a method similar to Pope et al. (1994). As in that previous paper, there is a clear advantage to spawning prior to the time of a seasonal bloom, but the most successful cohorts stay at the peak of the wave of abundance that follows a plankton bloom.

3.2 Size spectrum dynamics with seasonal blooms

3.2.1 Size spectrum model

A community size-spectrum model with two parts is considered; a phytoplankton spectrum dominated by primary producers, and a predation-driven consumer spectrum (Figure 3.1). The consumer spectrum consists of pelagic fish species, but also includes zooplankton which feed in a size-based fashion. This is similar to previous models (e.g. Maury et al., 2007a; Law et al., 2009; Blanchard et al., 2009, Chapter 1). A seasonal pulse of abundance is added to the phytoplankton spectrum to simulate springtime blooms observed in empirical data (e.g. Navarro and Thompson, 1995; Irigoien et al., 2005). The consequences of the bloom on the shape of the consumer

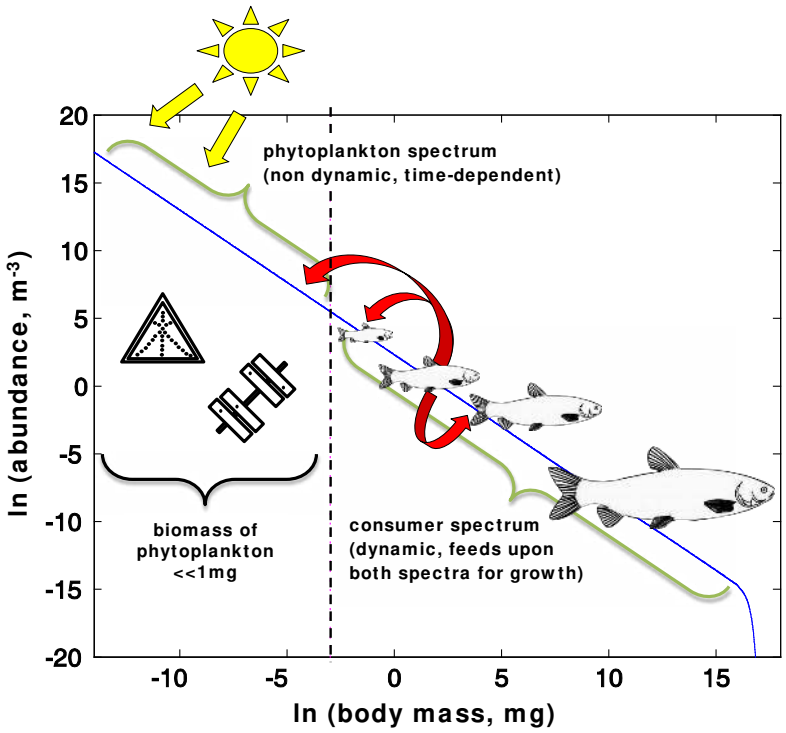

Figure 3.1: The size spectrum, plotting the log mass of organisms against the log abundance. The spectrum is split into a phytoplankton spectrum occupying the left-hand side of the size spectrum, and a consumer spectrum, where organisms are able to feed upon both spectra for growth. The spectra are separated by the dashed line. Image of grass carp (*Ctenopharyngodon idella*) used with permission of Vlado.

spectrum are investigated. The individual growth and survival rates of cohorts born at different times of year are examined, to establish the success of cohorts relative to the time of emergence.

Consumer spectrum

It has been shown in previous models that the predation process alone can produce a power-law steady state (Benoît and Rochet, 2004; Law et al., 2009). Here the McKendrick-von Foerster equation with diffusion is used because it emulates the stability properties of the more detailed jump-growth equation more closely than the widely used McKendrick-von Foerster equation without diffusion (Chapter 2), whilst being less numerically demanding than the full jump-growth equation. The McKendrick-von Foerster equation with diffusion has the form

$$\frac{\partial u(x)}{\partial t} = -\mu u - \frac{\partial}{\partial x}(gu) + \frac{1}{2}\frac{\partial}{\partial x}\left(e^{-x}\frac{\partial}{\partial x}(du)\right). \tag{3.1}$$

where μ, g and d are terms representing, in turn, death (either due to predation or other factors), growth due to predation, and diffusion in growth. The rates of these

processes are defined as

$$\mu = A{w_0}^{\alpha} \int_{x_0}^{x_\infty} s(e^{x'-x}) e^{\alpha x'} u(x') dx' + M(x), \tag{3.2}$$

$$g = A{w_0}^{\alpha} K e^{(\alpha-1)x} \int_{x_p}^{x_\infty} s(e^{x-x'}) e^{x'} \left(p(x') + u(x')\right) dx', \tag{3.3}$$

$$d = A{w_0}^{\alpha} K^2 e^{(\alpha-1)x} \int_{x_p}^{x_\infty} s(e^{x-x'}) e^{2x'} \left(p(x') + u(x')\right) dx'. \tag{3.4}$$

The phytoplankton spectrum is labelled as $p(x,t)$ and the consumer spectrum is labelled as $u(x,t)$. $p(x)$ and $u(x)$ are functions describing the density of individuals per unit volume at size x. For convenience, size is expressed as $x = \ln(w/w_0)$ where w is weight in milligrams and w_0 is a reference weight. dx' is the log weight range to be integrated over, which by convention is the whole real range $(-\infty, \infty)$, but needs to be restricted when performing numerical simulations (see Section 3.3). K describes the feeding efficiency with which prey biomass is converted to predator biomass (Chapter 1), which is assumed to be constant across the size spectrum. A mortality rate $M(x)$, which allows organisms to die due to non-predation factors is also included. The feeding of organisms is assumed to consist of two weight dependent terms. One scales with the weight of the predator (Aw^{α}), from evidence of allometric scaling between the volume covered by an organism per unit time and the weight of the organism (Ware, 1978). Here A is a constant defining the predator search volume per unit mass$^{-\alpha}$ per unit time and α is the scaling exponent. The other term $(s(x,y))$ is a function of the mass ratio of predator x and prey y, following the observation that the size of prey compared to its predator is an important factor in feeding (Cohen et al., 1993), and in aquatic systems more so than the prey species (Ursin, 1973; Andersen and Ursin, 1977; Boudreau and Dickie, 1992; Jennings and Mackinson, 2003). The lower bounds are x_p for the phytoplankton spectrum and x_0 for the consumer spectrum, and the upper bound for the consumer spectrum is x_∞.

Analytically a power-law steady state for the McKendrick-von Foerster equation with diffusion has been proven (Chapter 1), given by

$$\hat{u}(x) = u_0 e^{(1-\gamma)x} \tag{3.5}$$

where u_0 determines the scaling of the size spectrum, and $1-\gamma$ is the steady state exponent. This is with the caveats that the weight range is the real line $x \in (-\infty, \infty)$, and that all organisms feed in a size-based way.

Phytoplankton spectrum

The phytoplankton spectrum spans the range $x_p \leq x < x_0$. The processes driving the dynamics of phytoplankton and the acquisition of energy from nutrients and light are not explicitly modelled here (see Moloney and Field, 1991; Fuchs and Franks, 2010). Instead, it is assumed that organisms can be preyed upon by larger organisms, but are assumed to replace themselves quickly enough so as to make predation effects negligible (e.g. Maury et al., 2007a; Law et al., 2009; Blanchard et al., 2011). Models have tested the response of the size spectrum to bottom-up perturbations before, by increasing the height of the phytoplankton size classes uniformly for a short period of time (Maury et al., 2007b; Blanchard et al., 2011). Here a similar approach is taken. Following the approach of Pope et al. (1994) the seasonal size-time phytoplankton spectrum is characterized by the von Mises distribution, and the dynamics are therefore independent of the consumer spectrum. The phytoplankton bloom is thus modelled by the following time-dependent equation,

$$p(x,t) = u_0 e^{(1-\gamma)x}\left(1 + \frac{(D-1)e^{\zeta(\cos(2\pi(t-t_0)))}}{I_0(\zeta)}\right) \tag{3.6}$$

where $D \geq 1$ controls the ratio of the cumulative bloom abundance over the whole year and cumulative steady state abundance (i.e. $D = 1$ gives no bloom), ζ is an inverse measure of the duration of the bloom (as ζ increases the bloom becomes shorter and sharper) and t_0 corresponds to the point in time over the year where the bloom is at its peak (with $0 < t_0 < 1$, and time t measured in years). $I_0(\zeta)$ is a modified Bessel function of the first kind and order zero (Pope et al., 1994) and is a normalising factor such that, for fixed D, as ζ is altered, the integral of (3.6) over a year (the total number of phytoplankton) remains constant. For all parameter values, the mean phytoplankton spectrum over the course of a year is a power-law distribution.

Empirical data rarely show the cumulative phytoplankton abundance over a year; more often, samples are regularly taken throughout a time period giving the phytoplankton abundance at those points in time (Navarro and Thompson, 1995; Huete-Ortega et al., 2010). For this reason it can be simpler to specify D by using estimates for ζ and the ratio of abundance at the bloom peak and during the rest of the year (which is labelled R), and rearranging (3.6) to give

$$D = (R-1)I_0(\zeta)e^{-\zeta} + 1. \tag{3.7}$$

An example of the shape of the bloom is shown in Figure 3.2.

As well as the well-documented qualitative rise in abundance of phytoplankton during the bloom period, there is evidence to suggest that the majority of the increase takes place in larger size classes, i.e. the nanophytoplankton weight range of 20-

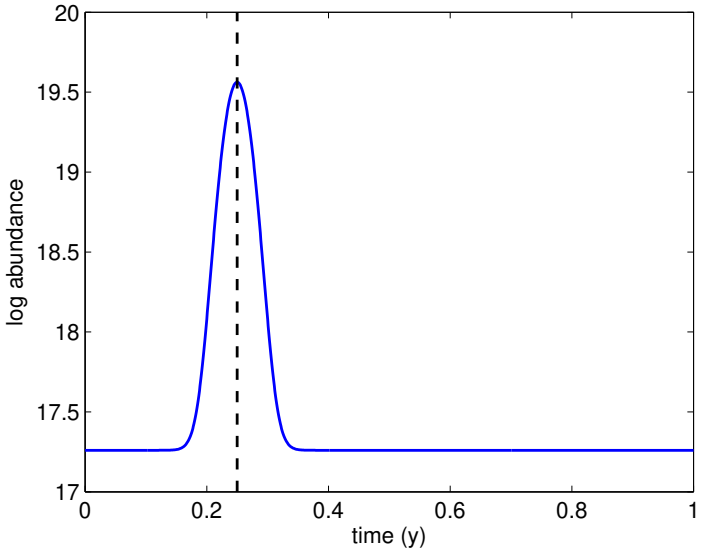

Figure 3.2: The abundance of phytoplankton over a year. The peak of the bloom is highlighted by the vertical dashed line.

200μm equivalent spherical diameter (Li and Logan, 1995; Mari and Burd, 1998). Thus two alternative forms of the bloom are considered, as well as (3.6). In the first instance, following size spectrum data showing that the slope of the phytoplankton spectrum becomes less negative during the course of a bloom (Echevarria and Rodriguez, 1994; Huete-Ortega et al., 2010), the gradient of the phytoplankton spectrum is altered during the bloom. Here the equation for the bloom is

$$p_1(x,t) = u_0 e^{(1-\gamma)x_p + \gamma^*(t)(x-x_p)} \tag{3.8}$$

where

$$\gamma^*(t) = \gamma + (\gamma_p - \gamma)e^{\zeta(\cos(2\pi(t-t_p))-1)} \tag{3.9}$$

with γ_p picked to give the specified bloom:steady state abundance of the largest phytoplankton. Hence $p_1(x_p,t)$ is fixed, and phytoplankton become relatively more abundant during the bloom for larger x.

In the second instance a change in the relative contributions of large:small phytoplankton is investigated by holding the lower part of the phytoplankton spectrum constant ($x_p \leq x \leq x_n$, where x_n represents the minimum weight of nanophytoplankton), and allowing only the upper part of the phytoplankton spectrum ($x_n < x \leq x_0$) to increase during the bloom. In this case the equation for the bloom is

$$\begin{aligned} p_2(x,t) &= u_0 e^{(1-\gamma)x} && \text{for } x_p \leq x < x_n \\ p_2(x,t) &= u_0 e^{(1-\gamma)x}\left(1 + \frac{(D-1)e^{\zeta(\cos(2\pi(t-t_0)))}}{I_0(\zeta)}\right) && \text{for } x_n \leq x < x_0 \end{aligned} \tag{3.10}$$

The effects of the three blooms (3.6), (3.8) and (3.10) on the consumer spectrum are compared using numerical simulations.

3.2.2 System parameters

Gaussian feeding preference function

Before the size spectrum model can be evaluated numerically, the feeding preference of organisms in the dynamic spectrum must be set. For this, a Gaussian feeding preference is incorporated following previous work (Ursin, 1973; Andersen and Ursin, 1977) which has the form

$$s(e^{x-y}) = \frac{1}{\sqrt{2\pi}\sigma} \cdot e^{\frac{-(x-y-\beta)^2}{2\sigma^2}} \tag{3.11}$$

where x is the predator log weight and y the prey log weight, β is the log of the preferred predator : prey mass ratio and σ controls the width of the Gaussian shape, and is a measure of diet breadth. The shape of the feeding preference function (3.11) is given in Figure 3.3.

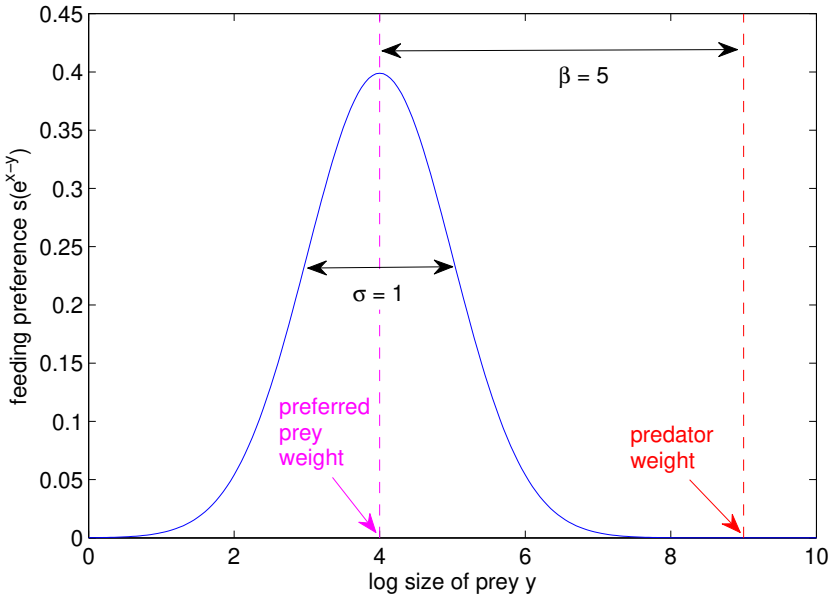

Figure 3.3: The shape of the Gaussian feeding preference function (3.11), with $x = 9$, $\beta = 5$ and $\sigma = 1$.

The kernel (3.11) is not truncated at $x = y$, so in theory organisms can feed on prey larger than themselves, but in the numerical simulations β and σ are set so the value of (3.11) becomes negligible as the prey weight approaches the predator weight.

Non-predation mortality

A weight-dependent non-predation mortality term is included, which affects all organisms in the dynamic spectrum. This is to account for other sources of mortality, such as starvation, fishing and natural causes. A second death rate is also included for extremely large organisms, to limit numbers at the right-hand end of the size spectrum. Thus a senescent mortality term increases exponentially by a factor θ from some starting weight x_f, following from previous work (Law et al., 2009, Chapter 1). Overall the non-predation death rate has the form

$$M(x) = \begin{cases} \eta e^{(\alpha-\gamma+1)x} & \text{if } x < x_f \\ \eta \left(e^{(\alpha-\gamma+1)x} + e^{\theta(x-x_f)} \right) & \text{if } x \geq x_f. \end{cases} \tag{3.12}$$

If η is set so that $\eta/(Au_0)$ is sufficiently small, then with reasonable parameter values (see Table 3.1 for details) γ is calculated to be approximately 2.05. Empirically observed size spectrum slopes have similar values (e.g. Huete-Ortega et al., 2010; Barnes et al., 2011), and thus non-predation mortality scales approximately with $e^{-0.25x}$ (where $\alpha = 0.8$, see Ware (1978)). This is in agreement with metabolic theory, which suggests that the metabolic rate for organisms scales with $w^{3/4}$, leading to a death rate scaled by $w^{-1/4}$ (Peters, 1986).

Boundary condition

Because of the different processes driving the behaviour of the two size spectra, organisms from the phytoplankton spectrum do not grow in mass to enter the consumer spectrum. Thus an assumption is required for the smallest individuals in the consumer spectrum, as there is no influx of biomass from smaller organisms. Previous simulations used a "renewal" spectrum as the boundary condition, with a fixed abundance but from which organisms could grow out of by predation (Law et al., 2009, Chapter 1). Unlike those models, the phytoplankton spectrum in this chapter has seasonally varying abundance, so such a fixed boundary could oversimplify the dynamics of real systems. The smallest organisms in the consumer spectrum considered here are zooplankton, and increased zooplankton abundance following a phytoplankton bloom have been observed (Heath, 1995; Zhou et al., 2009). Thus, to model the trend of zooplankton populations following a bloom, the abundance of the smallest organisms in the dynamic spectrum x_0 scales with the phytoplankton abundance, i.e.

$$u(x_0, t) = u_0 e^{(1-\gamma)x_0} \left(1 + \frac{(D-1)e^{\zeta(\cos(2\pi(t-t_0)))}}{I_0(\zeta)} \right). \tag{3.13}$$

Organisms can grow out from this weight along the consumer spectrum, although the abundance $u(x_0, t)$ is unaffected. The dynamics of zooplankton populations are more complex than the modelled population here; the work presented is a first step towards more realistic approaches (see Section 3.4 for further discussion).

3.2.3 Survival and growth rates at steady state

The non-predation mortality has the form (3.12) so that, in the absence of senescent mortality, an analytical power-law steady state can be derived (Chapter 1 Capitan and Delius, 2010). Using the Gaussian feeding preference (3.11), the death and growth rates are given respectively by

$$\mu = Ce^{-mx} \tag{3.14}$$

$$g = De^{-mx} \tag{3.15}$$

where the constants C, D and m are given by

$$\begin{aligned} C &= Aw_0{}^{\alpha} u_0 e^{m(\beta+\frac{1}{2}\sigma^2 m)} + \eta \\ D &= Aw_0{}^{\alpha} K u_0 e^{(\gamma-2)(\beta+\frac{1}{2}\sigma^2(\gamma-2))} \\ m &= \gamma - \alpha - 1. \end{aligned} \tag{3.16}$$

Generally $m > 0$ for realistic parameters, i.e. both death and growth in the power-law steady state decrease exponentially with log body weight.

For organisms whose majority diet is the phytoplankton spectrum (approximately the range $[x_0, x_0 + \beta - 2\sigma]$) the growth rate (3.15) will scale with the phytoplankton spectrum, although the result is no longer exact once individuals grow enough to feed upon the consumer spectrum.

3.2.4 Numerical simulations

The system of $p(x)$ and $u(x)$ is initialised at the analytical power-law steady state given by equation (3.1), with natural mortality (3.12) but without senescent death; γ is calculated from parameter values as specified in Table 3.1. The spectrum is discretised into weight "boxes" of width δx (ln weight is used for both axes throughout the simulations), and the initial distribution is set up with the abundance for weight x_i equating to $u(x_i) = u_o e^{(1-\gamma)x_i}$ (with $\delta x = x_i - x_{i-1}$). A Newton-Raphson iterative scheme is then used to calculate the numerical steady state using mortality term (3.12) including senescence, and this is taken as the initial distribution for the simulations.

To perform numerical integrations, the timescale is discretised into time steps of size δt, and a discretised form of equation (3.6) is used for the distribution of the phyto-

plankton spectrum $p(x,t)$. A semi-implicit Euler method (similar to that of Hartvig et al. (2011)) is implemented to calculate subsequent population distributions for the consumer spectrum $u(x)$ using the McKendrick-von Foerster equation with diffusion (3.1). For numerically calculating the integrals (3.2), (3.3) and (3.4) Simpson's rule is used. All parameter values are given in Table 3.1. To test reliability of the numerical results, an ODE solver in Matlab incorporating a fourth-order Runge-Kutta method is used to model the discretised system and confirm results.

At the community level, the dynamic behaviour of the consumer spectrum resulting from a phytoplankton bloom is investigated over the course of one year. This allows comparison with empirical observations observed across time in the consumer spectrum (Heath, 1995). Size-based feeding behaviour is used to explain the observed changes in abundance across the spectrum and across time. Phytoplankton blooms in nature vary in abundance, duration and shape, depending on location and time (Echevarria and Rodriguez, 1994; Mari and Burd, 1998; Huete-Ortega et al., 2010; Zhou et al., 2010). The effect of varying bloom amplitude and duration are studied, by altering R and ζ in (3.7) and (3.6) respectively. The shape of the bloom is also altered to model data which suggest large phytoplankton are primarily responsible for phytoplankton blooms (Li and Logan, 1995; Huete-Ortega et al., 2010) using both (3.8) and (3.10) (henceforth referred to as shallow and nanophytoplankton blooms respectively). These are compared to the usual bloom shape (3.6) where the whole spectrum keeps the same gradient throughout the year (henceforth referred to as a uniform bloom). Spectra are averaged over the year and plotted for comparison of the gradients with empirical time-averaged spectra (e.g. Jennings and Mackinson, 2003).

At the individual level, the growth and death rates calculated from (3.1) can be used to plot the weight and survival rate of organisms born at any point on the spectrum across time. At the steady state the growth and death rates are constant for any given weight, but in a seasonal environment there will be variation depending upon the timing of emergence in relation to the phytoplankton bloom. To calculate the growth and death rates the method of characteristics is used (Benoît and Rochet, 2004; Law et al., 2009). The focus in the model is on newborn fish larvae. The weight of a larva starting at weight x_e at time $t = 0$ can be calculated by solving

$$\frac{dx}{dt} = g(x(t)) \tag{3.17}$$

where $g(x,t)$ is taken from (3.3). To test whether the model growth rates for larvae are realistic, growth rates are calculated over the course of several years, and are compared with widely available weight-at-age data for common fish species (Fishbase, 2011), to validate the model parameters used. From a list of twelve of the most common species in the North Sea (comprising: cod, dab, grey gurnard, haddock, herring, Norway pout, plaice, saithe, sand eel, sole, sprat, and whiting) sole and cod are se-

lected because of their relatively low and high adult weights respectively, to give a realistic size range for individuals to grow to. At steady state growth is expected to correlate closely with (3.15); individual mass over time is explicitly derived as

$$x(t) = \frac{1}{m}\ln(mDt + 1). \tag{3.18}$$

Note this differs from the predicted trajectory for organisms which undergo von Bertalanffy type growth (von Bertalanffy, 1957), where the mass over time is derived to be

$$x(t) = x_\infty + b\ln\left(1 - e^{\kappa(t-t_0)}\right) \tag{3.19}$$

where x_∞ is the mean asymptotic log mass of the species, κ is a rate factor, t_0 is the theoretical age at length zero and b is the exponent of the length-weight relationship (generally centred around 3).

The survival rate of an individual over time $f(t)$ is found in a similar method to the growth rate (3.17), by solving

$$f(t) = e^{\int_0^t -\mu(x(\tau),\tau)\,d\tau} \tag{3.20}$$

with $\mu(x(t))$ taken from (3.2). At steady state survival over time is derived as

$$f(t) = (mDt + 1)^{-\frac{C}{mD}}. \tag{3.21}$$

At the cohort level, the match/mismatch hypothesis can be investigated. A combination of fast growth and low mortality has been predicted to maximise the biomass of fish larvae (e.g. Anderson, 1988; Horwood et al., 2000). In this model, "cohort" refers to the abundance of biomass of individuals remaining across time. All cohorts are started with equivalent biomass at the egg weight x_e, and the biomass is then calculated by multiplying the weight of the cohort across time with the corresponding survival rate. After a fixed amount of time has elapsed, the biomass of cohorts with different times of emergence can be compared to establish the most successful cohort by plotting the abundance remaining.

3.3 Results

3.3.1 The consequences of phytoplankton blooms on size spectrum dynamics

A phytoplankton bloom is added to the size-spectrum at steady state, and the resulting behaviour over the course of a year is shown in Figure 3.4. There is no vari-

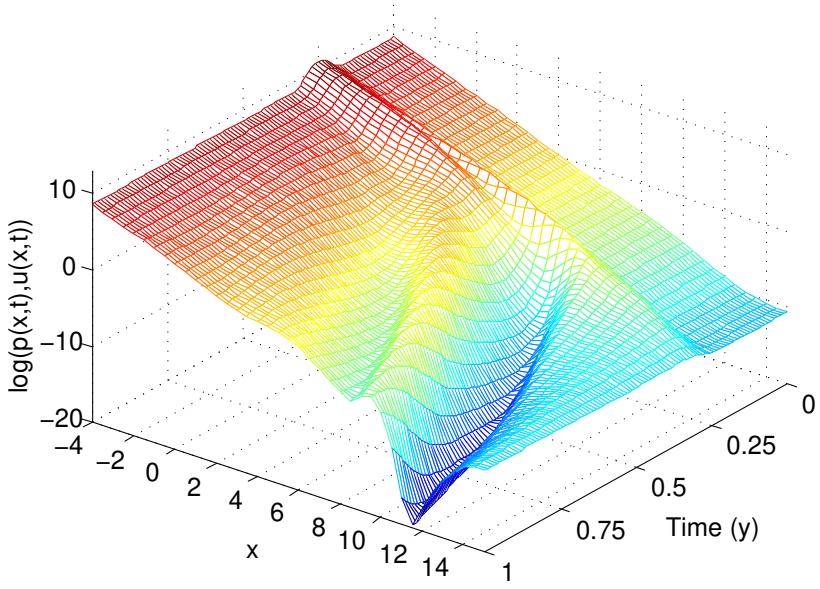

Figure 3.4: The size spectrum over a year, with a phytoplankton bloom introduced (centred at time $t = 0.25$).

ation in the spectrum until the introduction of the bloom (beginning around time $t = 0.2$), at which point the added abundance of the phytoplankton bloom causes an increase at the left-hand end of the consumer spectrum (i.e. the range of organisms whose diet range lies mainly in the phytoplankton spectrum). This rise in abundance quickly spreads to the whole consumer spectrum via the predation process. As the phytoplankton population returns to its original abundance, peaks and troughs are observed to move through the spectrum. For closer inspection of the dynamics occurring in the consumer spectrum, snapshots taken at different time of year are compared (Figure 3.5). At the peak of the bloom the abundance of the consumer spectrum is

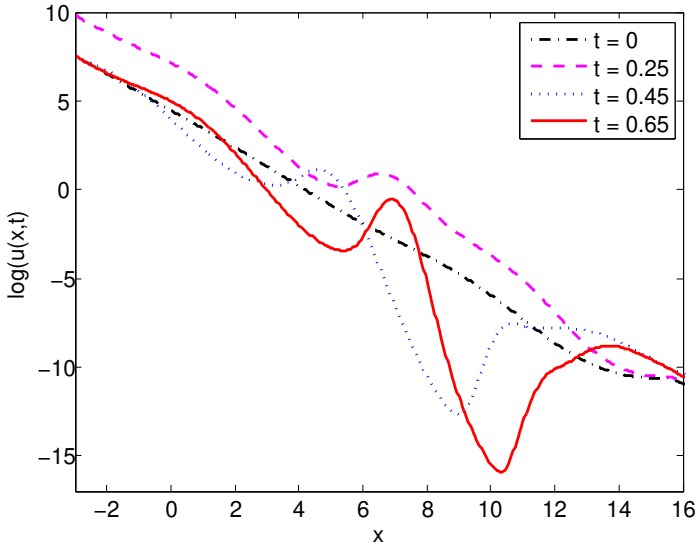

Figure 3.5: Snapshots of the consumer spectrum at different points during the year.

higher than at steady state. A peak of abundance is visible around $x = 7$, which moves along the size spectrum and induces a trough further down the spectrum, caused by the increased predation mortality on organisms in the feeding range of the abundance peak. This trough causes lower predation even further down the spectrum, leading to establishment of a second peak later in the year (Figure 3.5). At the end of the year the two peaks are still present, and the trough has become amplified as it moves across the spectrum. Similar observations were also noted by Maury et al. (2007b) who used a similar short-term increase (also $10\times$) of phytoplankton abundance as the "bottom-up" effect to induce the waves of abundance. Waves of abundance have also been induced by picking parameters which destabilised the power-law steady state, with the period of the peaks linked to feeding behaviour (Law et al., 2009, Chapter 1).

The dynamics of the spectrum are investigated under different blooms (Appendix 3.5.2). As the abundance of the bloom (R) increases there is a larger increase in abundance in the beginning of the consumer spectrum, as organisms have a higher prey abundance upon which to feed. These organisms experience faster growth, leading to a greater community abundance further along the spectrum, along with a more pronounced trough at the left-hand end of the consumer spectrum (Figure 3.12a). As ζ increases the duration of the bloom decreases, leading to a greater shift away from the steady state in the consumer spectrum (Figure 3.12b). This is intuitive, as a shorter sharper bloom leads to a larger variability in the growth rate of consumers feeding upon the phytoplankton spectrum. Note that the total annual phytoplankton biomass is equivalent for $\zeta = 10$ and $\zeta = 40$, and by the time of the snapshot in Figure 3.12b both blooms are over. Thus the peaks and troughs are at similar points in the spectrum, as consumers have the same total phytoplankton biomass to feed upon. The uniform bloom has a larger effect on the consumer distribution than either the shallow or nanophytoplankton blooms (Figure 3.12c). This is due to the cumulative phytoplankton biomass over the year being greatest for the uniform bloom, and reduced for either of the other blooms (which have similar total biomasses).

Time-averaged consumer spectra resemble power-law distributions for all tested blooms (Figure 3.6). Year-averaged gradients of the consumer spectrum are close to the steady state gradient (-1.04) for all tested blooms Average gradients throughout the year range from -1.16 to -0.922 in numerical simulations. Comparing this to empirical data on pelagic species which the model best describes, Jennings and Mackinson (2003) observed a size spectrum slope of -1.2 over the weight range 2-256g, while Boudreau and Dickie (1992) aggregated data to produce a slope of -1.04 (converted from the slope of the biomass spectrum). The results are thus closely correlated, although it is noted that fishing effects are not explicitly included in the model, and are known to decrease the slope of the size spectrum (e.g. Bianchi et al., 2000).

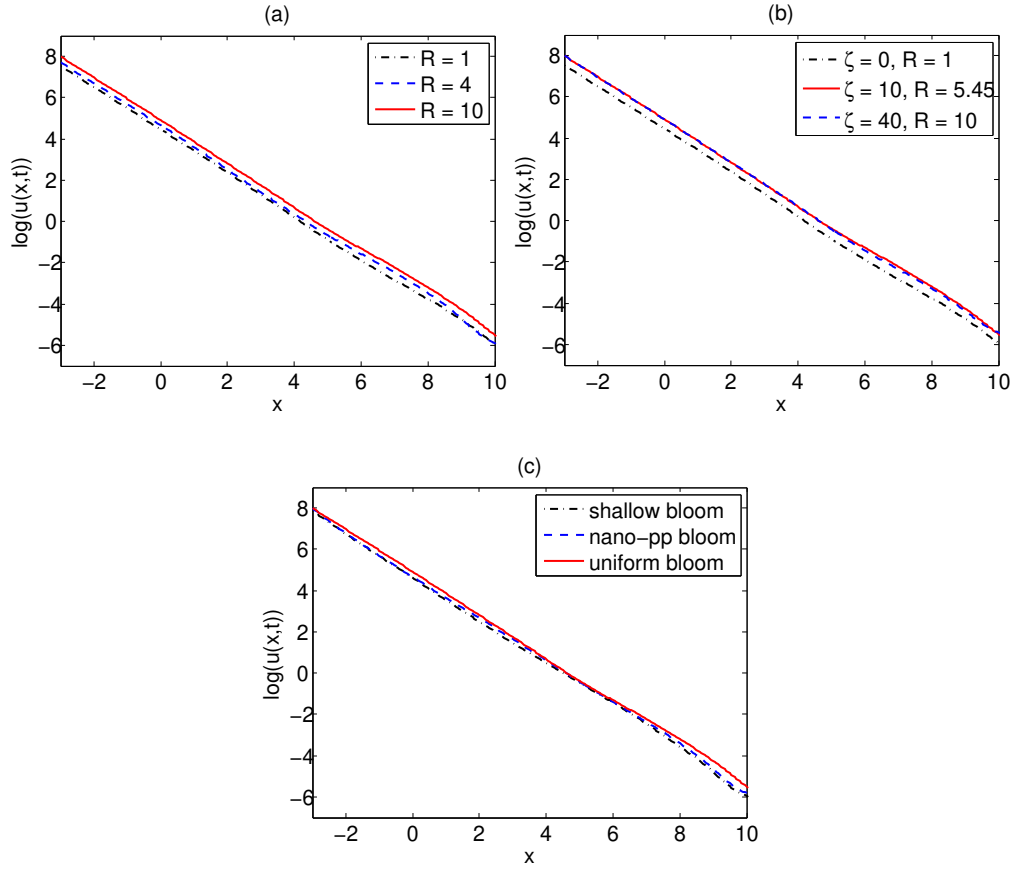

Figure 3.6: The average size spectrum across the year, altering the phytoplankton bloom: (a) blooms of different amplitude: $R = 1$, $R = 4$, $R = 10$; (b) blooms of different durations: $\zeta = 0$, $\zeta = 10$, $\zeta = 40$; (c) with different shapes of bloom: uniform bloom, nanophytoplankton bloom, shallow bloom.

3.3.2 Individual level effects of the bloom

Growth of individuals

The growth rates of individuals born into the spectrum displayed in Figure 3.4 were observed to increase during the phytoplankton bloom (Figure 3.7). In the absence of a bloom there is no variation in the success of individuals, and the same weight is reached after 0.1 years independent of the timing of emergence ($x = 3.44$, 31mg). In the presence of a bloom, growth is strongly influenced by prey abundance; organisms born at time $t = 0.215$ (just prior to the bloom peak) have the fastest growth (reaching $x = 9.31$, 11g), while cohorts born outside of the bloom period reach approximately the same weight as in the steady state spectrum. The growth rates are equivalent to 0.094 and 0.26 day^{-1} ln weight increase for individuals in the steady state and seasonal spectra relatively; these are within the ranges of growth rates for fish larvae of different species observed by Houde (1989). An advantage is observed in laying eggs

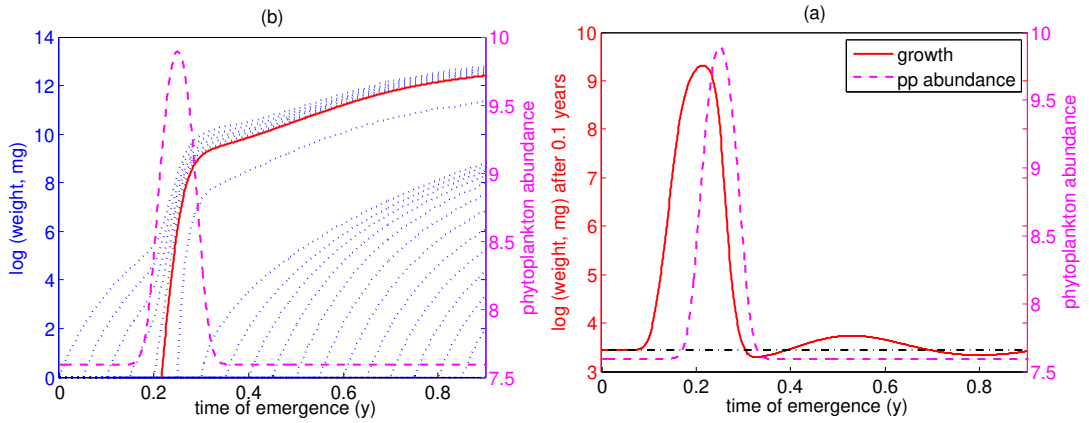

Figure 3.7: (a) The growth trajectories of individuals born throughout the year; the fastest growing individuals after 0.1 years is highlighted by the solid line.(b) The weight of individuals emerging throughout the year at weight x_e after 0.1 years (solid line), in a size spectrum subject to a phytoplankton bloom (dashed line). The horizontal dot-dash line indicates the growth of individuals in the steady state spectrum.

so that larvae hatch before the bloom peak, to ensure they have a greater abundance of food, reflecting the 'match' part of the match/mismatch hypothesis. Empirical evidence has indicated higher recruitment levels of larvae born prior to the bloom peak (e.g. Platt et al., 2003; Buckley and Durbin, 2006). Food availability is thus inferred to be a limiting factor to larval growth, and newborns with a higher growth rate have a shorter larval stage duration (Searcy and Sponaugle, 2000), avoiding the high levels of mortality that fish larvae are subject to (Leggett and Deblois, 1994).

The growth trajectories for an individual born in the steady state spectrum compare unfavourably with empirical data for cod and sole (Figure 3.8). In the steady state spectrum, the individual growth trajectory is similar to a logarithm curve as predicted by (3.18). The model growth rate (which is assumed to represent an "average" pelagic fish) starts slower than expected, and subsequently lies within the bounds of the empirical data for a short period within the first three years. The model individual then grows outside of the upper bound set by cod. The empirical growth rates are postulated to slow down in later life due to reproduction, which begins at maturity and allocates resources from incoming biomass to produce eggs. The reproduction process is not modelled in this study, and improved models explicitly account for biomass losses to produce offspring (Maury et al., 2007a; Blanchard et al., 2011; Hartvig et al., 2011; Plank and Law, 2011). It is observed that in a seasonal size spectrum growth of an individual is unrealistically rapid, and organisms reach the far end of the consumer spectrum (roughly 65kg) within the first year. Thus the model may not be realistic for modelling the effect of phytoplankton blooms on all size ranges, as the growth rate increases unrealistically for large consumers.

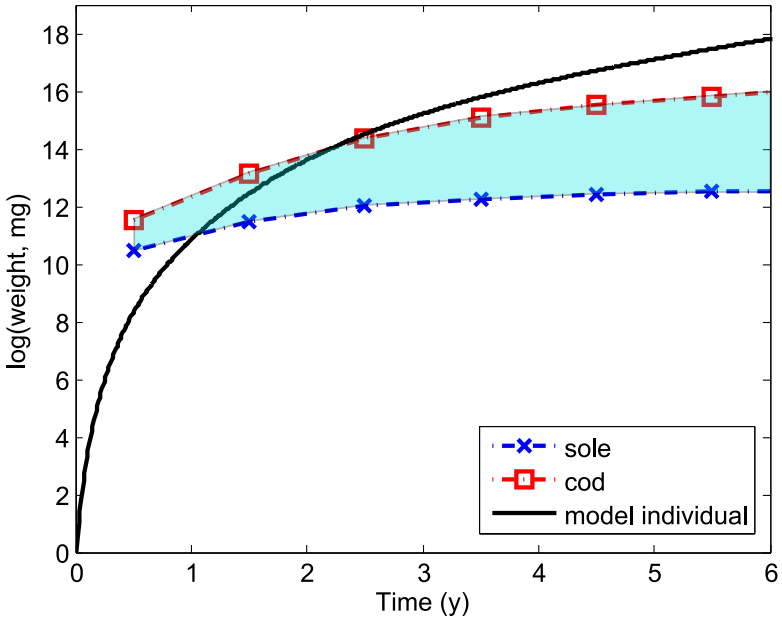

Figure 3.8: The weight-at-age plots for sole (cross markers) and cod (square markers). Data taken from Fishbase (2011). These are compared with the growth of individuals in the steady state spectrum (solid line).

Survival of individuals

There is little variation in survival until around the time of the peak of the phytoplankton bloom where the survival curve becomes steeper (Figure 3.9a). This is due to an increase in abundance of organisms in the weight range $[3, 7]$ during the bloom, which prey heavily on newborn larvae at weight 0. The survival of larvae rises and falls in a negative correlation with predation mortality over the year; the abundance of predators drops soon after the bloom, before rising later in the year (see Figure 3.5), corresponding relatively to the peak and second trough observed in Figure3.9b. In the model by Pope et al. (1994) the survival of newborns was observed to decrease as the wave of abundance moved to larger size classes able to prey upon them; the consumer spectrum here displays more complex behaviour due to the dynamics of the size-based feeding process. Mortality rates due to starvation and mortality are high for fish larvae (Rosenberg and Haugen, 1982; Ware, 1975), with ranges of $1 - 50\%$ day^{-1} reported (Houde, 1989); in comparison, daily mortality for larvae in the model is roughly 17% day^{-1}, and approximately 1% of individuals survive the first 0.1 years in the steady state spectrum (horizontal line in Figure 3.9b).

3.3.3 Cohort level effects of the bloom

A combination of fast growth and low mortality maximises the biomass of cohorts growing out of the larval stage (Figure 3.10). Cohort biomass generally decreases over

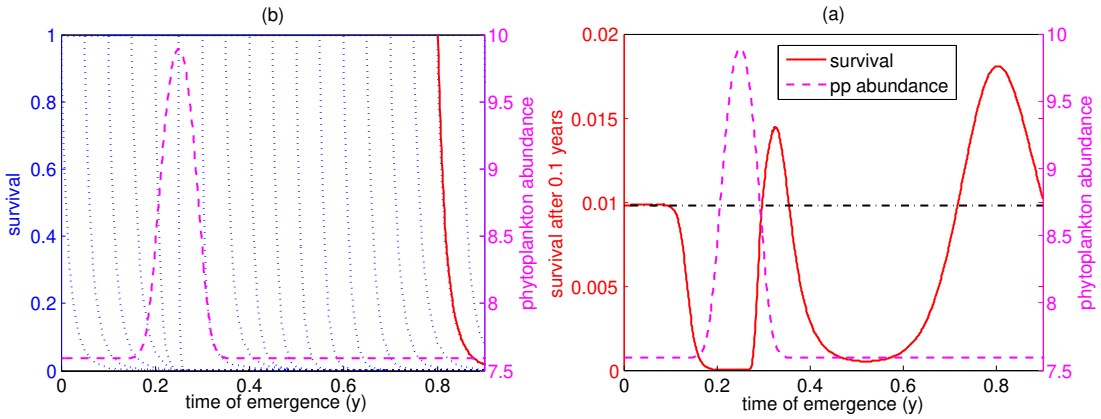

Figure 3.9: (a) The survival of individuals born throughout the year; the individuals with highest survival after 0.1 years is highlighted by the solid line. (b) The survival rate of individuals emerging throughout the year at weight x_e after 0.1 years (solid line), in a size spectrum subject to a phytoplankton bloom (dashed line). The horizontal dot-dash line indicates the survival rate of individuals in the steady state spectrum.

time as predation mortality removes the majority of individuals. However, cohorts born prior to the bloom have higher growth rates, leading to an increase in biomass over the bloom period (Figure 3.10a). The biomass of the most successful cohort over 0.1 years, born at time $t = 0.152$, reaches its maximum at the bloom peak, before dropping again as predation pressure causes a decrease in survival (Figure 3.9b). Additionally, a long-term strategy is revealed in the simulation; for cohorts born after the bloom ($t = 0.302$), survival is initially higher and allows the cohort to persist for a longer time-period (see dot-dash line in Figure 3.10a). However, the initial stage of larval growth (i.e. the first days and weeks of life) is commonly cited to be an important factor for recruitment success (Cushing and Horwood, 1994; Horwood et al., 2000), and larval stage duration is usually short (see Houde, 1989; Searcy and Sponaugle, 2000). Recruitment models also generally focus upon short time frames (e.g. 40-80 days in Pitchford et al., 2005). In the model, emerging prior to the bloom peak is observed to maximise cohort abundance in the larval stage, in agreement with empirical findings (Bradford, 1992).

3.3.4 Tracking successful cohorts through the spectrum

In order to gauge the "success" of cohorts, remaining cohort biomass is chosen, as it combines growth and survival into a single variable, both of which affect the chance of larval recruitment. The location of the cohorts with the largest remaining biomass (after 0.1 years and 0.4 years) is tracked on the backcloth of the seasonal size spectrum (Figure 3.11). In the cases of both cohorts, the trough of abundance in the spectrum is avoided due to the high levels of predations affecting individuals. The most successful cohort over 0.1 years is born ahead of the wave of abundance caused by the

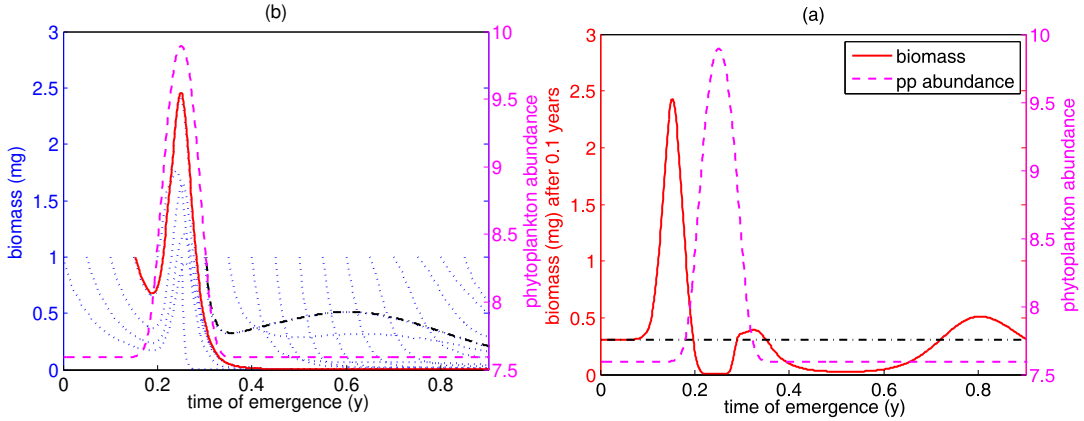

Figure 3.10: (a) The remaining biomass of cohorts born throughout the year; highlighted are the cohort with highest biomass after 0.1 years (solid line) and 0.4 years (dot-dash line). (b) The remaining biomass of individuals emerging throughout the year at weight x_e after 0.1 years (solid line), in a size spectrum subject to a phytoplankton bloom (dashed line). The horizontal dot-dash line indicates the remaining biomass of individuals in the steady state spectrum.

phytoplankton bloom. The extra abundance leads to an increased growth rate, and by the time the phytoplankton spectrum returns to the steady state level, the cohort is on the peak of abundance which remains following the bloom. Thus the cohort avoids the high level of predation that other cohorts born in the time period [0.2,0.3] are subject to (Figure 3.9b), and remains ahead of the trough for the rest of the year. For maintaining biomass over a longer time period, emerging post-bloom is a better tactic; the successful cohort in this case follows the second peak of abundance that follows the trough in the spectrum. The second peak is subject to lower mortality due to a reduced abundance of predators in the trough, leading to higher long-term survival.

The results are in agreement with those of Pope et al. (1994); the successful cohort stays ahead of the peak of abundance which causes higher mortality for cohorts born later in the year. The difference with the dynamic model is that in the previous model the wave of abundance was set externally, meaning cohorts were always eventually overtaken by the pulse, which moved through the entire spectrum (the weight range [1μg, 100kg]) in a year. In the dynamic model the peaks of abundance move via the feeding process, and thus cohorts can grow at the same rate as the pulses. The timescale is therefore very different once the feedbacks and realistic parameters for growth and mortality are considered. The speed of the wave is observed to vary little for the range of blooms considered here.

3.4 Discussion

The motivation behind this work was to investigate the consequences of seasonal pulses of abundance on the behaviour of the dynamical size spectrum model. Varia-

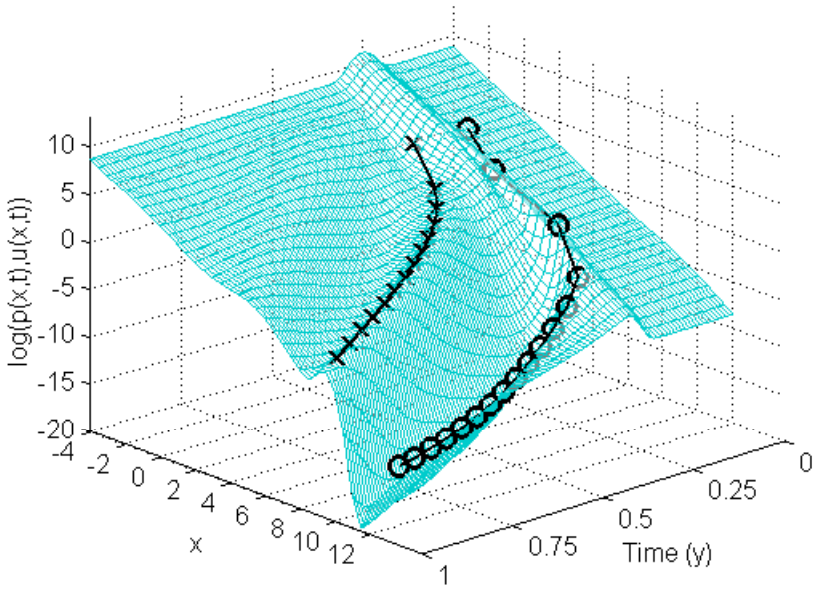

Figure 3.11: The seasonal size spectrum, with the growth trajectories of the most successful cohorts after 0.1 years (circle markers) and 0.4 years (cross markers).

tions in the abundance of phytoplankton over the course of a year have been observed (Menzel and Ryther, 1960), and the consequences of this have spurred on debate over how fish species time their spawning to take advantage of this extra prey availability (Cushing, 1975).

Adding a bloom to this system had the effect of perturbing the system away from the power-law steady state, and in doing so introducing peaks and troughs of abundance in the consumer spectrum, which moved along the spectrum over time through predation (Figure 3.4). Temporal spectra have shown a similar pattern of variation in zooplankton spectra. An empirical study by Heath (1995) over the course of a year displayed a springtime bloom of small organisms leading to a propagation of biomass up the spectrum. It is noted that the peak of biomass took approximately 100 days to reach the largest size class in the empirical study (around 5.5mm equivalent spherical diameter), much slower than the dynamic model used here. The simplistic boundary condition used here does not sufficiently describe the interactions between phytoplankton and zooplankton, and future work should focus on more detailed modelling of the boundary.

A variety of plankton blooms were introduced to the system, in order to view the time-averaged spectra produced over the course of a year. All were close to power-law distributions (Figure 3.6), supporting empirical data which aggregates spectra recorded at different times of year (Li, 2002; Jennings et al., 2002b). The blooms were chosen to represent the diversity of phytoplankton trends observed; blooms of different abundances, durations and forms have been recorded (e.g. Menzel and Ryther, 1960; Navarro and Thompson, 1995; Batten et al., 2003; Huete-Ortega et al., 2010).

Other studies have simulated variations in plankton spectra to examine "bottom-up" effects. Oscillating phytoplankton input using a sine function resulted in peaks and troughs which expanded while propagating up the spectrum (Benoît and Rochet, 2004). Maury et al. (2007b) simulated a temporary increase of phytoplankton abundance, which led to amplified peaks of biomass further up the spectrum, over a year after the bloom had ended. Stock et al. (2008) tested the response of a size-structured functional group model to bottom-up effects, and found biomass increased scaled with the square root of the perturbation size.

Snapshots at any particular time were often perturbed far from the steady state spectrum (Figure 3.5); likewise, snapshots of empirical spectra are rarely perfectly linear, but rather show variation between different size groups with a best fit line plotted over the data (Li and Logan, 1995; Jonsson et al., 2005). There is a lack of empirically observed temporal size spectra in the weight region where fish larvae are born; most sampling is either of the phytoplankton weight range (Huete-Ortega et al., 2010) or the fish weight range (Jennings and Mackinson, 2003), missing out the crucial range where fish larvae are born into the system. There is a large degree of overlap between the weights of large zooplankton and fish larvae, so it would be difficult to separate the effects of fish reproduction from the general behaviour of the spectrum using a community size spectrum model where zooplankton and fish larvae of the same weight are indistinguishable. To explore the interface between the phytoplankton and consumer spectra, a more detailed approach is required for zooplankton dynamics. Phytoplankton - zooplankton models are often used to describe predator-prey interactions (e.g. Truscott and Brindley, 1994; Edwards and Brindley, 1996; James et al., 2003), thus a separate size spectrum for zooplankton dynamics could be incorporated into the model (see Fuchs and Franks, 2010; Zhou et al., 2010).

The growth rate of organisms was observed to scale with the abundance of the spectrum u_0, for which a large range of values was observed from empirical data ($[10^0, 10^4]$, see Boudreau and Dickie (1992); Mari and Burd (1998); Cermeño et al. (2006); Zhou (2006); Zhou et al. (2009); Barnes et al. (2011)). A midrange value was chosen for simulations, and individuals in the steady state spectrum were observed to initially grow at a slower rate than empirical data would suggest, before continuing at a faster rate than the data showed beyond the first three years (Figure 3.8); an extra reproduction term is required to realistically model the allocation of energy to reproduction. Dynamic energy budget (DEB) models are commonly used to model the partitioning of incoming biomass into gonadic and somatic growth (see e.g. van der Veer et al., 2001; De Roos and Persson, 2002; Kooijman, 2009), and the methodology has been recently applied to size spectrum models (e.g. Hartvig et al., 2011; Plank and Law, 2011). The growth rate was observed to increase as phytoplankton abundance rose during the bloom. Hence fish larvae emerging within the bloom period experienced faster initial growth, keeping with both model predictions (Pope et al., 1994) and empirical

observations of larval growth rates (Gotceitas et al., 1996; Wright and Bailey, 1996). Larval mortality also increased with phytoplankton abundance; emerging in the window between the beginning and peak of the bloom resulted in very low survival rates. The dependence of recruitment on larval mortality is a subject of debate; it has been conjectured that slower growing larvae are exposed to both starvation and predation mortality for a longer time, leading to lower survival (Ware, 1975; Beverton and Holt, 1993). However, reliable empirical evidence of the predation levels of fish eggs and larvae, and the subsequent variation of recruitment, are limited (Bailey and Houde, 1989). In the model starvation of individuals was not explicitly modelled (see Hartvig et al., 2011), but was assumed part of the natural mortality that decreased with body mass; an advancement of the model would be to link low growth of newborns with increased mortality. This study has shown the importance of predation on larval survival, and is a first step towards more detailed modelling of mortality effects on larval recruitment.

When investigating the optimum time of emergence in the seasonal size spectrum, the conclusion reached was similar to that of Pope et al. (1994). To maximise the biomass remaining over time, cohorts were born in advance of the bloom, to take advantage of the bloom biomass and to avoid the high predation rates which closely followed the bloom (Figure 3.10). The successful cohort stayed on the peak of abundance which remained after the bloom for the rest of the year (Figure 3.11). Pope et al. (1994) found similar timing for the most successful cohort, and coined the term 'surfing the wave' to describe the tactic of staying ahead of the wave of abundance to maximise growth and minimise predation. The term is apt in that model because the wave of abundance necessarily moves through the entire size spectrum over one year (due to the setup of the system by Pope et al. (1994)), and so inevitably overtakes the cohort at some point - as a water wave eventually overtakes the surfer. Once the dynamics of feeding are incorporated in the spectrum, the wave of abundance is observed to move more slowly, and as a consequence the successful cohort in this model follows the peak of abundance over the year without being overtaken by the pulse. Spawning in time for the phytoplankton bloom has resulted in higher levels of recruitment (e.g. Platt et al., 2003; Buckley and Durbin, 2006), which is in agreement with the model findings; however, there is still much conjecture about which single life stage of fish (if any) is most indicative of recruitment success (see e.g. Bradford, 1992), and very few solid conclusions have been reached since the hypotheses proposed by Hjort (1914) and Cushing (1975).

The key improvement to the model would be an explicit reproduction function. In this model organisms in the consumer spectrum were introduced by the boundary condition (3.13). It is simplistic to assume that the birth rates of zooplankton correlate with the phytoplankton abundance, although the population size of zooplankton has been observed to follow peaks and troughs in phytoplankton abundance (Zhou et al.,

2010). More importantly, fish larvae are not produced by mature fish in the model; in this study growth and death rates were simply used to 'trace' the potential growth and survival rates of cohorts. An obvious step forward would be to allow adult fish to produce offspring, and to make the reproductive process time-dependent, so that the match/mismatch hypothesis can be more rigorously tested. The phytoplankton dynamics could also be explicitly modelled; rather than using the non-dynamic blooms utilised here, nutrient levels could be taken into account (e.g. Armstrong, 1994; Fuchs and Franks, 2010), along with other environmental factors such as temperature and turbulence (Cózar and Echevarría, 2005; Reul et al., 2005), which are known to affect the productivity of phytoplankton. The model used here is a stepping stone for more realistic dynamical models to investigate seasonality in aquatic systems.

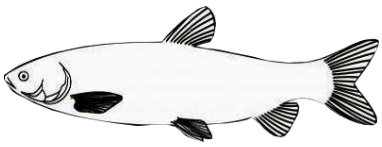

3.5 Appendix

3.5.1 Parameters for numerical integrations

Parameter values for the system are obtained from the literature, and are detailed in Table 3.1.

term	meaning	default value
δt	size of time steps	0.001 years
δx	size of weight brackets	0.05 ln(weight, mg)
x_p	minimum weight for phytoplankton	800pg
x_n	minimum weight for nanophytoplankton	500ng
x_0	maximum weight for phytoplankton	50μg
x_e	weight of newly hatched fish larvae	1mg
x_f	minimum weight for senescent death	5kg
x_∞	maximum weight for dynamic consumer spectrum	65kg
A	predator search volume	$2.548\text{m}^{-3}\text{mg}^{-\alpha}\text{y}^{-1}$
α	predator search exponent	0.8
β	preferred predator : prey mass ratio	100
σ	width of feeding preference function	2
K	feeding efficiency	0.2
u_0	scaling abundance of size spectrum	80m^{-3}
w_0	reference weight selected	1mg
$1-\gamma$	initial slope of size spectrum	-1.04
η	weight dependent mortality rate	0.1 years^{-1}
θ	senescent death exponent	3
t_0	time of phytoplankton bloom peak	0.25 years
R	ratio of bloom : steady state abundance	10
ζ	concentration of peak	40

Table 3.1: Parameter definitions and default values used for numerical integrations. Sources for values are as follows: x_n (Mari and Burd, 1998; Barnes et al., 2011), x_0 (Boudreau and Dickie, 1992; Huete-Ortega et al., 2010), x_e (Cury and Pauly, 2000), A (Ware, 1978; Peters and Wassenberg, 1983), α (Ware, 1978), β (Cohen et al., 1993; Jennings and Mackinson, 2003), σ (Ursin, 1973; Andersen and Ursin, 1977), K (Jennings et al., 2002b), u_0 (Zhou, 2006; Cermeño et al., 2006), R (Zhou et al., 2009), ζ (Navarro and Thompson, 1995; Buckley and Durbin, 2006). Conversions between lengths and masses use methods from the Appendix of Boudreau and Dickie (1992). Other parameter values chosen for numerical convenience.

3.5.2 Varying bloom parameters

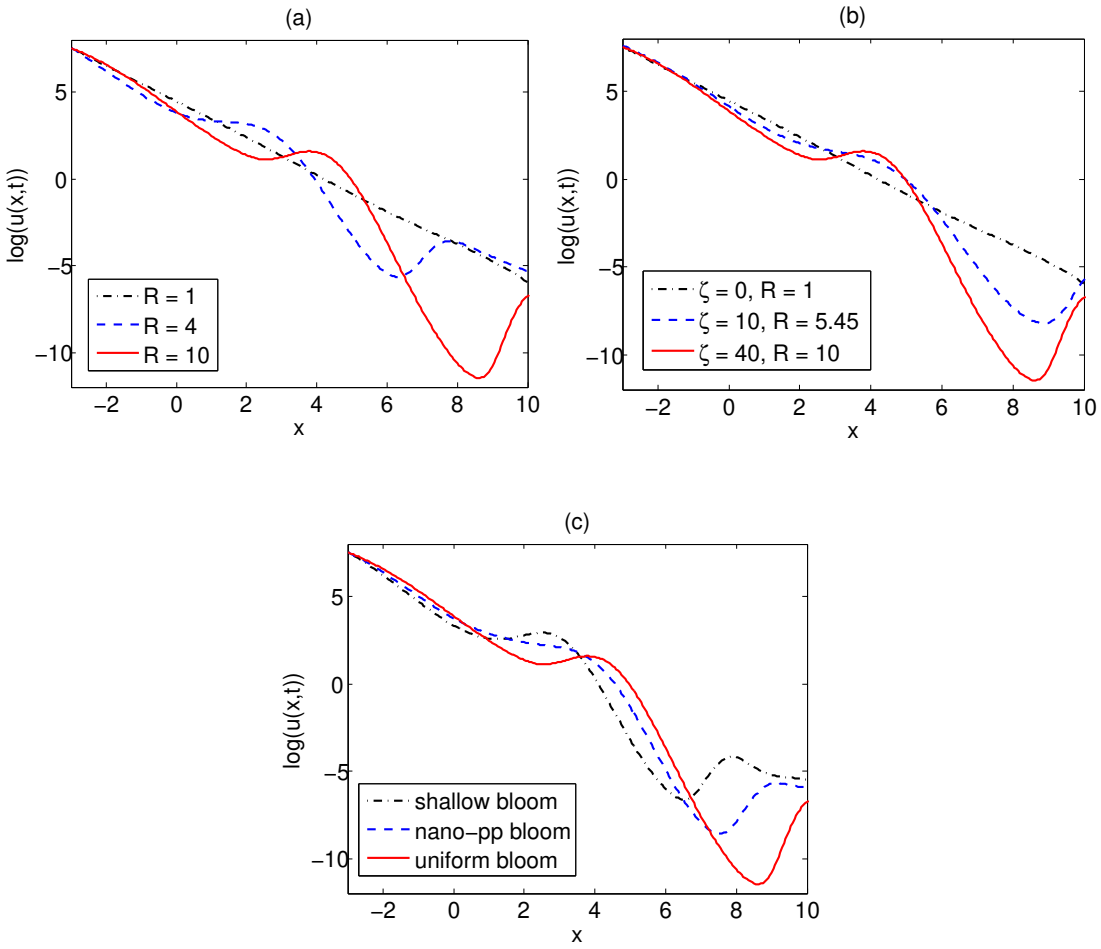

Figure 3.12: The effect of changing bloom parameters on the consumer spectrum: (a) bloom amplitude $R = 4, 10$ in (3.6), with $\zeta = 40$ for all simulations, compared to the steady state spectrum; (b) bloom duration $\zeta = 10, 40$ in (3.6), with R adjusted to give equal total numbers of phytoplankton over the year, compared to the steady state spectrum; (c) bloom shapes (3.6), (3.8), (3.10), with $R = 10$, $\zeta = 40$ for all simulations. Snapshots taken at time $t = 0.4$.

Chapter 4

Seasonal reproduction in size spectra

Samik Datta

Department of Biology,
University of York,
York YO10 5DD, U.K.[1]

[1]email: sd550@york.ac.uk

Abstract

In this chapter time-dependent reproduction is explicitly added to a size spectrum model, along with seasonal plankton blooms, in order to investigate the match/mismatch hypothesis that predicts recruitment success being dependent on prey abundance for newborn fish larvae. The reproduction process in aquatic species is scaled up from an individual level process to the community, and incorporated into the McKendrick-von Foerster equation with diffusion. The process is assumed to be time-dependent, for the first time in a community size-spectrum model. Waves of abundance propagate up the spectrum when time-dependent spawning periods are included. The combined effects of the timing and seasonality of reproduction coupled with the timing of the plankton bloom are then investigated. It is revealed that the growth rate of newborn larvae is high around the plankton bloom, and mortality rates generally decrease for later spawning; to maximise biomass cohorts should be born prior to the bloom peak. As the spawning duration is decreased, the average cohort has lower survival but a higher variability in growth, leading to possible pay-offs in spawning seasonally rather than constantly.

Keywords: marine ecosystem; seasonality; size-spectrum; McKendrick-von Foerster equation; phytoplankton bloom; match/mismatch hypothesis; reproduction

4.1 Introduction

Fish stocks are subject to large fluctuations across time (Horwood et al., 2000), and yet the fisheries industry relies on catches for food sources, with aquaculture recognised as the fastest growing animal food-producing sector (FAO, 2008). Marine communities have thus been heavily investigated, to identify possible causes for interannual variability. Hjort (1914) was the first to hypothesise that the level of recruitment of fish to the adult population was linked to the first year of life for fish larvae (much more strongly than to later life stages), and the growth and mortality they experienced during this time; this was termed the "critical period" hypothesis. Advances in larval fish ecology have happened slowly, over the course of decades rather than

years. Breakthroughs have included the use of otoliths to pinpoint the age and habitat of larvae (Pannella, 1971), advances in technology enabling the modelling of hydrodynamical processes which several hypotheses have predicted have a large effect on larval survival (Werner et al., 2001), and more advanced computing software to deal with the complexities of spatial and temporal processes involved. These advances have allowed a more thorough analysis of the early life stages of fish.

The concept of a critical period has been expanded upon, thanks in large part to the work by Cushing (1975, 1990), who coined the "match/mismatch" hypothesis, which links the timing of the birth of fish larvae to annual springtime plankton blooms; these organisms (specifically zooplankton) act as the majority diet for newly hatched larvae. It is postulated that synchrony between the spawning and bloom periods will result in higher survival of larvae leading to greater levels of recruitment. The idea has gained empirical backing from various studies on seasonally spawning fish species since its conception (e.g. Bergenius et al., 2002; Buckley and Durbin, 2006). Further studies have found that larval mortality decreases with size (Bradford, 1992; Puvanendran and Brown, 1999), adding weight to the postulation that a fish larva has a greater chance of reaching recruitment if growth is faster during the early life stages where mortality from starvation and predation is at its highest. Many studies, both empirical and theoretical, have followed Cushing's proposal, and whose results either confirm the hypothesis (Mertz and Myers, 1994; Pope et al., 1994), or show no significant correlation between success of fish larvae and availability of food (Bollens et al., 1992; Johnson, 2000). Other studies have observed that other abiotic factors such as temperature are more important then plankton abundance in determining growth rates of larvae (e.g. Meekan et al., 2003).

Anderson (1988) summarised recruitment theory and provided an overview of the hypotheses over what governs growth and mortality in the larval stage of fish species; it was concluded that no one factor was solely responsible for governing recruitment success, and it was most likely a combination of various biotic and abiotic factors which controlled the early life stages of fish species. However, the results seemed to support a size-based theory to predict success of fish larvae, in terms of both maximising growth and minimising mortality in the early life stages, which indicates that models taking into account the size of fish may be beneficial in predicting recruitment success of newborn larvae.

It has been shown that the frequency distributions of all aquatic organisms across the body mass range, irrespective of taxa, yields a power-law distribution. Sheldon and Parsons (1967) found that plotting log(abundance) against log(mass) gave a roughly linear relationship, which has become referred to as the "size spectrum" (Sheldon et al., 1972). This phenomenon is not limited to microscopic particles, the size range for which the pattern was first observed, and the linear trend remains reg-

ular at different size ranges, in a variety of aquatic communities (e.g. Boudreau and Dickie, 1992; Kerr and Dickie, 2001; San Martin et al., 2006). The slope of the size spectrum is observed to be close to -1 (Jennings and Mackinson, 2003; Huete-Ortega et al., 2010; Barnes et al., 2011), indicating that there are equivalent amounts of biomass in logarithmically increasing weight brackets. This pattern has been understood using metabolic scaling theory (Brown and Gillooly, 2004), and more recently using the idea of scale invariance in the life processes of marine organisms (Capitan and Delius, 2010).

In order to investigate larval survival within the aquatic community, the reproduction process must be modelled. Fecundity has been shown to scale with body mass (Duarte and Alcaraz, 1989), and the maturity weight and asymptotic weight of fish species have been linked (Beverton, 1992). Thus there is evidence for a size-based approach to simulating the spawning process. Modelling reproduction in a size-spectrum model has been accomplished before (e.g. Shin and Cury, 2004; Maury et al., 2007a; Hartvig et al., 2011); in short, models generally used a fraction of the assimilated body mass from predation to produce eggs of a fixed weight, following the dynamic energy budget theory of Kooijman (1986, 2009). This resulted in an influx of biomass at some fixed weight in the spectrum, following the observation that regardless of fish species, egg size is fairly constant among many pelagic fish species (Ware, 1975; Cury and Pauly, 2000). However, size spectrum models with time-dependent reproduction are less common; one example is a model proposed by Persson et al. (1998), where preallocated mass is transformed into a batch of new cohorts at the beginning of each season. It is well established that some fish species spawn only at certain times in the year, such as cod, sole and sprat (see e.g. Mertz and Myers, 1994; Johnson, 2000; Armstrong et al., 2001), to take advantage of the extra food abundance from the plankton bloom, if the match/mismatch hypothesis is to be believed (Beaugrand et al., 2003).

Previous work on the timing of larval hatching used a fixed temporal "background" spectrum, and then followed cohorts born at different times to calculate the best time of year to be born in terms of fast growth and low mortality (Pope et al., 1994). Following this, an updated model made the consumer spectrum fully dynamic, specifying only the phytoplankton spectrum over the year, including seasonal blooms in the springtime (Chapter 3). However, neither of these models had a robust reproductive function, the latter model specifying the abundances of the smallest organisms in the consumer spectrum at all times, independent of the abundance of adults capable of spawning. Size spectrum models which take time-dependent phytoplankton abundance into account have been studied (Zhou et al., 2010), where the observed phytoplankton abundances through several years were used to model zooplankton abundance over the same period, with comparable results to observed population sizes. For an analysis of the match/mismatch hypothesis both growth and mortality of larvae subject to variable prey abundance should be studied, to determine the

best time to be born. Hence, in this study, both seasonal blooms and seasonal reproduction are incorporated in a simple community-level size spectrum model, and the consequences of the timing of spawning in relation to the plankton bloom are investigated.

This work builds upon the approach from Chapter 3, by adding reproduction to the seasonal size spectrum established in numerical simulations. By systematically altering both the timing and duration of the spawning peak, the success of cohorts is compared to investigate the timing needed to maximise cohort biomass. It is found that, as in previous work, being born prior to the bloom peak results in the highest amount of surviving cohort biomass, and that gambling with shorter spawning periods increases variability within the success of a cohort.

4.2 Setting up the size spectrum model

4.2.1 Splitting the size spectrum into two

A community size-spectrum with two parts is considered, following the setup in previous work (Chapter 3). Previously, the method of growth was used to disaggregate the spectrum into autotrophs (the phytoplankton spectrum) and heterotrophs (the consumer spectrum). The focus was on the dynamics of the size spectrum subject to annual phytoplankton blooms. The area of study is now shifted to the timing of reproduction of fish species in relation to plankton blooms (where "plankton" now comprises of both the phyto- and zooplankton communities). It has been shown that the weight of eggs spawned from marine teleost fish lie in a narrow range around 1mg (Ware, 1975; Cury and Pauly, 2000); thus, reproduction to a single fixed egg weight in the spectrum is considered, which is the boundary between the plankton and consumer spectra.

An identical equation is used to model the plankton spectrum as in previous work (3.6); see Chapter 3 for details. The consumer spectrum is altered to introduce reproduction to the system, for which the individual-level process is initially considered.

4.2.2 Model for reproduction

In previous work, the jump-growth equation for modelling the predation process was derived from a basic stochastic process involving one individual eating another and gaining weight (Chapter 1). In a similar way, to model reproduction the individual level process is initially considered, summarised in Figure 4.1. From this basic stochas-

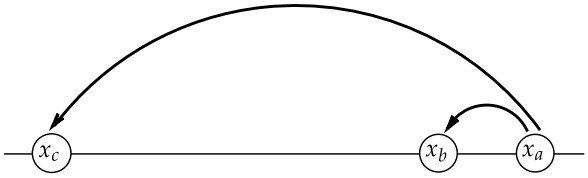

Figure 4.1: The change in abundances at different weights during a single reproductive event. A fish of weight x_a loses a small amount of weight (to become weight x_b) while depositing a large number of eggs further down the spectrum at x_c.

tic process Capitan and Delius (2010) derived the macroscopic model, given by

$$\left(\frac{\partial u(x,t)}{\partial t}\right)_b = \int dx' \int dx'' \Bigg(-r(x,x',x'',t)u(x,t) + r(x',x,x'',t)u(x',t) + \frac{e^{x'} - e^{x''}}{e^x} r(x',x'',x,t)u(x',t) \Bigg) \tag{4.1}$$

where $r(x,x',x'',t)$ is the rate at which individuals of weight x reduce to weight x' by producing offspring of weight x''. Note that the subscript b indicates that only the reproductive process is considered at present; reproduction is incorporated into the full dynamic model in the next section.

Using the model (4.1) for reproduction would be computationally demanding, and require extremely fine discretisation of the weight range for numerical simulations, as noted for the jump-growth equation (Chapter 1). Thus a simplified model is used here for the reproductive process; for the sake of argument, the continuous weight range is discretised into weight brackets, as in Chapter 1, for a more intuitive grasp of the system. The following assumptions are now made. Firstly, the mass of eggs tends to vary little in many pelagic species (Ware, 1975; Cury and Pauly, 2000). Secondly, mature fish generally weigh much more than the eggs they produce (several orders of magnitude larger is commonplace); it is therefore reasonable to assume that a parent fish has similar weights before and after a reproductive event. Thus the model of reproduction appears similar to the metabolic loss term of Capitan and Delius (2010); in a discretised system fish simply move to the weight bracket below in a reproductive event, while the appropriate amount of mass moves to the weight bin where offspring are born, and converted into the appropriate number of offspring (Figure 4.2).

The log weight of newborns is labelled x_0 (note that this is equivalent to x_e from Chapter 3). The equation for reproduction is now given by

$$\begin{aligned} \left(\frac{du_i}{dt}\right)_b &= r_{i+1}u_{i+1} - r_i u_i \qquad \text{for } i \neq 0 \\ \left(\frac{du_0}{dt}\right)_b &= \sum_j \left(\frac{e^{x_j} - e^{x_{j-1}}}{e^{x_0}} r_j u_j\right) \Delta \end{aligned} \tag{4.2}$$

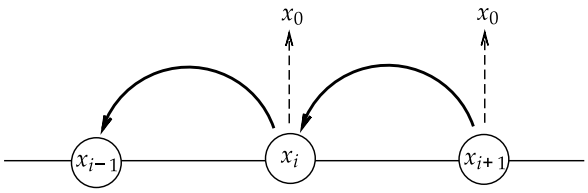

Figure 4.2: A simplified version of the changes in abundance during a reproductive event. Individuals of weight x_{i+1} lose weight Δ in each reproductive event to become weight x_i, where $\Delta = x_{i+1} - x_i$ (Δ is independent of x). The mass lost moves to some fixed weight bin x_0 further down the spectrum. In the same way, individuals at weight x_i lose egg weight and move down to become weight x_{i-1}.

By taking the limit $\Delta \to 0$ the continuum limit of (4.2) is derived. This follows steps taken in previous work (Chapter 1, Capitan and Delius (2010)). Thus the number $u_i(t)$ becomes a number density per unit volume $u(x,t)$, such that $u(x_i,t) = u_i(t)/\Delta$, and $r_i(t)$ becomes $r(x_i,t)$, such that $r(x_i,t) = r_i(t)\Delta$. The sum in (4.2) is replaced by an integral. Rewriting the fraction in (4.2) as

$$\begin{aligned} \frac{e^{x_j} - e^{x_{j-1}}}{e^{x_0}} &= \frac{e^{x_j}(1 - e^{-\Delta})}{e^{x_0}} \\ &\approx e^{x_j - x_0}\Delta, \end{aligned} \tag{4.3}$$

where the first order approximation for $1 - e^{-\Delta}$ is taken, then taking $\Delta \to 0$ changes the sum $\sum \Delta$ to an integral $\int dx$. Thus the reproductive process in the continuum limit is given by

$$\begin{aligned} \left(\frac{\partial u(x,t)}{\partial t}\right)_b &= \frac{\partial}{\partial x}(r(x,t)u(x,t)) \qquad \text{for } x \neq x_0 \\ \left(\frac{\partial u(x_0,t)}{\partial t}\right)_b &= \int e^{x-x_0} r(x,t)u(x,t)\, dx \end{aligned} \tag{4.4}$$

where time-dependence has been re-introduced to the reproduction and abundance functions.

It is noted that the assumptions used to derive (4.4) only hold as long as the loss in weight during reproductive events is small. Thus, if spawning individuals are close in mass to that of newborns, or many offspring are produced over a short period of time, then the approximation to (4.1) becomes worse. This is analogous to the McKendrick-von Foerster equation being a suitable approximation to the jump-growth equation only when prey are generally much smaller than predators (Chapter 1).

4.2.3 Including reproduction in the model

Reproduction is included in the McKendrick-von Foerster equation with diffusion by altering the the first order term in (4.5), which moves biomass up the spectrum. As reproduction involves individuals losing weight, biomass is shifted the opposite way;

the overall flux of biomass is the difference of the two rates. Thus, the McKendrick-von Foerster equation with diffusion becomes

$$\frac{\partial u(x)}{\partial t} = -\mu u - \frac{\partial}{\partial x}\left((g-r)u\right) + \frac{1}{2}\frac{\partial}{\partial x}\left(e^{-x}\frac{\partial}{\partial x}(du)\right) \tag{4.5}$$

where $r(x,t)$ is the reproduction rate (other terms are identical to the equation without reproduction (3.1)) and $g-r$ is labelled the overall growth rate. The abundance of offspring is given by

$$\frac{\partial u(x_0)}{\partial t} = -\mu(x_0)u(x_0) - g(x_0)u(x_0) + \int_{x_0}^{\infty} e^{x-x_0} r(x,t)u(x,t)\, dx. \tag{4.6}$$

which is similar to the boundary condition of Blanchard et al. (2011), although reproduction has explicit time-dependence here.

A size- and time-based approach is used to model fecundity. Realistically a number of different factors affect reproductive output (Lambert, 2008), and a simple model is employed to allow greater tractability. The maturity weight of fish is labelled x_m in the spectrum; below this weight, organisms do not reproduce. The reproduction function $r(x)$ is specified as

$$r(x,t) = f(t) \cdot h(x) \tag{4.7}$$

where

$$f(t) = \frac{e^{\nu\cos(2\pi(t-t_r))}}{I_0(\nu)} \tag{4.8}$$

$$h(x) = \left(1 + e^{\rho(x_m - x)}\right)^{-1} (Fe^{qx}). \tag{4.9}$$

Thus the time dependence (4.8) is a von Mises distribution as in the plankton bloom (3.6), albeit now centred around time t_r, independent of t_p. This takes into account the possibility of non-uniform reproduction across time, which is present in batch spawners such as cod and haddock (e.g. Bollens et al., 1992; Knijn et al., 1993; Johnson, 2000). Setting the period duration $\nu = 0$ means time-independent reproduction (but still dynamic, scaling with the abundance of mature organisms in the spectrum). From the form of (4.7) waves of abundance are expected to result from non-constant reproduction, as the boundary condition is oscillatory in time. The rate at which individuals reproduce is described by $h(x)$, which scales with body mass following evidence that log fecundity increases linearly with log size (Duarte and Alcaraz, 1989; Blanchard, 2000). The first bracket in (4.9) is a switching function, similar to that of Hartvig et al. (2011), which fixes where reproduction starts, with x_m as the weight where 50% of organisms are mature, and ρ determining the steepness of the slope. F and q are constants; F is the rate at which organisms reproduce and q is the weight-dependent scaling factor. Values for F and q are chosen to match with the aggregated fecundity curve from 97 teleost fish species (Duarte and Alcaraz, 1989), reflecting the fact that

this community model simulates reproduction (and other life processes) for an "average" pelagic fish (Blanchard et al., 2009). Both male and female fish are assumed to contribute equal biomass to reproduction. Note that for simplicity the stages between spawning (i.e. incubation, hatching and yolk resorption) are not modelled here (see Duarte and Alcaraz, 1989), and offspring are assumed to immediately feed in a size-based way.

The setup of the size spectrum model incorporating reproduction is summarised in Figure 4.3.

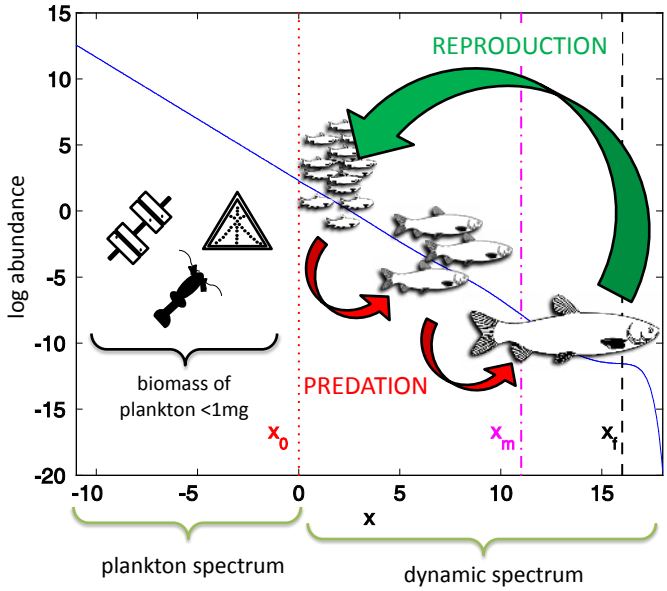

Figure 4.3: The size spectrum, consisting of the plankton and dynamic spectra. Organisms in the plankton spectrum do not grow by predation, and their population is set externally. Organisms in the dynamic spectrum feed upon both spectra for growth. Organisms above maturity weight x_m can reproduce; offspring enter at the boundary of the dynamic spectrum, at weight x_0. x_f is the weight at which extra mortality starts to affect the spectrum, to prevent organisms growing unreasonably large. Image of grass carp (*Ctenopharyngodon idella*) used with permission of Vlado.

Note that in the setup of the model the reproduction rate r is independent of the growth rate g, in a departure from the dynamic energy budget methods (Kooijman, 2009) commonly used in size spectrum models to allocate incoming mass to somatic and reproductive mass (e.g. Maury et al., 2007a; Blanchard et al., 2011); here the physiology of egg production is not explicitly modelled, and size-based fecundity is assumed. One issue with using a reproduction rate which is dependent on the instantaneous growth rate of organisms is that fish species reproduce over different time scales (see Appendix 4.5); for species such as haddock and cod spawning occurs over a limited period of time in the year (a matter of weeks or months, see Mertz and Myers (1994); Armstrong et al. (2001)), and in such cases constant reproduction is not an accurate representation of the system. Also, for models with growth-dependent repro-

duction, a temporal decrease in the growth rate (for example, due to spatial variability of prey) causes the reproduction rate to likewise be reduced. Here the focus is on the consequences of seasonality, so reproduction is modelled in a simple way. This is not to say that food supply does not affect reproductive rate in the long term; studies have shown correlations between rations received by fish and egg production (e.g. Wootton, 1977). An in-depth modelling of the physiology of marine organisms would be required for the robust modelling of egg production from food intake, and is beyond the scope of this work.

4.2.4 The match/mismatch hypothesis

The match/mismatch hypothesis (Cushing, 1969, 1990) is summarised in Figure 4.4, adapted from Mertz and Myers (1994). The hypothesis suggests that larval survival

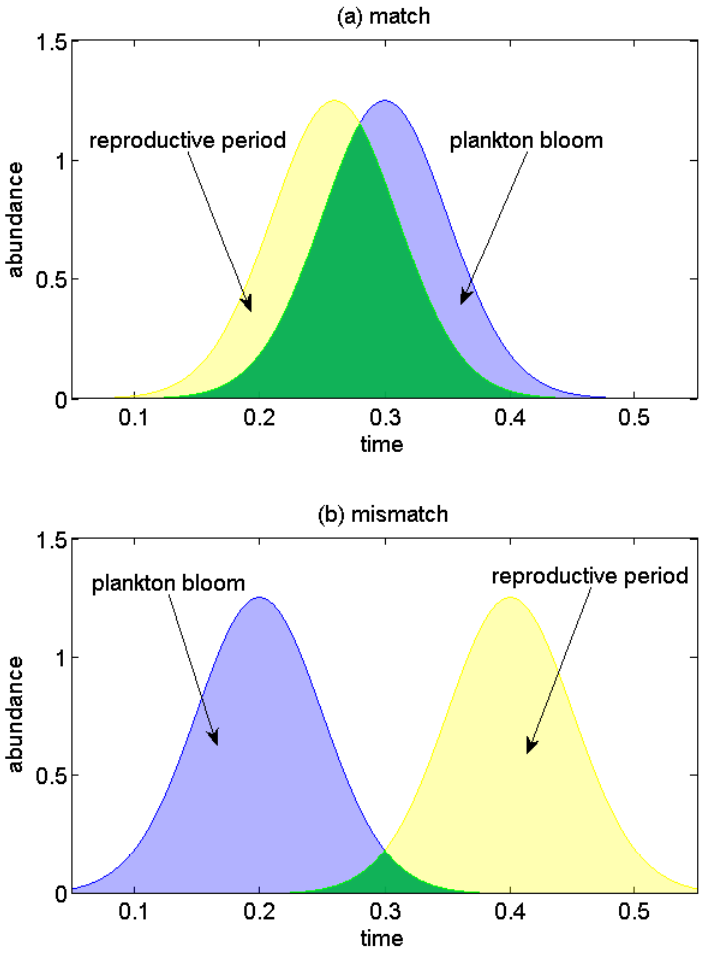

Figure 4.4: Illustration of plankton blooms (shown in blue) and reproductive periods (shown in yellow); the area of overlap of the two is shown in green. The match/mismatch hypothesis indicates that eggs can (a) hatch in time to take advantage of the increased prey abundance from the plankton bloom, leading to greater recruitment, or (b) miss the bloom, and have lower food availability, with fewer fish larvae surviving to adulthood.

is linked to prey availability, and that faster growing larvae are more likely to reach recruitment as they are subject for a shorter amount of time to the high starvation and predation mortalities affecting fish larvae (Leggett and Deblois, 1994). There is empirical evidence to back up the hypothesis; for example, data from Wright and Bailey (1996) suggests that the larvae of sandeel (*Ammodytes marinus*) which are born closer to the phytoplankton bloom undergo faster growth, and have a higher survival rate than those born significantly before or after the plankton bloom. Platt et al. (2003) also accounted for 89% of the variation in haddock larval survival by the timing of spring-time phytoplankton blooms, using ocean satellite data recorded over seven years. Extensive testing of the hypothesis was not possible until recently, when the technology for detailed spatial and temporal recording of marine systems became more widely available. Satellite data recording chlorophyll *a* levels (a proxy for phytoplankton abundance) of ocean surfaces (Platt et al., 2003; Barnes et al., 2011) and frequent cruise sampling (Li, 2002; Zhou et al., 2010) have led to more detailed temporal phyto- and zooplankton data, enabling comparisons of plankton abundances with those of well-established data on fish eggs and larvae (Armstrong et al., 2001; Meekan et al., 2003; Genner et al., 2010).

The interplay between the plankton bloom and spawning period is examined numerically here. A fixed plankton bloom is set up during the year, and the spawning period is varied to find correlations between cohort success and the timing and duration of reproduction.

4.2.5 Numerical simulations

The system of $p(x)$ and $u(x)$ is initialised at the analytical power-law steady state as in Chapter 3; γ is calculated from parameter values as specified in Table 4.1. The spectrum is discretised into weight "boxes" of width δx (ln weight was used for both axes throughout the simulations), and the initial distribution is set up with the abundance for weight x_i equating to $u(x_i) = u_o e^{(1-\gamma)x_i}$ (with $\delta x = x_i - x_{i-1}$). A Newton-Raphson iterative scheme is then used to calculate the numerical steady state for the model (4.5), with constant reproduction ($\nu = 0$) and the senescent mortality rate of (3.12). This is taken as the initial distribution for the simulations. The plankton and consumer spectra through time are then calculated as in Chapter 3, with the boundary condition now specified by (4.6). Initially the plankton spectrum is held constant, and a bloom is later introduced to test the varying success of cohorts over the course of the year.

The growth trajectory of an individual is tested as in Chapter 3, using the method of characteristics (Law et al., 2009; Rochet and Benoît, 2011). The growth of an individual is calculated by solving (3.17), and compared to both empirical weight-at-age data and the growth trajectory of an individual in the steady state spectrum in Chapter 3. The

reproduction present in this model is predicted to slow down growth at larger sizes, and the trajectory is expected to fall within or closer to the bounds set by the empirical data for cod and sole. These species are chosen to represent pelagic species with large and small asymptotic sizes respectively (Fishbase, 2011).

The effect of seasonal reproduction on the dynamics of the consumer spectrum is investigated, to simulate the batch spawning behaviour of various pelagic fish species (e.g. Armstrong et al., 2001). Waves of abundance previously resulted from phytoplankton blooms, where the boundary condition was assumed to follow the phytoplankton abundance (Chapter 3). A similar pattern is expected due to the time-dependent reproduction function controlling influx of new individuals at the boundary (4.7). The growth trajectory of a mature individual is traced over the course of the year, to observe temporal variability in the overall growth rate (i.e. growth - reproduction). This is expected to drop during the spawning period as resources are diverted to reproduction.

A plankton bloom is added to the spectrum lasting 2-3 months (Navarro and Thompson, 1995), and the consumer spectrum is simulated over the course of a year, systematically varying the timing of spawning. A spawning window with the same duration as the plankton bloom is picked, reflecting behaviour of pelagic batch spawners (e.g. Johnson, 2000). The method of characteristics is employed to calculate the growth trajectories (3.17) and survival (3.20) of offspring through the year. This is then used to investigate the success of cohorts, i.e. the amount of biomass remaining after a fixed time period. In Chapter 3 abundance at the boundary scaled with the phytoplankton spectrum, and to eliminate the effects of this the per capita biomass was calculated (i.e. where all cohorts start with the same abundance). Here the abundance depends explicitly on the reproduction function (4.7), and this is taken into account by scaling the initial biomass with $u(x_0, t)$. The average growth, death and remaining biomass of different cohorts are compared to investigate the optimal time to be born. The effect of varying spawning duration ν is tested in the cases where reproduction occurs around the time of the plankton bloom, and where it occurs after the bloom has ended (representing the 'match' and 'mismatch' components of the match/mismatch hypothesis respectively). Both the average and maximum biomass are plotted, in order to study both the general trend and variability in biomass as spawning becomes more peaked.

4.3 Results

4.3.1 Model specifics for numerics

Table 4.1 summarises the values assigned to system parameters for the numerics. Most parameter values are taken from Chapter 3 and generally chosen to represent bi-

ologically reasonable process rates. A higher feeding efficiency $K = 0.6$ (Hartvig et al., 2011) is required to take reproduction into account; although the reproduction function (4.7) is independent of food intake, for a numerical steady state to be achieved it was found that all organisms needed positive overall growth rates. As in Chapter 1, the steady state can be destabilised by increasing the preferred predator:prey mass ratio β or decreasing diet breadth σ. As the growth rate of individuals scales with K, the scaling abundance of the size spectrum is reduced to $u_0 = 30$ for realistic growth trajectories. A reduced exponent for senescent death is included as reproduction affects large individuals more strongly, so less mortality is required to keep abundance low at the end of the spectrum.

term	meaning	default value
	dynamic spectrum $u(x)$	
x_p	min weight of plankton	-11 (16ng)
x_0	weight of newborn consumers	0 (1mg)
x_m	maturity weight of individuals	11 (60g)
x_f	wt at start of senescent death	15.35 (5kg)
x_∞	max wt of consumers	18 (65kg)
A	predator search volume	$2.548\text{m}^{-3}\text{mg}^{-\alpha}\text{y}^{-1}$
α	search volume exponent	0.8
β	log preferred pred:prey mass ratio	5
σ	width of feeding kernel	2
K	mass conversion efficiency	0.6
η	natural mortality rate	$0.2\ \text{years}^{-1}$
$1-\gamma$	slope of initial size spectrum	-0.955
θ	senescent death exponent	2
u_0	abundance of size spectrum	30m^{-3}
	plankton spectrum $p(x)$	
t_p	time of plankton bloom peak	0.5 years
ζ	width of bloom peak	10 (0.25 years)
R	ratio of bloom : steady state abundance	5
	spawning period	
t_r	time of spawning peak	varies
ν	width of reproduction window	10 (0.25 years)
F	rate of reproduction	$1.8\ \text{years}^{-1}$
q	reproduction exponent	0.01
ρ	exponent of switching function	5
	numerical integration	
δx	weight bracket for integration	0.05 ln(weight, mg)
δt	time step for integration	0.001 years

Table 4.1: Default parameter values used in figures (realised values shown in brackets).

The size spectrum is split into several sections, each subject to different predation and mortalities. The weight spectrum x is subdivided as follows:

- $[x_p, x_0)$ is the plankton spectrum. Predation from the consumer spectrum does not affect the abundance of individuals (which are assumed to replace them-

selves immediately, see Chapter 1). Organisms do not grow across the boundary. The system is subject to a seasonal bloom, corresponding to equation (3.6).

- $[x_0]$ is the boundary between the two spectra, and where new consumer offspring (produced by mature fish at the upper end of the spectrum) are born into the spectrum. Newborns are subject to both natural and predation mortality, and are able to grow through the consumer spectrum (4.6).
- (x_0, x_f) is the consumer spectrum, which undergoes death, growth, reproduction and diffusion processes as in (4.5), feeding upon both the plankton and consumer spectra. The reproduction rate is negligible until x_m where it increases exponentially with ln body mass. The natural death rate of (3.12) affects all organisms.
- $[x_f, x_\infty]$ is subject to all the processes above, plus the extra senescent death term in (3.12), in order to limit abundance for extremely large organisms.

4.3.2 Steady state with time-independent reproduction

Setting $\nu = 0$, the reproduction rate is time-independent. Figure 4.5 shows the steady state derived using parameter values as shown in Table 4.1. A discontinuity is ob-

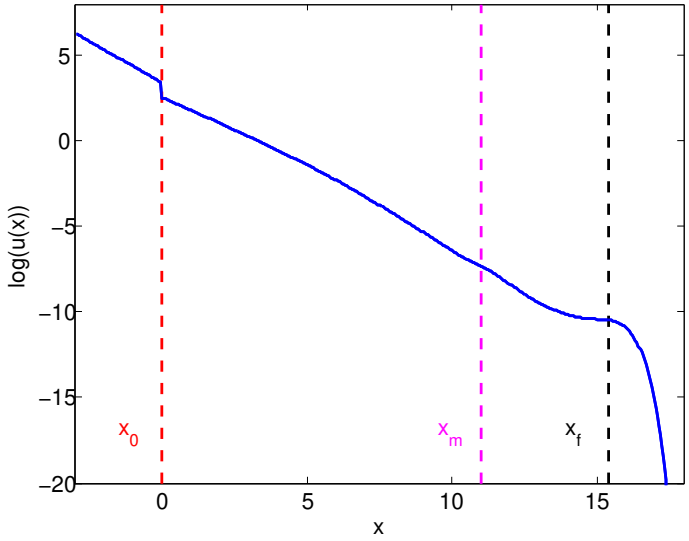

Figure 4.5: The steady state solution to the McKendrick-von Foerster equation with diffusion (4.5), with a fixed plankton spectrum and uniform reproduction ($\nu = 0$). The vertical dashed lines indicate, from left to right: the boundary between the plankton and consumer spectra, the maturity weight for organisms in the spectrum, and the point where senescent mortality begins to affect organisms.

served at the boundary between the two spectra where offspring are born. Similar behaviour has been observed in other models specifying reproductive boundaries (Blanchard et al., 2011). The slope of the consumer spectrum becomes steeper around

weight x_m as biomass begins to be allocated to reproduction from mature individuals. The overall growth rate $(g - r)$ is a smooth positive function of x at the steady state (results not shown here).

The growth trajectory for an individual born in the steady state spectrum compares favourably with empirical data when reproduction is included as a size-dependent process (Figure 3.8). The model growth rate is slower than in the previous chap-

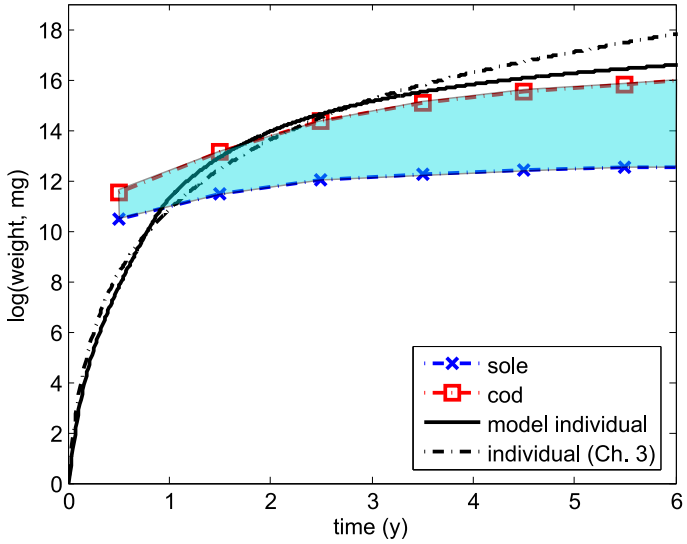

Figure 4.6: The growth of a model individual in the steady state spectrum (solid line), compared to individuals from Chapter 3 (dot-dash line) and empirical weight-at-age curves for sole (cross markers) and cod (square markers). These species are chosen to represent lower and upper bounds of growth for pelagic species, and the shaded region indicates the expected size range for individuals of different ages.

ter where reproduction was not modelled. The growth curve starts similar to the logarithm-shaped curve from Chapter 3, and becomes flatter after the cohort reaches maturity, as growth is reduced by reproductive output. The curve has a similar shape to that of cod in years 4-6, although exceeding the weight-at-age curve slightly. Nevertheless, at a qualitative level the behaviour of an individual through time seems to reflect real weight-at-age curves better than when reproduction is not taken into account.

4.3.3 Peaked reproduction

For $\nu > 0$ reproduction rates are low for the majority of the year, and peak around time t_r. The dynamics reveal a wave of abundance moving through the system (Figure 4.7). The abundance at the boundary decreases initially, as reproductive effort is low at the start of the year. Abundance increases and reaches its peak at time $t = t_r$, before then decreasing again for the rest of the year. This fluctuation at the boundary causes a wave of abundance to move up the size spectrum, similar to the bottom-up

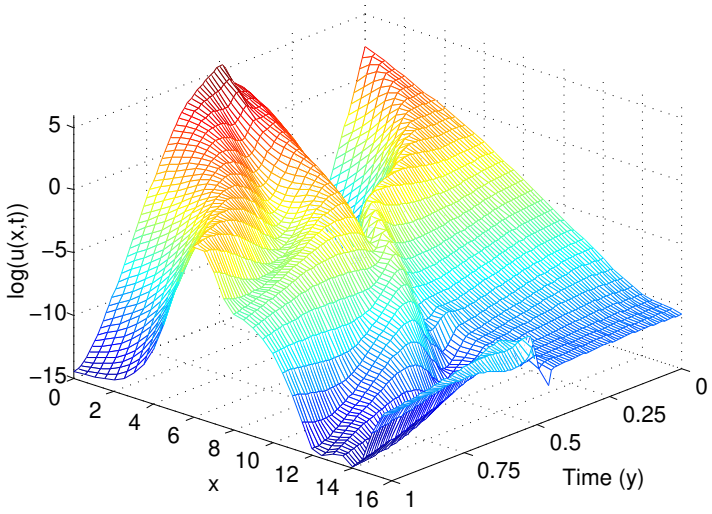

Figure 4.7: The size spectrum over the course of a year, with seasonal spawning centred at $t_r = 0.5$.

effect of seasonal plankton blooms (Pope et al., 1994; Heath, 1995, Chapter 3). The abundance at size x_0 follows the shape of the time-dependent function (4.8), as expected, although variations in the abundance of mature organisms lead to deviations from the exact shape of $f(t)$. Importantly, the lack of reproduction at the start of the year leads to a deficit of the predators of larvae further up the spectrum, which is observed to rise sharply as spawning reaches its peak. Predation mortality plays a crucial role in the survival of fish larvae (Leggett and Deblois, 1994), and the dynamics of the community have been simplified greatly for the model.

The overall growth rate for mature individuals is observed to drop below zero during the reproductive period (Figure 4.7a). Initially reproductive effort is low, so the

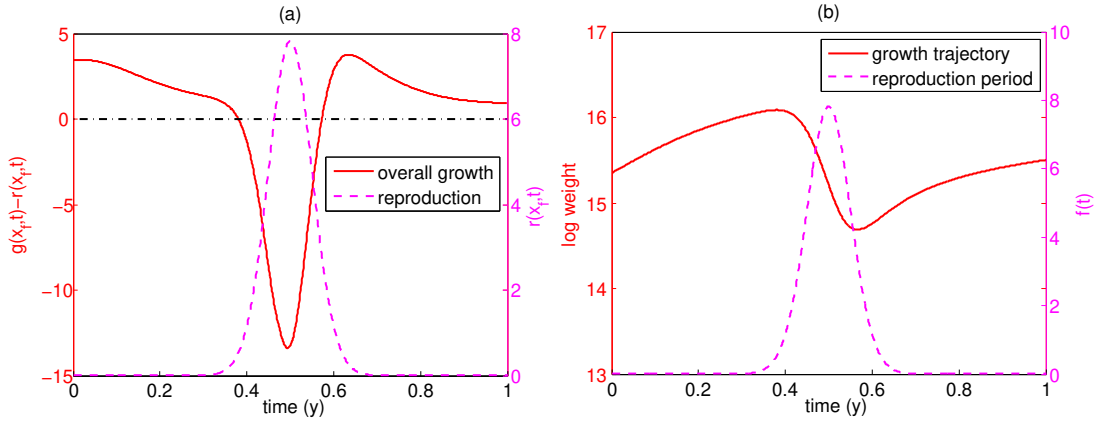

Figure 4.8: The growth of mature organisms which undergo seasonal spawning around $t_r = 0.5$ (spawning period highlighted by dashed line): (a) the overall growth rate of a mature individual (mass x_f) across the year ($g - r = 0$ indicated by horizontal dot-dash line), (b) tracing the mass of a mature individual (with an initial weight of 4.6kg) over the course of a year.

majority of biomass is used for somatic growth. As the reproductive period begins, overall growth decreases, and drops below zero around time $t = 0.4$. The minimum is reached at $t = 0.5$ when reproductive effort is highest, before increasing again. There is thus the possibility for individuals to lose weight over the reproductive period (Figure 4.8b), which depends upon the ratio of growth rate g to reproduction rate r. Although the physical dimensions of fish have not been observed to decrease from field studies in the wild over the reproductive period, it is feasible for the body mass to decrease if the mass lost in laying eggs is not compensated by the biomass assimilated through predation, a phenomenon which has been observed in laboratory-based studies (Wootton, 1977). The mature individual in Figure 4.8b is observed to be approximately the same weight at the beginning and end of the year; this is unlikely, as fish grow continuously for the majority of their lives. The model is less realistic for simulating growth of larger organisms in the spectrum than for larvae.

4.3.4 Cohort success

Timing of reproduction

A plankton bloom (3.6) is now introduced to the spectrum; this is given a von Mises shape following empirical evidence (see Chapter 3), centred at $t_p = 0.5$ and lasting approximately 2-3 months. Different timings of the spawning peak are tested to investigate the growth, survival and biomass of cohorts (Figure 4.9). Both growth and biomass are observed to peak around the peak of the bloom. The death rate increases slowly until the bloom, after which it decreases more significantly over the rest of the year. In Chapter 3 the death rate was observed to be highest at the peak of the bloom; here the same result is observed, although there is a relatively high abundance of predators of larvae at the start of the year (Figure 4.7) due to the initial steady state condition. Predation biomass varies more with the reproductive boundary condition than in Chapter 3, as there is little flow up the spectrum from the smallest consumers outside of the reproductive period. The peak for cohort biomass is around $t = 0.5$, where growth rates are high, and drops sharply after the bloom peak. Hence spawning prior but close to the peak is the best tactic for maximising biomass, in agreement with previous models (Pope et al., 1994, Chapter 3) and empirical results (Platt et al., 2003; Buckley and Durbin, 2006). An early peak in biomass is observed at $t = 0.25$, and possible causes are currently being investigated.

Duration of reproduction

The shorter the spawning period is, the lower the average biomass of the cohort (Figure 4.10a). This applies for both 'match' and 'mismatch' conditions, although cohorts

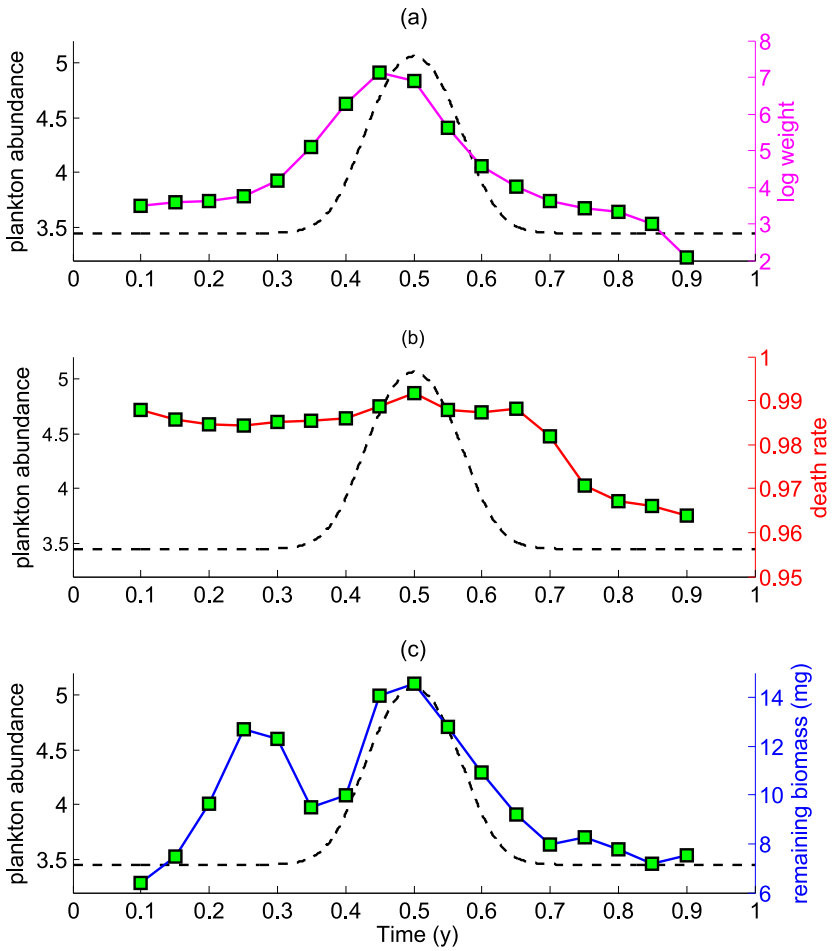

Figure 4.9: Characteristics of cohorts born in different reproductive periods throughout the year, in a system subject to a plankton bloom: (a) average weight after 0.1 years; (b) average per capita death rate after 0.1 years; (c) average biomass remaining after 0.1 years. Reproductive periods simulated at regular intervals between $t_r = 0.1$ and $t_r = 0.9$. Plankton abundance shown by dotted line.

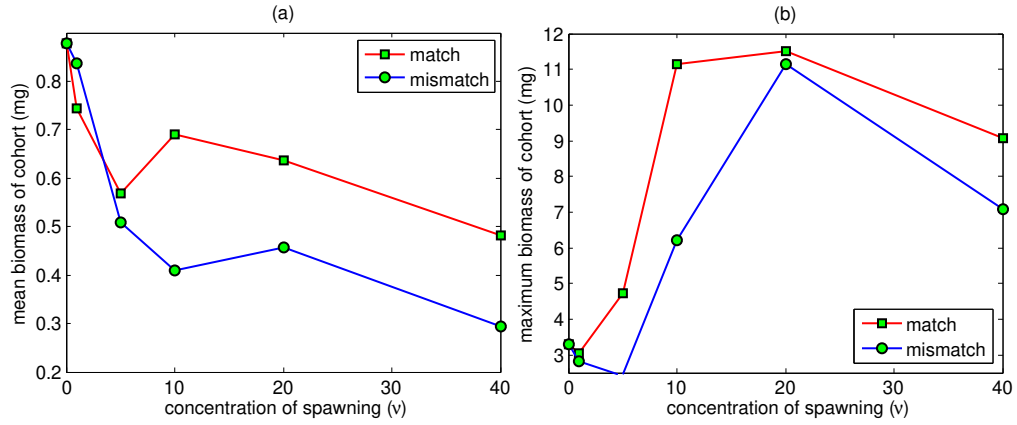

Figure 4.10: Testing the effect of spawning duration on cohorts born close to ($t = 0.45$, 'match') and away from ($t = 0.75$, 'mismatch') the plankton bloom, with decreasing spawning duration: (a) the average biomass of cohorts; (b) the maximum biomass of cohorts.

born close to the bloom generally have larger sizes due to increased prey biomass. This would seem to indicate that a "bet-hedging" strategy of constant spawning ($\nu = 0$) would maximise the total biomass of fish larvae (note that the integrated amount of reproduction biomass is equal for all values of ν). However, the maximum biomass of cohorts is shown to increase as reproduction becomes more peaked (Figure 4.10b). This is in agreement with the simple model by Mertz and Myers (1994), where recruitment variability increased as the width of spawning decreased. The maximum biomass in both cases dropped for $\nu = 40$ (corresponding to spawning duration close to a month), and numerical work is currently being carried out to explain this.

Recruitment levels in nature are generally low for fish larvae, with high mortality rates for newborns (Pitchford et al., 2005); if fewer large individuals are more likely to be recruited than many smaller individuals, then gambling by producing many eggs in a shorter time period could result in higher levels of recruitment. However, these results do not support a firm conclusion for this.

4.4 Discussion

A simple community size spectrum model used in the context of resolving size-dependent predation, growth, mortality and reproduction processes of an "average" species was developed in this chapter, incorporating predation, seasonality and, for the first time in a community size-spectrum model, continuous time-dependent reproduction. Previous models used a pulse of reproductive effort at the start of each time period (Persson et al., 1998); this was extended over a longer time period in this model, in keeping with empirical data (Quéro, 1984; Knijn et al., 1993; Johnson, 2000). Previous models which simulate the production of new offspring into size-based models have divided incoming biomass from the predation process into somatic growth and egg production (De Roos and Persson, 2002; Maury et al., 2007a; Blanchard et al., 2011; Hartvig et al., 2011); here reproduction was independent of the instantaneous feeding rate of organisms, which in reality is subject to spatial and temporal variation. Instead, the simple assumption was made of making reproduction both weight-dependent (Wootton, 1977; Duarte and Alcaraz, 1989; Blanchard, 2000) and time-dependent based on the batch spawning method used by some pelagic species, in keeping with empirical observations (see Appendix 4.5).

The incorporation of reproduction into the model involved a method similar to the derivation of the deterministic jump-growth model (Chapter 1); starting with an individual stochastic process whereby an organism produces offspring of a lower weight and, in doing so, loses a portion of its own weight (Figure 4.1). However, rather than deriving a macroscopic model from the master equation describing this process (Capitan and Delius, 2010), it was simply assumed that the amount of weight lost in each

event was quite small, leading to a first-order approximation (4.4). This is similar to the growth term (3.3) in the McKendrick-von Foerster equation (Benoît and Rochet, 2004; Law et al., 2009), although the reproductive term moves mass down rather than up the spectrum. This led to a modified equation which incorporated the reproductive process into the population dynamics (4.5).

When performing numerical integrations of the system, a power-law steady state was attained when reproduction was spread equally across the year (Figure 4.5) with a discontinuity between the plankton and consumer spectra. Realistic parameter values were chosen, and the discontinuity did not cause fluctuations as in other work (Rochet and Benoît, 2011), so this artifact did not affect the dynamics. Empirical spectra which measure abundances of newborn larvae are uncommon, and so reductions in abundance when moving between different taxonomic groups may exist; rigorous sampling at the size of larvae is needed to test this.

The value used for the feeding efficiency K (estimated to be around 0.1-0.2 for aquatic species, see Paloheimo and Dickie (1966)) was larger than expected to assure positive overall growth for organisms with constant reproduction. Recent work by Hartvig et al. (2011) suggest a higher assimilation efficiency when dynamic action, excretion and egestion are accounted for. The energetic trade-off in the adult life stage should be explicitly modelled in future work, to account for maturation of organisms. An arbitrary value for the maturity weight x_m of approximately 60g was chosen here, although variation between species is high, and has been linked to the asymptotic weight (Beverton, 1992). An improvement to the model would thus be a multi-species spectrum (each species having its own maturity, reproductive schedule and asymptotic weight) where species are allowed to feed upon each other, such as those studied by Andersen et al. (2009). The success of species with different spawning behaviour could be compared, and the dynamics of predation would be more robust than the simplistic model here, where predator abundance decreased at times when reproduction did not occur. Coexistence and stability of multi-species spectra can be difficult to achieve, and a recent model (incorporating constant reproduction) used random coupling strengths between species until stability was established (Hartvig et al., 2011).

Making reproduction a seasonal process induces waves of biomass which move up the size spectrum, as the population of offspring rises and falls throughout the year (Figure 4.7). Waves of abundance have been observed in the past (Law et al. (2009), Chapter 1) when parameter values were chosen which destabilised the steady state distribution. Adding a plankton bloom has a similar effect, as organisms whose feeding range lies within the plankton spectrum are subject to higher growth rates (Benoît and Rochet (2004); Maury et al. (2007a), Chapter 3). Here it was observed that seasonal forcing via the reproductive process also pushes the system away from the steady state. With both plankton blooms and time-dependent reproduction occurring si-

multaneously, departures from the well-established power-law distribution (Sheldon et al., 1972) are expected. Real systems show greater variation when observations are recorded without averaging results temporally or spatially (e.g. Heath, 1995; Barnes et al., 2011).

An important feature of the reproductive model used here is the ability for organisms to have negative overall growth rates (i.e. lose mass) during the reproductive period (Figure 4.8). Previous models used biomass from predation to produce offspring (e.g. Blanchard et al., 2011; Hartvig et al., 2011; Plank and Law, 2011). The difference in the model here is the disaggregation of instantaneous growth rate and reproductive rate. The conjecture behind making the reproduction growth-independent is that spawning is generally fixed to a certain period of the year for some fish species (Durant et al., 2007). Other models have also enabled organisms to lose weight during reproduction; for example, Persson et al. (1998) incorporated a discrete reproductive period once a year, where all offspring for that year were produced at the same time in the spring. For this, "reversible mass" was built up over the rest of the year which could be lost in reproduction (or used for metabolism in the case of low food supply), as opposed to "irreversible mass" which made up the bones and organs and was assumed not to decrease. A loss in weight has been observed in sticklebacks during the reproductive period (Wootton, 1977), supporting the qualitative nature of the results.

It has been shown that recruitment to the adult population depends on the growth and death rates that larvae are subject to (Cushing and Horwood, 1994; Beaugrand et al., 2003; Platt et al., 2003). Variability in larval mortality has also been linked to the width of the spawning window (Mertz and Myers, 1994). This was observed in the numerical simulations (Figure 4.9); offspring born after the plankton bloom had a higher survival rate, although did not grow as fast. Conversely, being born close to the bloom promoted fast growth but a higher death rate. Overall the biomass was maximised by being born prior to and close to the peak of the bloom, with a sharp drop in biomass following the bloom (Figure 4.9c). Platt et al. (2003) observed unusually high levels of recruitment in years where the plankton bloom was early, and it was postulated that fish which spawned over a longer period of time (hence both earlier and later in the year) resulted in larvae which avoided high starvation mortalities after the bloom ended. The dynamics of the consumer spectrum were heavily affected by the time-dependent reproduction boundary in our model; in reality, different fish species spawn over different periods of time (see Appendix 4.5), so a dip at the beginning of the consumer spectrum for most of the year is unrealistic.

The optimum strategy for recruitment is still unclear from the results of the analysis; as mortality in the early life stages of fish is high (Duarte and Alcaraz, 1989; Leggett and Deblois, 1994), recruitment is unlikely for the average larva (Pitchford et al., 2005), and thus fewer larger organisms may be more likely to be recruited than many smaller

organisms. Spawning over shorter periods of time resulted in lower average amounts of biomass after 0.1 years (roughly 37 days, an appropriate amount of time to reach recruitment, see Houde (1989); Searcy and Sponaugle (2000)) but higher variability in the size range within the cohort. This is in agreement with the model findings of Mertz and Myers (1994), who found recruitment variability increased as spawning duration decreased, and empirical data showing stronger size classes where spawning was more peaked (Johnson, 2000). However, it is still unclear whether fewer large individuals or greater numbers of small individuals are more likely to be recruited from this model. An extension of the model would be to allow offspring to grow sufficiently to reach maturity. Running the model over several decades, it could be observed how recruitment and community abundance varied in the long-term when timing the reproductive period away from, or close to the plankton bloom.

There is still work to be done to prove or disprove the match/mismatch hypothesis of Cushing (1990) and alternate hypotheses subsequently proposed (see Durant et al., 2007). Models have shown a variety of factors important in reaching maturity: for some models growth rate is the most important factor in recruitment (Meekan and Fortier, 1996), while others have concluded mortality in the larval stage as the more important factor (Rice et al., 1993). Other factors such as climate and hydrodynamics have been studied to investigate the interannual variability in larval recruitment (Houde, 1989; Durant et al., 2007). The role of mortality (from starvation and predation) on the survival of larvae is less documented empirically than the growth process (Leggett and Deblois, 1994), and further work investigating the temporal changes in mortality will lead to a greater understanding of the tactics to maximise survival in dynamic size-structured communities. What has been presented here is a first step towards more general approaches to simulating seasonal reproduction.

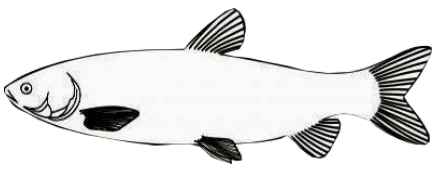

4.5 Appendix: Reproductive periods for North Sea species

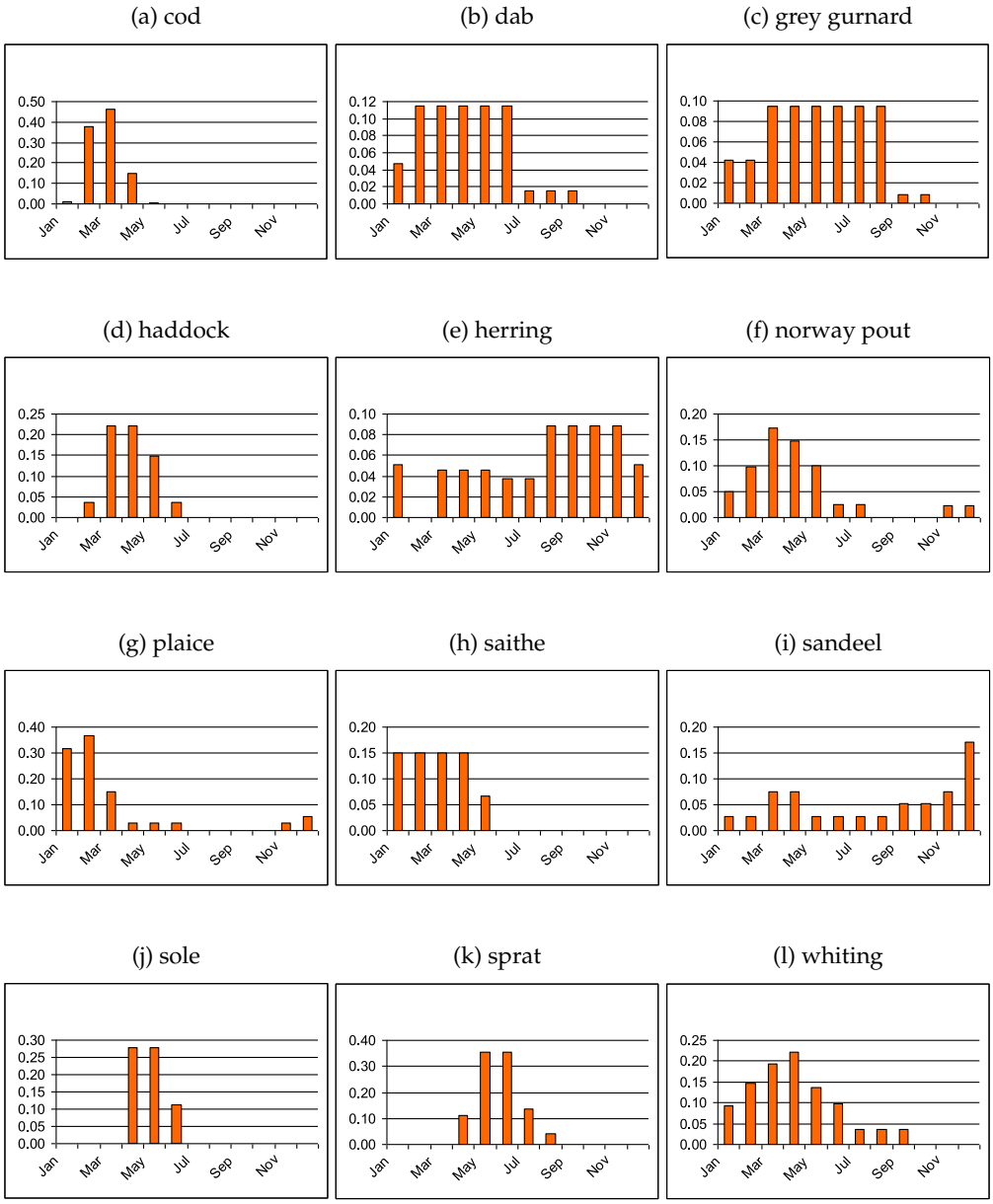

Figure 4.11: The variety in spawning periods of twelve common fish species in the North Sea, aggregated from Bowers (1954); Quéro (1984); Alheit (1988); Knijn et al. (1993); Albert (1994); Brander (1994); Hunter et al. (2003).

Concluding Remarks

Marine ecosystems are an important source of food, employment and economic growth for humans (FAO, 2010) and have been heavily exploited within the last century, leading to recent stock collapses (Longhurst, 1998; FAO, 2010; Hutchings and Rangeley, 2011). Furthermore, the wider effects of overexploitation have included large-scale alterations in fish communities and whole ecosystems (Jennings et al., 2002a; Salomon et al., 2008). The density of large predators at high trophic levels has decreased due to increasing fishing effort, leading to altered size compositions of fish communities with higher proportions of smaller organisms (Bianchi et al., 2000). In order to interpret and predict the consequences of human-induced changes, an understanding of the fundamental processes that drive the dynamics of marine ecosystems is needed, including their natural variation and resilience to different types of perturbations. Size-based models have been widely used to simulate the basic life processes that organisms in aquatic environments are subject to, and for understanding community level responses to perturbations (Silvert and Platt, 1978; Camacho and Solé, 2001; Andersen and Beyer, 2006; Maury et al., 2007a; Law et al., 2009; Hartvig et al., 2011). In this thesis a mathematical perspective was taken to improve understanding and further develop size-based models and theory. The motivation for modelling ecosystems in this way was the evidence of size-based behaviour observed widely in aquatic systems (Sheldon et al., 1972; Ursin, 1973), coupled with the need to make progress from an analytical viewpoint, which is difficult when using complex models that comprise all species and their separate size distributions.

There are important lessons to be learned from the work contained in this thesis, both in the context of size spectra and the wider field of ecology. These include: (1) the need for a mechanistic approach when modelling life processes of organisms, and to begin with individual-level interactions before scaling up to the community (Chapter 1), (2) new insights about the stability of size-structured communities, and analytical explanations for the effect of feeding parameters on stability (Chapter 2), (3) improved understanding of the consequences of seasonal perturbations from phytoplankton blooms on the dynamics of the size spectrum (Chapter 3), (4) a size-based analysis of the match/mismatch hypothesis including the seasonal timing and duration of reproduction, and the importance of predation mortality on cohort survival

(Chapter 4).

Size-based feeding is common in aquatic systems (Cohen et al., 2003), and linear trends in biomass in logarithmically increasing weight brackets have been observed in marine communities (Sheldon et al., 1972; Jennings and Mackinson, 2003). These observations have led to much work developing size-based models to simulate marine ecosystems. There are several factors allowing the species of organisms to be ignored in favour of body mass (or any other indicator of size, e.g. length, volume, equivalent spherical diameter for plankton); these include cannibalism, cross-predation and organisms growing up to six orders of magnitude over their lives (Cushing, 1975). The same arguments often do not apply for terrestrial systems; although size has been shown to be an important factor in prey selection for predators in terrestrial food webs (Cohen et al., 1993; Brose et al., 2006a), size-based feeding holds to a higher degree in marine systems, particularly in pelagic systems spanning in size from small zooplankton up to large fish predators. Factors such as group hunting strategies, strong interaction strengths between particular species, and asymptotic size being reached at an early life stage, may be more commonplace for terrestrial species. Thus size-based modelling may be less appropriate for terrestrial systems, and the conclusions reached in the thesis may be restricted to aquatic systems where many processes are strongly governed by size.

Accurate modelling of growth is needed in size spectrum models

The McKendrick-von Foerster equation (1.14) is widely used in size spectrum models (e.g. Benoît and Rochet, 2004; Andersen and Beyer, 2006; Law et al., 2009), to simulate the growth process. The equation was originally conceived to model the age distributions of individuals through time (McKendrick, 1926), with the convenience that age and time evolve at the same rate. The life expectancy of an individual is dependent upon the cumulative death rate across time: simple assumptions about reproduction and death were made to derive a steady state for the model (von Foerster, 1959).

The application of the McKendrick-von Foerster equation to model weight distributions seems intuitive. Platt and Denman (1978) were first to use a flux term to describe growth through the size spectrum, the logic being that biomass generally moves up the size spectrum, with large organisms eating small ones. While the assumption is reasonable, modelling growth in this fashion eliminates any variability in the growth trajectory of individuals; a group of organisms starting at the same weight in the size spectrum grow at identical rates over time. This may not be representative of marine organisms; fish larvae have low food supply and high mortality rates (Cushing, 1975; Cushing and Horwood, 1994), and stochastic models have emerged to take into account individual-based variability in growth (Beyer and Laurence, 1980; Pitchford

et al., 2005; Burrow et al., 2011).

A simple stochastic process of one organism eating another in order to grow larger was introduced in Chapter 1, and the macroscopic model for dynamics was derived from the master equation. The jump-growth equation (1.12) allows organisms to grow different amounts depending upon the size of their prey, which is intuitive: given a constant feeding efficiency, eating prey twice as large means growing by twice the amount. This model more accurately captures the feeding process of aquatic organisms, and a power-law steady state solution can be derived using size-based feeding (Section 1.2.6). The link to the McKendrick-von Foerster equation is shown via a Taylor expansion in Section 1.2.5: for size spectra close to equilibrium and where prey are on average much smaller than their predators, the McKendrick-von Foerster equation is an appropriate approximation to use. These conditions do not always hold, and empirical data has shown both varying abundance over time (Boudreau and Dickie, 1992; Heath, 1995; Li, 2002; Zhou et al., 2010) and reduced predator:prey mass ratios for lower predator masses (Barnes et al., 2010). In cases such as these the McKendrick-von Foerster equation may be a less useful tool for representing the feeding process, as individuals may grow significantly within a single feeding event. The invariance in growth for individuals can lead to an overestimate of numerical instability in comparison to the jump-growth equation (Figure 1.4), which could be mistaken for biological properties of the system. In these instances the jump-growth equation (or a higher order approximation) are necessary to capture feeding behaviour more accurately.

Variation in growth stabilises the size spectrum

Time-averaged power-law distributions can be observed upon aggregating data (e.g. Boudreau and Dickie, 1992; Barnes et al., 2011), and a power-law steady state has been proven analytically (Platt and Denman, 1978; Camacho and Solé, 2001; Benoît and Rochet, 2004, Chapter 1). However, contrary to the evidence to suggest marine systems are at steady state, perturbations to aquatic ecosystems occur due to various biotic and abiotic factors. These include temperature, plankton blooms and fishing (Hutchings and Myers, 1994; Echevarria and Rodriguez, 1994; Bianchi et al., 2000). The literature reports an increasing variation in fished populations compared to unexploited populations (Hsieh et al., 2006; Anderson et al., 2008), with the latter providing hypotheses for the observed increase; these include fluctuating fishing levels leading to higher variability in population size, and truncation effects of removing the largest individuals of species.

The stability analysis carried out in Chapter 2 is the first that I am aware of in the context of size spectrum models; numerical local stability analyses of size spectra have previously been carried out (Law et al., 2009; Blanchard et al., 2011). Stability analyses

of food web models (which generally involve a finite number of nodes corresponding to different species or functional groups) have been carried out previously (see e.g. Brose et al., 2005a; Rooney et al., 2006). For size spectra the difference is that there are an infinite number of 'nodes' as a continuous weight scale is instead considered. A previous stability analysis, performed by Arino et al. (2004), also used a continuous weight scale for the analysis, although there growth was not explicitly linked to predation, and feeding was only a function of the predator size rather than predator:prey mass ratio. It can thus be argued that the analysis in Chapter 2 models predator-prey interactions more realistically, although certain parameter restrictions were required to carry out the analysis.

Adding a diffusion term to the McKendrick-von Foerster equation (2.3) allows a cohort of organisms to spread out in weight when feeding, rather than following a fixed trajectory. This allows for stochasticity due to both environmental and demographic sources (Pitchford et al., 2005; McKane and Newman, 2005). In Chapter 2 the diffusion term had the effect of stabilising the system to short wave perturbations (Figures 2.1, 2.2), due to the presence of the non-oscillatory $-k^2$ term in (2.26). Thus stable eigenvalue spectra were achieved with the equation with diffusion and the full jump-growth model, but never with the McKendrick-von Foerster equation. Similarly, Benoît and Rochet (2004) had to incorporate a diffusion term into feeding in the absence of non-predation mortality for the community to persist in their model. Adding diffusion is a simple, yet mathematically derived, method to account for stochasticity within the feeding process of aquatic organisms.

The eigenvalue spectra were more closely correlated with those of the jump-growth equation than those of the McKendrick-von Foerster equation without diffusion, as expected of a higher-order approximation (Figures 2.1, 2.2). The jump-growth equation was derived as a deterministic equation specifically to model the generic feeding process of marine predators that primarily feed according to body size (such as many fish and pelagic invertebrate species), and hence should be taken as the yardstick for comparing other size-based predation models to. An issue when running the equation numerically is the fine discretisation required to ensure non-zero growth for reasonable parameter values (see Section 1.4). In this sense the McKendrick-von Foerster equation with diffusion can be seen as a compromise of modelling the predation process with numerical accuracy, while avoiding the high computational power needed to reasonably run the full jump-growth model.

Smaller feedback loops stabilise size spectra

The feeding parameters tested in Chapter 2 consisted of: the feeding efficiency, the preferred predator:prey mass ratio, and the diet breadth. Stability was shown to in-

crease in cases where feeding efficiency was high, predator:prey mass ratios were small and diet breadths were broad. Chapter 3 displayed a tendency for perturbations (caused by phytoplankton blooms) to move through the spectrum faster when efficiency was higher, and for the amplitude to be reduced when feeding was more localised (results not shown).

All three observations can be explained by feedback processes: the longer an organism takes to grow from weight y to weight x which feeds upon y, the larger the feedback loop is, which can potentially destabilise the system (Blanchard et al., 2008). From the form of the growth rate (3.3) it is clear that organisms will grow through the spectrum faster with increasing efficiency K (this is also intuitive). Low predator:prey mass ratios and broad diet breadths will reduce the average distance between prey and predator weights, thus reducing the feedback of individuals being removed by the predation process.

Previous numerical work has shown that increasing predator:prey mass ratios can destabilise the power-law steady state of size spectra (Blanchard et al., 2008), and with certain parameter values lead to travelling waves (Law et al., 2009, Chapter 1). An empirical analysis of 74 sites across the North Sea also revealed a tendency for more stable environments to have lower mass ratios (Jennings and Warr, 2003), supporting the numerical results found in Chapters 1, 2 and 3.

Interestingly, Brose et al. (2006b) found that in complex food web models, stability (i.e. where all species in the web persisted) rose with increasing predator:prey mass ratio, which was hypothesised to lower the per unit biomass interaction strength between predators and prey (Yodzis and Innes, 1992; Brose et al., 2005a). This result agreed with the proposal of May (1972) that lowered interaction strengths increase food web stability. The result seems to contradict the observation in size spectrum models that lower predator:prey mass ratios are stabilising. In fact the situation is more complicated. Comparison of the results of Brose et al. (2006b) with the size-based distributions used in this thesis is possible by discretising the continuous size range into N countable nodes (each node y_i representing a body mass range $[x_i, x_i + \delta x)$ rather than a species), and adding links between nodes where the feeding kernel is non-negligible. Lowering the average interaction strength I in the discretised distribution is achieved by increasing the diet breadth σ, but this also raises the number of links from each node (and hence the probability P that two nodes will interact). The stability condition of May (1972) states stability is likely if $I < 1/\sqrt{NP}$, so closer examination is required before any conclusions about agreement can be drawn. Nevertheless, stability was observed to be enhanced by high values of σ in the models used in this thesis. Also, in the discretised distribution the biomass at node y_i scales with $e^{(2-\gamma)x_i}$; in the case $\gamma = 2$ there are invariant amounts of biomass at each node, so the consumption rate is independent of β, an observation which separates the size-based models of this

thesis and the complex food webs of Brose et al. (2006b). It is clear that predator-prey interactions are non-trivial, and further work should shed light on how size-based feeding affects size spectrum dynamics.

Phytoplankton blooms lead to perturbed size spectra

Phytoplankton abundance can vary little over time, or be subject to seasonal blooms (Frost, 1991). These blooms manifest themselves in the springtime (e.g. Navarro and Thompson, 1995; Wang et al., 2006; Zhou et al., 2010) and, to a lesser extent, in the autumn (Herring, 2002; Kaiser et al., 2005; Findlay et al., 2006). The mechanisms of how blooms occur are well understood, and the combination of nutrients, advection and sunlight that are involved are not studied in this thesis (see e.g. Kaiser et al., 2005). I chose instead to focus on the net effect: a temporal rise in phytoplankton abundance, and the consequences for a size-spectrum model of these seasonal perturbations.

To incorporate phytoplankton blooms a von Mises distribution was selected (Pope et al., 1994), for its similarity in shape to recorded temporal abundance data (Navarro and Thompson, 1995; Irigoien et al., 2005). The method in Chapter 3 followed the work by Pope et al. (1994), but importantly with a dynamic consumer spectrum rather than a fixed background spectrum for the weight distribution. The subsequent dynamic size spectrum showed behaviour approximating that of empirical spectra measured across time (Heath, 1995), where peaks of abundance moved up through the spectrum by predation, followed closely by a trough of abundance. Temporal and spatial averaged spectra (e.g. Kamenir et al., 2004; Cermeño et al., 2006) often smooth over these perturbations, although spectra sampled at certain points in time reveal seasonal oscillations in abundance (e.g. Figure 5b of Zhou (2006), Figure 9 of Zarauz et al. (2009), Figure 5a of Schartau et al. (2010)).

For all blooms introduced to the system, an increase in the abundance of the consumer spectrum was observed. The same observation was assumed by Pope et al. (1994), and has been observed both in models and empirically (e.g. Benoît and Rochet, 2004; Maury et al., 2007a; Zhou et al., 2010; Blanchard et al., 2011). The perturbations tended to dampen and spread out as biomass shifts up the size spectrum via predation, due to feeding by larger organisms and variation in growth caused by the diffusion term in the model. A return to the steady state was observed for all spectra following the bloom, provided no further blooms were introduced; in reality, annual phytoplankton blooms are a component of many marine ecosystems, so the concept of a steady state may be misleading in such environments.

A simple fixed boundary condition between the autotrophic phytoplankton spectrum and heterotrophic consumer spectrum was assumed in Chapter 3, and a dynamic reproductive boundary was introduced in Chapter 4. These simple boundary condi-

tions enabled interpretations of the responses of the consumer spectrum to seasonal "bottom-up" effects to be made. Other studies have extended work on dynamic producer (or background) spectra with a variety of methods. Semi-chemostatic growth has been assumed to allow feedback between predation by consumers and the abundance of the producer spectrum (e.g. De Roos and Persson, 2002; Hartvig et al., 2011). Other studies provided detailed coupling between nutrient levels and phytoplankton, zooplankton and fish spectra (Baird and Suthers, 2007; Stock et al., 2008). Both nutrient and sunlight levels were simulated by Fuchs and Franks (2010) for a detailed investigation of phytoplankton - zooplankton dynamics. Further work is required in investigating the links in dynamics between phytoplankton, zooplankton and predators to understand the nature of bottom-up perturbations in size spectra better. Adding complexity to the basic size spectrum model introduced here will improve knowledge of the dynamics involved in biomass transfer to larger organisms, and thorough examination of temporal data is required.

Successful cohorts are born prior to the phytoplankton bloom

The match/mismatch hypothesis, first conceptualised by Hjort (1914), predicts that survival at the early life stages of fish species is an important determinant of year-class strength. It postulates that planktonic food availability at the time when larvae exhaust the egg yolk supply and switch to external feeding is critical in the survival of larvae to recruitment. The term 'match/mismatch' was coined by Cushing (1975) to highlight the possibility of the spawning period of fish to time with the peak of zooplankton abundance (match) or away from the peak (mismatch). Larval mortality is variable depending upon the synchrony of these two periods, as larvae with insufficient food are more susceptible to starvation and grow more slowly, increasing vulnerability to predation. Due to high larval mortality, Mertz and Myers (1994) propose that "the larval stage may be the principal determinant of year-class strength" (also see Chambers and Trippel, 1997; Horwood et al., 2000).

Empirical studies have been carried out due to debate over the plausibility of the match/mismatch hypothesis. Recruitment in cod has been linked to variation in the timing of reproduction with the planktonic prey peak (Beaugrand et al., 2003), and larval growth rate has been shown to correlate strongly with prey biomass (Buckley and Durbin, 2006; Koeller et al., 2009). Platt et al. (2003) used surveys measuring both juvenile abundance of haddock from 1970, and the timing of the plankton bloom each year from ocean colour sensors, in order to measure the correlation between the survival of year classes and the timing between the spawning and bloom period. Most of the variation in larval survival (89%) was explained by the timing of the springtime plankton bloom. Durant et al. (2007) extended the match/mismatch hypothesis by investigating its applicability to terrestrial systems.

In Chapter 3 cohort biomass after 0.1 years was maximised by being born slightly prior to the phytoplankton bloom (Figure 3.10), due to an increased growth rate once the bloom was introduced (Figure 3.7) combined with a lower predation rate than cohorts born during the bloom were subject to. A marked increase of the predators of offspring was observed during the bloom, leading to a higher death rate (Figure 3.9a), and the most successful cohort avoided this through fast growth to advance ahead of the predator range (Figure 3.11). Interestingly, Platt et al. (2003) found that in both 1981 and 1999, where the survival of haddock larvae was exceptionally high, the plankton blooms were observed to be unusually early. They hypothesised that adult haddock may have begun to spawn earlier in the year (and for a longer duration), so that fewer of the total number of larvae perished from starvation (although starvation mortality was not measured to validate this). From Figure 3.9 the death rate for larvae born before the bloom is not as severe as after the bloom has initiated, so the empirical findings of Platt et al. (2003) are consistent with the results in Chapter 3.

Explicitly modelling the reproductive process adds an additional feedback to the model, with only organisms above a threshold weight x_m able to reproduce. Reproduction in size spectrum models has mostly been modelled as a constant process, with no time dependence (e.g. Shin and Cury, 2004; Maury et al., 2007a; Blanchard et al., 2011; Hartvig et al., 2011; Plank and Law, 2011). Here, for the first time in a dynamic community size spectrum model, the reproductive period is limited to certain times of year and is independent of growth rate. Many fish species exhibit spawning seasons with different timing and durations; some fish species reproduce fairly constantly over the course of the year (for example, herring and sandeel), while other species have extremely peaked reproduction over only two or three months, such as cod and haddock (Quéro, 1984; Rice et al., 1993). Thus the match/mismatch hypothesis seems more appropriate for these latter species (see Meekan and Fortier (1996) for one such analysis on Atlantic cod) than for non-seasonal spawners. Appendix 4.5 shows spawning periods of 12 common North Sea species.

Adding time dependence to the influx of consumers perturbed the spectrum, as expected (Figure 4.7); along with plankton blooms, this is another example of a bottom-up effect that marine systems are subject to. The growth rate of mature organisms was observed to decrease during the reproductive period, as resources are diverted to producing offspring (Figure 4.8), characterised by a drop in mass over the spawning period (Wootton, 1977). When investigating the effect of reproductive period on cohort growth and survival in the seasonal spectrum, high rate of both growth and death were observed during the bloom period (Figure 4.9a, b). This agrees with observations from the previous chapter (Figures 3.7a and 3.9a). Overall biomass remaining after 0.1 years was observed to reach a maximum leading up to the peak of the plankton bloom (Figure 4.9c), where growth rates were highest, leading to the conclusion that being born leading up to the peak of the bloom maximised cohort abundance over time, a

result mirrored in recent empirical data (Platt et al., 2003; Buckley and Durbin, 2006).

Pitchford et al. (2005) highlight that as recruitment is an unlikely event for an individual larva, deterministic models may not adequately capture the randomness involved in larval survival. From the results of Figure 4.10, making the spawning period shorter and sharper resulted in lower mean cohort biomass, yet increased the variability in biomass, meaning a small number of individuals were able to grow significantly. It is not obvious which individuals are more likely to reach recruitment, as mortality is observed to decrease with body weight, both in the model (3.14) and in observations of real systems (Bradford, 1992; Puvanendran and Brown, 1999). The growth trajectories of cohorts must be followed for longer periods of time to establish recruitment probabilities, and predation mortality must be made explicitly time-dependent in models. Results from this early work are the first stage of further studies required to answer the question of reproduction timing and its consequences.

Factors aside from prey availability will influence the survival of fish larvae, and authors have criticised the match/mismatch hypothesis for ignoring other processes involved in successful recruitment (e.g. Leggett and Deblois, 1994). Empirical studies have been conducted which show no significant correlation between the timing of reproduction and bloom periods and larval survival (Bollens et al., 1992; Johnson, 2000). Buckley and Durbin (2006) reported that, although strong correlations were observed between the timing of *Pseudocalanus* blooms and larval growth, aggregating the four main copepod species present showed a weaker correlation, and abundance of *Calanus finmarchicus* alone were unrelated to growth rate. This highlights how the knowledge of prey selection can impact on interpretations from empirical data, and is an example of the importance of specific species links, even in marine systems where size-based interactions are thought to be dominant. Other factors such as potential energy gain and morphological relationship between predators and their prey influence the choice of prey (Gill and Hart, 1994). The importance of photoperiod and water temperature in larval survival are also cited, and the difficulties of adequately sampling prey abundance (Buckley et al., 2006).

Alternative hypotheses have been suggested to explain observed variations in year class strength, such as the member-vagrant hypothesis of Sinclair (1988). He postulates that the survival of offspring populations are attributed to the numbers of ”member” larvae remaining together in geographical space over time, minus ”vagrants” which become separated by advection currents in the ocean. Platt et al. (2003) emphasised the need for data which adequately captures fine-scale spatio-temporal processes at the correct time of sampling the fish eggs / larvae and geographical location (thus requiring an understanding of oceanographic processes, such as currents and turbulence). A summary of alternate hypotheses is provided by Durant et al. (2007). Thorough testing of hypotheses with high resolution data will yield a greater

understanding of the important life processes involved in larval survival and year class strength.

Limitations and improvements of the work presented

In this thesis a deeper mathematical understanding of the dynamics driving community size spectra has been achieved, and results obtained (both analytically and numerically) have been in agreement with observations of real community size spectra and previous modelling work. Although size-based modelling can explain many of the patterns observed in aquatic communities, there are drawbacks and limitations of the approach.

One of the key assumptions made when adopting the size spectrum method was to ignore species and classify organisms by their weight only. This allows conclusions to be drawn at the community level, i.e. the biomass distribution of an ecosystem as a function of body weight regardless of species, and the response of the spectrum to environmental effects dependent only on body weight. For example, fish species have different asymptotic sizes (Figure 3.8) and reproductive periods (Appendix 4.5), which were fixed at "average" community values in the work presented here. In order to expand knowledge of more in-depth processes, working with multiple populations and/or further disaggregation of organism traits may be needed to accurately model the dynamics. The analytical understanding of the dynamical processes gained in this thesis would be difficult with more complex models that contain species identities and their size distributions. The community-based approach has helped to gain more in-depth mathematical insight into community size spectrum models, which are being used to try to inform "an ecosystem approach" via the use of size-based indicators for tracking community and ecosystem-level impacts (e.g. Bianchi et al., 2000; Shin et al., 2005; Pope et al., 2006).

Multi-species models have been compared to single species models from a fishing perspective (Hollowed et al., 2000), where it was concluded that predation mortality varied little temporally in most systems, and multi-species models need to take size structure (as well as spatial effects and abiotic factors) into account. Size spectra have been modelled with multiple populations interacting, each with species-specific traits such as maturation, asymptotic mass and rates for life processes (De Roos and Persson, 2001; Pope et al., 2006; Blanchard et al., 2011). De Roos and Persson (2002) incorporated a physiological structured population model (dubbed the 'Escalator Boxcar Train' method, see De Roos (1988)) to model a three-component system consisting of size-structured predator and consumer populations and an unstructured resource population. A model describing the effect of fishing on size-structured populations was incorporated by Pope et al. (2006), although growth for the 13 species

studies was determined by von Bertalanffy growth curves, and not linked to predation (whereas mortality rates were dependent on predator abundance). Their results were in agreement with empirical and modelling observations of steeper size spectrum slopes emerging from heavily exploited systems (Bianchi et al., 2000; Shin et al., 2005). More recently, theoretical work has incorporated growth from predation into size spectrum models which model the interactions between 'species' as defined by a single life-history trait, asymptotic body size (Andersen and Beyer, 2006; Andersen et al., 2009). More recently, the work has been extended to explicitly model the dynamics and physiological processes of these species including reproduction (Andersen and Pedersen, 2010) and, by using random interaction matrices, equilibrium states have been reached (Hartvig et al., 2011). The multi-species spectra investigated allow inferences to be made at both the community level and individual species level and is a quickly progressing area of research.

The closed form expressions derived in this thesis allowed the power-law steady state to be analysed, and to quantify the dependence of stability upon feeding parameters (Chapter 2). To keep the dynamic size spectrum model simple and allow analytical progress to be made, many of the parameters in the system were assumed to be constant, and only body mass distinguished individuals in the spectrum. There is evidence of changing predator:prey mass ratios and feeding efficiency as body size increases (Barnes et al., 2010), and choosing functions (with weight as the variable) for these and other parameters is a simple step that could be taken to add more realism to the model. Other traits may be species-specific, rather than size-based, so it is important to gain understanding of the important factors affecting ecosystem stability and dynamics. Metabolism has been modelled simplistically in the work presented here, as an allometric function scaling with body weight in the feeding kernel. Many life processes have been shown to scale with body size (Peters, 1986; Brown et al., 2004), and in-depth analyses of basic functions of organisms at a cellular level could yield valuable results for size spectrum models. Although egg size has been shown to vary little between marine teleost fish species (Ware, 1975; Cury and Pauly, 2000), evidence suggests that winter and spring spawners produce larger eggs, and for batch spawners to produce progressively smaller eggs over the summer (Ware, 1975). Alternative studies link egg size to pelagic / demersal spawning (Duarte and Alcaraz, 1989). This is just one example of species-specific traits which could be integrated into a multi-species model; others include asymptotic weight (as used by Hartvig et al. (2011)), swimming speed and species-specific feeding rates.

Phytoplankton have not been modelled dynamically in the studies in this thesis. In Chapter 1 the phytoplankton spectrum was held constant and in Chapters 3 and 4 a time-dependent bloom was introduced, although this was done independently of the abundance in the consumer spectrum. Simple non-dynamic models for the producer spectrum were used to analyse the behaviour of seasonal forcing on the consumer

spectrum, without explicitly modelling the various factors which trigger blooms such as temperature and nutrients. Other studies have used semi-chemostatic models for the producer spectrum, to enable the abundance to drop by predation and rebuild from population growth and invasion (e.g. De Roos and Persson, 2002; Hartvig et al., 2011). The dynamics of nutrient levels on the abundance of producers has been modelled; Irwin et al. (2006) used a constant nutrient influx with logistic growth to model phytoplankton abundance, while more complex dynamics have been incorporated into models with phytoplankton, zooplankton and fish spectra (Baird and Suthers, 2007; Stock et al., 2008). A benthic size spectrum consisting of detritivores was modelled by Blanchard et al. (2009), although the plankton spectrum was held constant in simulations. Temperature and sunlight are also important factors in the emergence of blooms, and the modelling of these in conjunction with nutrient levels should provide robust models for phytoplankton abundance (see Fuchs and Franks, 2010); recent work has also linked size spectrum slopes to a dynamic model of phytoplankton and nutrients using remote sensing (Roy et al., 2011). Another subject of interest associated with phytoplankton spectra is coagulation, and the role it plays in observed size-abundance patterns (Jackson, 1995; Li and Logan, 1995; Mari and Burd, 1998). It would be valuable to see what effects (if any) this would have on the shape and slope of the size spectrum.

As well as modelling the phytoplankton spectrum separately from the dynamic consumer spectrum, there are reasons to support disaggregating the zooplankton from other marine predators. Zooplankton have a maximum weight much lower than fish species (approximately in the order of 1g, see Zhou et al. (2009)), feeding primarily on phytoplankton (Heath, 1995) and forming the majority of the diet of newly hatched fish larvae (Cushing, 1990). The debate spurred on by the last observation has led to PZF (phytoplankton - zooplankton - fish larvae) models to simulate explicitly the dynamics of the three interacting populations (e.g. Moloney and Field, 1991; Armstrong, 1994; James et al., 2003). However, there is little literature to describe size-based zooplankton spectra; Zhou et al. (2010) discuss a lack of models for describing details of life processes of zooplankton. Concerted efforts are being made to remedy this (see e.g. Stock et al., 2008; Fuchs and Franks, 2010), and connecting in a size-based way up to larger predators. Empirical studies focusing on the zooplankton spectra are not widely available (Heath, 1995), and more data needs to be made available before modelling efforts can be validated.

Environmental effects have not been extensively tested in the work presented here. Of particular interest in light of climate change is water temperature, and the impact on the life processes of aquatic organisms. Growth and fecundity have been shown to scale linearly with temperature (Hirst and Bunker, 2003), and temperature is intrinsically linked to physiological rates of organisms (Houde, 1989; Kooijman, 2009; Gillooly et al., 2001; Brown et al., 2004). This is integrated into size spectrum models,

for example, in that of Maury et al. (2007a). Scaling the three dynamic processes of death, growth and diffusion presented in the model used in Chapters 3 and 4 could provide valuable insight to the potential impacts of warming climates. Abiotic factors such as temperature, turbulence and upwelling are spatially affected, and incorporating this into the model would require extensive changes to the model setup. One of the main assumptions in deriving the jump-growth equation is that over large enough spatial scales, the numbers of organisms is proportional to volume. Once this is no longer the case, model assumptions will need to be re-evaluated. However, spatial effects are important: for example, sunlight, temperature and oxygen levels vary along the water column (Echevarria and Rodriguez, 1994). The added randomness of environmental variation means adding stochasticity to the model could be justified. The master equation approach used (van Kampen, 1992) in Chapter 1 to derive the deterministic model for predation (the jump-growth equation) also yielded a Fokker-Planck equation to describe the demographic fluctuations of the deterministic model, which scaled with the square root of the system size and hence was assumed to be negligible for a large enough community. Stochastic size spectra were run alongside the jump-growth equation and McKendrick-von Foerster equation to confirm observations from the two models (Section 1.3). In Chapter 2 it was concluded that demographic stochasticity had only small effects on the stability of the power-law steady state, and the fluctuations could be ignored. More work is required in order to determine the consequences of environmental effects using the models developed in this thesis.

To conclude, a size-based approach incorporating individual-level processes of predation, growth, death and reproduction has been constructed, and are consistent with empirical observations of the structure, dynamics and stability of marine community size spectra. Variable growth in size-based models has been shown to capture the feeding process more realistically; the McKendrick-von Foerster equation can often result in numerically unstable systems due to the rigid growth trajectories of organisms, which the diffusion term from the second order approximation remedied. To empirically test the findings in this thesis, high resolution temporal spectra could be sampled in the size range for pelagic fish species (e.g. 2-2048g as sampled by Jennings et al. (2002b)), to observe the possibility of waves of abundance moving through the spectrum, which were caused in numerical simulations by both unstable steady states and bottom-up seasonal effects. The importance of feedback loops in the stability of the studied models was not investigated in great detail. Analytical findings suggest that feeding over a wide weight range with low predator:prey mass ratios is stabilising, and temporal spectra could reveal higher variability in communities where the preferred mass ratio is higher. To further improve the simple models used to test the match/mismatch hypothesis, alternates such as the member/vagrant and stable ocean hypotheses could be tested; this would involve modelling spatial variation of

plankton abundance and simulating the effects of turbulence, as the majority of hypotheses for larval recruitment success are explained using mixing and upwelling processes in the ocean (see Durant et al., 2007). The importance of predation mortality in larval survival was concluded from the studies carried out in Chapters 3 and 4, and further in-depth analyses should be carried out on temporal variations in predator abundance, with the aid of real data of larval mortality following hatching. A combination of appropriate empirical data and theoretical model setups will facilitate a deeper understanding of recruitment variability.

"The man in black fled across the desert, and the gunslinger followed."

- Stephen King, **The Gunslinger** (1982).

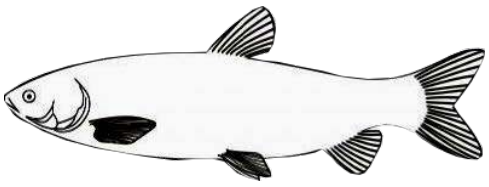

Bibliography

Albert, O., 1994. Biology and ecology of Norway pout (*Trisopterus esmarki Nilsson*, 1855) in the Norwegian Deep. ICES Journal of Marine Science 51 (1), 45.

Aldous, D. J., 1999. Deterministic and stochastic models for coalescence (aggregation and coagulation): a review of the mean-field theory for probabilists. Bernoulli 5 (1), 3–48.

Alheit, J., 1988. Reproductive biology of sprat (*Sprattus sprattus*): factors determining annual egg production. ICES Journal of Marine Science 44 (2), 162.

Allaby, M. (Ed.), 2010. A dictionary of ecology, 4th Edition. Oxford University Press, Oxford.

Andersen, K., Beyer, J., Lundberg, P., 2009. Trophic and individual efficiencies of size-structured communities. Proceedings of the Royal Society B: Biological Sciences 276 (1654), 109.

Andersen, K., Pedersen, M., 2010. Damped trophic cascades driven by fishing in model marine ecosystems. Proceedings of the Royal Society B: Biological Sciences 277 (1682), 795.

Andersen, K. H., Beyer, J. E., 2006. Asymptotic size determines species abundance in the marine size spectrum. The American Naturalist 168, 54–61.

Andersen, K. P., Ursin, E., 1977. A multispecies extension to the Beverton and Holt theory of fishing, with accounts of phosphorus circulation and primary production. Meddr Danm. Fisk.- og Havunders 7, 319–435.

Anderson, C. N. K., Hsieh, C., Sandin, S. A., Hewitt, R., Hollowed, A., Beddington, J., May, R. M., Sugihara, G., 2008. Why fishing magnifies fluctuations in fish abundance. Nature 452, 835–839.

Anderson, J. T., 1988. A review of size dependent survival during pre-recruit stages of fishes in relation to recruitment. Journal of Northwest Atlantic Fishery Science 8, 55–66.

Arino, O., Shin, Y., Mullon, C., 2004. A mathematical derivation of size spectra in fish populations. Comptes Rendus Biologies 327 (3), 245–254.

Armstrong, M. J., Connolly, P., Nash, R. D. M., Pawson, M. G., Alesworth, E., Coulahan, P. J., Dickey-Collas, M., Milligan, S. P., O'Neill, M. F., Witthames, P. R., Woolner, L., 2001. An application of the annual egg production method to estimate the spawning biomass of cod (*Gadus morhua* L.), plaice (*Pleuronectes platessa* L.) and sole (*Solea solea* L.) in the Irish Sea. ICES Journal of Marine Science 58, 183–203.

Armstrong, R. A., 1994. Grazing limitation and nutrient limitation in marine ecosystems: steady state solutions of an ecosystem model with multiple food chains. Limnology and Oceanography 39(3), 597–608.

Aulbach, B., Garay, B. M., 1993. Linearizing the expanding part of noninvertible mappings. Z. angew. Math. Phys. 44 (3), 469–494.

Bailey, K., Houde, E., 1989. Predation on eggs and larvae of marine fishes and the recruitment problem. Advances in Marine Biology 25, 1–83.

Baird, M., Suthers, I., 2007. A size-resolved pelagic ecosystem model. Ecological Modelling 203 (3-4), 185–203.

Bardos, D. C., 2005. Probabilistic Gompertz model of irreversible growth. Bulletin of Mathematical Biology 67, 529–545.

Barnes, C., Irigoien, X., De Oliveira, J., Maxwell, D., Jennings, S., 2011. Predicting marine phytoplankton community size structure from empirical relationships with remotely sensed variables. Journal of Plankton Research 33 (1), 13.

Barnes, C., Maxwell, D., Reuman, D., Jennings, S., 2010. Global patterns in predator-prey size relationships reveal size dependency of trophic transfer efficiency. Ecology 91 (1), 222–232.

Batten, S., Walne, A., Edwards, M., Groom, S., 2003. Phytoplankton biomass from continuous plankton recorder data: an assessment of the phytoplankton colour index. Journal of plankton research 25 (7), 697.

Beaugrand, G., Brander, K., Lindley, J., Souissi, S., Reid, P., 2003. Plankton effect on cod recruitment in the North Sea. Nature 426 (6967), 661–664.

Benoît, E., Rochet, M., 2004. A continuous model of biomass size spectra governed by predation and the effects of fishing on them. Journal of Theoretical Biology 226 (1), 9–21.

Bergenius, M., Meekan, M., Robertson, R., McCormick, M., 2002. Larval growth predicts the recruitment success of a coral reef fish. Oecologia 131 (4), 521–525.

Berlow, E., Neutel, A., Cohen, J., De Ruiter, P., Ebenman, B., Emmerson, M., Fox, J., Jansen, V., Iwan Jones, J., Kokkoris, G., Logofet, D., McKane, A., Montoya, J., Petchey, O., 2004. Interaction strengths in food webs: issues and opportunities. Journal of Animal Ecology 73 (3), 585–598.

Berryman, A., 1992. The orgins and evolution of predator-prey theory. Ecology 73 (5), 1530–1535.

Beverton, R., 1992. Patterns of reproductive strategy parameters in some marine teleost fishes. Journal of Fish Biology 41, 137–160.

Beverton, R., Holt, S., 1993. On the dynamics of exploited fish populations. Vol. 11. American Fisheries Society.

Beyer, J., 1989. Recruitment stability and survival: simple size-specific theory with examples from the early life dynamic of marine fish. Dana 7, 45–147.

Beyer, J., Laurence, G., 1980. A stochastic model of larval fish growth. Ecological Modelling 8, 109–132.

Bianchi, G., Gislason, H., Graham, K., Hill, L., Jin, X., Koranteng, K., Manickchand-Heileman, S., Paya, I., Sainsbury, K., Sanchez, F., Zwanenburg, K., 2000. Impact of fishing on size composition and diversity of demersal fish communities. ICES Journal of Marine Science 57 (3), 558.

Blanchard, J., Dulvy, N., Jennings, S., Ellis, J., Pinnegar, J., Tidd, A., Kell, L., 2005. Do climate and fishing influence size-based indicators of Celtic Sea fish community structure? ICES Journal of Marine Science: Journal du Conseil 62 (3), 405.

Blanchard, J., Law, R., Castle, M., Barnes, C., Jennings, S., 2008. Predator-prey size ratios, food web stability and the variability of marine fish populations. In: ICES Annual Science Conference. Halifax, Canada, pp. 1–24.

Blanchard, J., Law, R., Castle, M., Jennings, S., 2011. Coupled energy pathways and the resilience of size-structured food webs. Theoretical Ecology 4 (3), 289–300.

Blanchard, J. L., 2000. Maternal contribution to the reproductive potential of a recovering fish stock: variability in the fecundity and condition of haddock (*Melanogrammus aeglefinus*) on the Scotian Shelf. Master's thesis, Dalhousie University.

Blanchard, J. L., Jennings, S., Law, R., Castle, M. D., McCloghrie, P., Rochet, M., Benoît, E., 2009. How does abundance scale with body size in coupled size-structured food webs? Journal of Animal Ecology 78 (1), 270–280.

Bollens, S., Frost, B., Schwaninger, H., Davis, C., Way, K., Landsteiner, M., 1992. Seasonal plankton cycles in a temperate fjord and comments on the match-mismatch hypothesis. Journal of plankton research 14 (9), 1279.

Boudreau, P., Dickie, L., 1992. Biomass spectra of aquatic ecosystems in relation to fisheries yield. Canadian Journal of Fisheries and Aquatic Sciences 49 (8), 1528–1538.

Bowers, A., 1954. Breeding and growth of whiting (*Gadus merlangus* L.) in Isle of Man waters. Journal of the Marine Biological Association of the United Kingdom 33 (01), 97–122.

Bradford, M., 1992. Precision of recruitment predictions from early life stages of marine fishes. Fishery Bulletin - National Oceanic And Atmospheric Administration 90, 439–439.

Brander, K., 1994. The location and timing of cod spawning around the British Isles. ICES Journal of Marine Science 51 (1), 71.

Brose, U., Berlow, E., Martinez, N., 2005a. Scaling up keystone effects from simple to complex ecological networks. Ecology Letters 8 (12), 1317–1325.

Brose, U., Cushing, L., Berlow, E., Jonsson, T., Banasek-Richter, C., Bersier, L., Blanchard, J., Brey, T., Carpenter, S., Blandenier, M., Cohen, J., Dawah, H., Dell, T., Edwards, F., Harper-Smith, S., Jacob, U., Knapp, R., Ledger, M., Memmott, J., Mintenbeck, K., Pinnegar, J., Rall, B., Rayner, T., Ruess, L., Ulrich, W., 2005b. Body sizes of consumers and their resources. Ecology 86 (9), 2545–2545.

Brose, U., Jonsson, T., Berlow, E., Warren, P., Banasek-Richter, C., Bersier, L., Blanchard, J., Brey, T., Carpenter, S., Blandenier, M., Cushing, L., Dawah, H., Dell, T., Edwards, F., Harper-Smith, S., Jaob, U., Ledger, M., Martinez, N., Memmott, J., Mintenbeck, K., Pinnegar, J., Rall, B., Rayner, T., Reuman, D., Ruess, L., Ulrich, W., Williams, R., Woodward, G., J.E., C., 2006a. Consumer-resource body-size relationships in natural food webs. Ecology 87 (10), 2411–2417.

Brose, U., Williams, R., Martinez, N., 2006b. Allometric scaling enhances stability in complex food webs. Ecology Letters 9 (11), 1228–1236.

Brown, J., Maurer, B., 1989. Macroecology: the division of food and space among species on continents. Science 243 (4895), 1145.

Brown, J. H., Gillooly, J. F., 2004. Ecological food webs: high-quality data facilitate theoretical unification. Proceedings of the National Academy of Sciences 100(4), 1467–1468.

Brown, J. H., Gillooly, J. F., Allen, A. P., Savage, V. M., West, G. B., 2004. Toward a metabolic theory of ecology. Ecology 85, 1771–1789.

Buckley, L., Caldarone, E., Lough, R., St Onge-Burns, J., 2006. Ontogenetic and seasonal trends in recent growth rates of Atlantic cod and haddock larvae on Georges Bank: effects of photoperiod and temperature. Marine Ecology Progress Series 325, 205–226.

Buckley, L., Durbin, E., 2006. Seasonal and inter-annual trends in the zooplankton prey and growth rate of Atlantic cod (*Gadus morhua*) and haddock (*Melanogrammus aeglefinus*) larvae on Georges Bank. Deep Sea Research Part II: Topical Studies in Oceanography 53 (23-24), 2758–2770.

Burrow, J., Horwood, J., Pitchford, J., 2011. The importance of variable timing and abundance of prey for fish larval recruitment. Journal of Plankton Research (submitted).

Butler, G., Hsu, S., Waltman, P., 1983. Coexistence of competing predators in a chemostat. Journal of Mathematical Biology 17 (2), 133–151.

Camacho, J., Solé, R. V., 2001. Scaling in ecological size spectra. Europhysics Letters 55 (6), 774–780.

Capitan, J. A., Delius, G. W., 2010. Scale-invariant model of marine population dynamics. Physical Review E 81 (6), 061901.

Carpenter, S., Kitchell, J., Hodgson, J., Cochran, P., Elser, J., Elser, M., Lodge, D., Kretchmer, D., He, X., Von Ende, C., 1987. Regulation of lake primary productivity by food web structure. Ecology 68 (6), 1863–1876.

Cermeño, P., Marañón, E., Harbour, D., Harris, R., 2006. Invariant scaling of phytoplankton abundance and cell size in contrasting marine environments. Ecology Letters 9 (11), 1210–1215.

Chambers, R. C., Trippel, E. A., 1997. Early life history and recruitment in fish populations. Vol. 21. Springer.

Chase, J., 1999. Food web effects of prey size refugia: variable interactions and alternative stable equilibria. American Naturalist, 559–570.

Chen, X., Cohen, J., 2001. Global stability, local stability and permanence in model food webs. Journal of Theoretical Biology 212 (2), 223–235.

Cohen, J. E., Jonsson, T., Carpenter, S. R., 2003. Ecological community description using the food web, species abundance, and body size. Proceedings of the National Academy of Sciences (USA) 100 (4), 1781–1786.

Cohen, J. E., Pimm, S. L., Yodzis, P., Saldana, J., 1993. Body sizes of animal predators and animal prey in food webs. Journal of Animal Ecology 62, 67–78.

Cook, R. M., Sinclair, A., Stefansson, G., 1997. Potential collapse of North Sea cod stocks. Nature 385 (6616), 521–522.

Cózar, A., Echevarría, F., 2005. Size structure of the planktonic community in microcosms with different levels of turbulence. Scientia Marina 69(2), 187–197.

Cury, P., Pauly, D., 2000. Patterns and propensities in reproduction and growth of marine fishes. Ecological Research 15 (1), 101–106.

Cushing, D., 1990. Plankton production and year-class strength in fish populations: an update of the match/mismatch hypothesis. Advances in Marine Biology 26, 249–293.

Cushing, D. H., 1969. The regularity of the spawning season of some fishes. ICES Journal of Marine Science 33 (1), 81.

Cushing, D. H., 1975. Marine ecology and fisheries. Cambridge University Press, Cambridge.

Cushing, D. H., Horwood, J. W., 1994. The growth and death of fish larvae. Journal of Plankton Research 16(3), 291–300.

Damuth, J., 1981. Population density and body size in mammals. Nature 290 (5808), 699–700.

Datta, S., Delius, G. W., Law, R., 2010a. A jump-growth model for predator-prey dynamics: derivation and application to marine ecosystems. Bulletin of Mathematical Biology 72 (6), 1361–1382. Corrected version at http://arxiv.org/abs/0812.4968.

Datta, S., Delius, G. W., Law, R., Plank, M. J., 2010b. A stability analysis of the power-law steady state of marine size spectra. Journal of Mathematical Biology, doi: 10.1007/s00285–010–0387–z.

De Roos, A., 1988. Numerical methods for structured population models: the escalator boxcar train. Numerical Methods for partial differential equations 4 (3), 173–195.

De Roos, A., Mccauley, E., Wilson, W., 1991. Mobility versus density-limited predator–prey dynamics on different spatial scales. Proceedings: Biological Sciences, 117–122.

De Roos, A., Persson, L., 2001. Physiologically structured models: from versatile technique to ecological theory. Oikos 94 (1), 51–71.

De Roos, A., Persson, L., 2002. Size-dependent life-history traits promote catastrophic collapses of top predators. Proceedings of the National Academy of Sciences of the United States of America 99 (20), 12907.

Delgado, M., López-Gómez, J., Suárez, A., 2000. On the symbiotic Lotka-Volterra model with diffusion and transport effects. Journal of Differential Equations 160 (1), 175–262.

Drake, J., 1991. Community-assembly mechanics and the structure of an experimental species ensemble. American Naturalist, 1–26.

Duarte, C., Alcaraz, M., 1989. To produce many small or few large eggs: a size-independent reproductive tactic of fish. Oecologia 80 (3), 401–404.

Dulvy, N., Sadovy, Y., Reynolds, J., 2003. Extinction vulnerability in marine populations. Fish and Fisheries 4 (1), 25–64.

Durant, J., Hjermann, D., Anker-Nilssen, T., Beaugrand, G., Mysterud, A., Pettorelli, N., Stenseth, N., 2005. Timing and abundance as key mechanisms affecting trophic interactions in variable environments. Ecology Letters 8 (9), 952–958.

Durant, J. M., Hjermann, D. O., Ottersen, G., Stenseth, N. C., 2007. Climate and the match or mismatch between predator requirements and resource availability. Climate Research 33, 271–283.

Echevarria, F., Rodriguez, J., 1994. The size structure of plankton during a deep bloom in a stratified reservoir. Hydrobiologia 284 (2), 113–124.

Edwards, A., Brindley, J., 1996. Oscillatory behaviour in a three-component plankton population model. Dynamics and Stability of Systems 11 (4), 347–370.

Emmerson, M., Raffaelli, D., 2004. Predator–prey body size, interaction strength and the stability of a real food web. Journal of Animal Ecology 73 (3), 399–409.

Enquist, B. J., Economo, E. P., Huxman, T. E., Allen, A. P., Ignace, D. D., Gillooly, J. F., 2003. Scaling metabolism from organisms to ecosystems. Letters to Nature 423, 639–642.

FAO, 2008. The state of world fisheries and aquaculture. United Nations Food and Agriculture Program.

FAO, 2010. The state of world fisheries and aquaculture. United Nations Food and Agriculture Program.

Feller, W., 1941. On the integral equation of renewal theory. The Annals of Mathematical Statistics 12 (3), 243–267.

Findlay, H. S., Yool, A., Nodale, M., Pitchford, J. W., 2006. Modelling of autumn plankton bloom dynamics. Journal of Plankton Research 28(2), 209–220.

Finkelshtein, D., Kondratiev, Y., Kutoviy, O., 2009. Individual based model with competition in spatial ecology. SIAM Journal on Mathematical Analysis 41 (1), 297–317. URL http://arxiv.org/abs/0803.3565

Fishbase, 2011. Weight-at-age data of Atlantic cod (*Gadus morhua*) and sole (*Solea vulgaris*).
URL http://www.fishbase.org

Frank, K., Petrie, B., Choi, J., Leggett, W., 2005. Trophic cascades in a formerly cod-dominated ecosystem. Science 308 (5728), 1621.

Frost, B., 1991. The role of grazing in nutrient-rich areas of the open sea. Limnology and Oceanography 36 (8), 1616–1630.

Fry, B., 1988. Food web structure on Georges Bank from stable C, N, and S isotopic compositions. Limnology and Oceanography 33 (5), 1182–1190.

Fuchs, H., Franks, P., 2010. Plankton community properties determined by nutrients and size-selective feeding. Marine Ecology Progress Series 413, 1–15.

Gasol, J. M., Guerrero, R., Pedrós-Alió, C., 1992. Seasonal variations in size structure and procaryotic dominance in sulfurous Lake Cisó. Limnology and Oceanography 36(5), 860–872.

Gaston, K., Blackburn, T., 2000. Pattern and process in macroecology. Wiley Online Library.

Genner, M., Halliday, N., Simpson, S., Southward, A., Hawkins, S., Sims, D., 2010. Temperature-driven phenological changes within a marine larval fish assemblage. Journal of Plankton Research 32 (5), 699.

Gill, A., Hart, P., 1994. Feeding behaviour and prey choice of the threespine stickleback: the interacting effects of prey size, fish size and stomach fullness. Animal Behaviour 47 (4), 921–932.

Gillespie, D. T., 1976. A general method for numerically simulating the stochastic time evolution of coupled chemical reactions. Journal of Computational Physics 22, 403–434.

Gillespie, D. T., 2000. The chemical Langevin equation. Journal of Chemical Physics 113, 297–306.

Gillooly, J., Brown, J., West, G., Savage, V., Charnov, E., 2001. Effects of size and temperature on metabolic rate. Science 293 (5538), 2248.

Gillooly, J. F., Brown, J. H., West, G. B., Savage, V. M., Charnov, E. L., 2002. Effects of size and temperature on metabolic rate. Science 293, 2248–2251.

Gilpin, M., Ayala, F., 1973. Global models of growth and competition. Proceedings of the National Academy of Sciences 70 (12), 3590.

Goh, B., 1979. Stability in models of mutualism. The American Naturalist 113 (2), 261–275.

Gotceitas, V., Puvanendran, V., Leader, L., Brown, J., 1996. An experimental investigation of the 'match/mismatch' hypothesis using larval Atlantic cod. Marine ecology progress series. Oldendorf 130 (1), 29–37.

Grimm, V., 1999. Ten years of individual-based modelling in ecology: what have we learned and what could we learn in the future? Ecological modelling 115 (2), 129–148.

Grimm, V., Wyszomirski, T., Aikman, D., Uchmanski, J., 1999. Individual-based modelling and ecological theory: synthesis of a workshop. Ecological Modelling 115 (2-3), 275–282.

Gurney, W., Nisbet, R., Lawton, J., 1983. The systematic formulation of tractable single-species population models incorporating age structure. The Journal of Animal Ecology, 479–495.

Gurney, W. S. C., Veitch, A. R., 2007. The dynamics of size-at-age variability. Bulletin of Mathematical Biology 69, 861–885.

Haeckel, E., 1866. Generelle morphologie der organismen: allgemeine grundzüge der organischen formen-wissenschaft, mechanisch begründet durch die von Charles Darwin reformirte descendenz-theorie. G. Reimer.

Hall, S., Raffaelli, D., 1991. Food-web patterns: lessons from a species-rich web. Journal of Animal Ecology 60 (3), 823–841.

Hartvig, M., Andersen, K. H., Beyer, J. E., 2011. Food web framework for size-structured populations. Bulletin of Mathematical Biology 272, 113–122.

Hastings, A., 1978. Global stability in Lotka-Volterra systems with diffusion. Journal of Mathematical Biology 6 (2), 163–168.

Hastings, A., 1990. Spatial heterogeneity and ecological models. Ecology 71 (2), 426–428.

Heath, M. R., 1995. Size spectrum dynamics and the planktonic ecosystem of Loch Linnhe. ICES Journal of Marine Science 52, 627–642.

Hermann, A., Hinckley, S., Megrey, B., Napp, J., 2001. Applied and theoretical considerations for constructing spatially explicit individual-based models of marine larval fish that include multiple trophic levels. ICES Journal of Marine Science 58 (5), 1030.

Herring, P., 2002. The biology of the deep ocean. Oxford University Press, USA.

Hilton-Taylor, C., 2000. IUCN red list of threatened species. IUCN, Gland, Switzerland and Cambridge, UK 61.

Hinckley, S., Hermann, A., Megrey, B., 1996. Development of a spatially explicit, individual-based model of marine fish early life history. MEPS 139, 47–68.

Hirst, A., Bunker, A., 2003. Growth of marine planktonic copepods: global rates and patterns in relation to chlorophyll *a*, temperature, and body weight. Limnology and Oceanography 48 (5), 1988–2010.

Hjort, J., 1914. Fluctuations in the great fisheries of Northern Europe. Rapports et Procs-Verbaux Des Runions, Conseil International Pour l'Exploration de la Mer 20, 1–13.

Holling, C., 1959. The components of predation as revealed by a study of small mammal predation of the European Pine sawfly. The Canadian Entomologist 91, 293–332.

Holling, C., 1965. The functional response of predators to prey density and its role in mimicry and population regulation. Memoirs of the Entomological Society of Canada 45, 5–60.

Holling, C., 1973. Resilience and stability of ecological systems. Annual Review of Ecology and Systematics 4, 1–23.

Hollowed, A., Bax, N., Beamish, R., Collie, J., Fogarty, M., Livingston, P., Pope, J., Rice, J., 2000. Are multispecies models an improvement on single-species models for measuring fishing impacts on marine ecosystems? ICES Journal of Marine Science 57 (3), 707.

Horwood, J., Cushing, D., Wyatt, T., 2000. Planktonic determination of variability and sustainability of fisheries. Journal of Plankton Research 22 (7), 1419.

Horwood, J., Shepherd, J., 1981. The sensitivity of age-structured populations to environmental variability. Mathematical Biosciences 57 (1-2), 59–82.

Houde, E., 1989. Comparative growth, mortality, and energetics of marine fish larvae: temperature and implied latitudinal effects. Fishery Bulletin 87 (3), 471–495.

Hsieh, C., Reiss, C. S., Hunter, J. R., Beddington, J. R., May, R. M., Sugihara, G., 2006. Fishing elevates variability in the abundance of exploited species. Nature 443, 859–862.

Huete-Ortega, M., Marañón, E., Varela, M., Bode, A., 2010. General patterns in the size scaling of phytoplankton abundance in coastal waters during a 10-year time series. Journal of Plankton Research 32(1), 1–14.

Hunter, E., Metcalfe, J., Reynolds, J., 2003. Migration route and spawning area fidelity by North Sea plaice. Proceedings of the Royal Society of London. Series B: Biological Sciences 270 (1529), 2097.

Hutchings, J., Myers, R., 1994. Timing of cod reproduction: interannual variability and the influence of temperature. Marine Ecology Progress Series 108 (1), 21–32.

Hutchings, J., Rangeley, R., 2011. Correlates of recovery for Canadian Atlantic cod. Can. J. Zool 89, 386–400.

Irigoien, X., Flynn, K. J., Harris, R. P., 2005. Phytoplankton blooms: a loophole in microzooplankton grazing impact? Journal of Plankton Research 27 (4), 313–321.

Irigoien, X., Harris, R., Head, R., Harbour, D., 2000. North Atlantic Oscillation and spring bloom phytoplankton composition in the English Channel. Journal of Plankton Research 22 (12), 2367.

Irwin, A., Finkel, Z., Schofield, O., Falkowski, P., 2006. Scaling-up from nutrient physiology to the size-structure of phytoplankton communities. Journal of Plankton Research 28 (5), 459.

Jackson, G., 1995. Comparing observed changes in particle size spectra with those predicted using coagulation theory. Deep Sea Research Part II: Topical Studies in Oceanography 42 (1), 159–184.

James, A., Pitchford, J., Brindley, J., 2003. The relationship between plankton blooms, the hatching of fish larvae, and recruitment. Ecological modelling 160, 77–90.

Jennings, S., de Oliveira, J., Warr, K. J., 2007. Measurement of body size and abundance in tests of macroecological and food web theory. Journal of Animal Ecology 76 (1), 72–82.

Jennings, S., Greenstreet, S., Hill, L., Piet, G., Pinnegar, J., Warr, K., 2002a. Long-term trends in the trophic structure of the North Sea fish community: evidence from stable-isotope analysis, size-spectra and community metrics. Marine Biology 141 (6), 1085–1097.

Jennings, S., Greenstreet, S., et al., 1999. Structural change in an exploited fish community: a consequence of differential fishing effects on species with contrasting life histories. Journal of Animal Ecology 68 (3), 617–627.

Jennings, S., Mackinson, S., 2003. Abundance-body mass relationships in size-structured food webs. Ecology Letters 6, 971–974.

Jennings, S., Pinnegar, J., Polunin, N., Boon, T., 2001. Weak cross-species relationships between body size and trophic level belie powerful size-based trophic structuring in fish communities. Journal of Animal Ecology 70 (6), 934–944.

Jennings, S., Reynolds, J., Mills, S., 1998. Life history correlates of responses to fisheries exploitation. Proceedings of the Royal Society of London. Series B: Biological Sciences 265 (1393), 333.

Jennings, S., Warr, K., 2003. Smaller predator-prey body size ratios in longer food chains. Proceedings of the Royal Society of London. Series B: Biological Sciences 270 (1522), 1413.

Jennings, S., Warr, K., Mackinson, S., 2002b. Use of size-based production and stable isotope analyses to predict trophic transfer efficiencies and predator-prey body mass ratios in food webs. Marine Ecology Progress Series 240, 11–20.

Johnson, D. L., 2000. Preliminary examination of the match-mismatch hypothesis and recruitment variability of yellowtail flounder, *Limanda ferruginea*. Fisheries Bulletin 98(4), 854–863.

Jonsson, T., Cohen, J., Carpenter, S., 2005. Food webs, body size, and species abundance in ecological community description. Advances in Ecological Research 36, 1–84.

Judson, O., 1994. The rise of the individual-based model in ecology. Trends in Ecology & Evolution 9 (1), 9–14.

Kaiser, M. J., Attrill, M. J., Jennings, S., Thomas, D. N., Barnes, D. K. A., Brierley, A. S., Polunin, N. V. C., Raffaelli, D. G., le B Williams, P. J., 2005. Marine ecology: processes, systems and impacts. Oxford University Press, New York.

Kamenir, Y., Dubinsky, Z., Zohary, T., 2004. Phytoplankton size structure stability in a meso-eutrophic subtropical lake. Hydrobiologia 520 (1), 89–104.

Kerr, S. R., Dickie, L. M., 2001. The biomass spectrum: a predator-prey theory of aquatic production. Columbia University Press, New York.

Kingsland, S., 1995. Modeling nature: episodes in the history of population ecology. University of Chicago Press.

Kirchgraber, U., Palmer, K. J., 1990. Geometry in the neighborhood of invariant manifolds of maps and flows and linearization. Longman Scientific & Technical, Harlow, Essex, England.

Knijn, R. J., Boon, T. W., Heessen, H. J. L., Hislop, J. R. G., 1993. Atlas of North Sea Fishes: ICES Cooperative Research Report No. 194. ICES, Copenhagen, Denmark.

Koeller, P., Fuentes-Yaco, C., Platt, T., Sathyendranath, S., Richards, A., Ouellet, P., Orr, D., Skúladóttir, U., Wieland, K., Savard, L., et al., 2009. Basin-scale coherence in phenology of shrimps and phytoplankton in the North Atlantic Ocean. Science 324 (5928), 791.

Kooijman, S. A. L. M., 1986. Energy budgets can explain body size relations. Journal of Theoretical Biology 121, 269–282.

Kooijman, S. A. L. M., 2009. Dynamic energy budget theory, 3rd Edition. Cambridge University Press, Cambridge.

Kot, M., 2001. Elements of mathematical ecology. Cambridge Univ Press.

Krabs, W., Pickl, S., 2010. Dynamical Systems: Stability, Controllability and Chaotic Behavior. Springer Verlag.

Lambert, Y., 2008. Why should we closely monitor fecundity in marine fish populations? Journal of Northwest Atlantic Fisheries Science 41, 93–106.

Law, R., 1983. A model for the dynamics of a plant population containing individuals classified by age and size. Ecology 64 (2), 224–230.

Law, R., Morton, R., 1996. Permanence and the assembly of ecological communities. Ecology 77 (3), 762–775.

Law, R., Plank, M. J., James, A., Blanchard, J. L., 2009. Size-spectra dynamics from stochastic predation and growth of individuals. Ecology 90 (3), 802–811.

Leggett, W., Deblois, E., 1994. Recruitment in marine fishes: is it regulated by starvation and predation in the egg and larval stages? Netherlands Journal of Sea Research 32 (2), 119–134.

Leslie, P., 1945. On the use of matrices in certain population mathematics. Biometrika 33 (3), 183–212.

Levin, S., Paine, R., 1974. Disturbance, patch formation, and community structure. Proceedings of the National Academy of Sciences of the United States of America 71 (7), 2744.

Li, W. K. W., 2002. Macroecological patterns of phytoplankton in the northwestern North Atlantic Ocean. Nature 419, 154–157.

Li, X., Logan, B., 1995. Size distributions and fractal properties of particles during a simulated phytoplankton bloom in a mesocosm. Deep Sea Research Part II: Topical Studies in Oceanography 42 (1), 125–138.

Lomnicki, A., 1978. Individual differences between animals and the natural regulation of their numbers. Journal of Animal Ecology 47, 461–475.

Lomnicki, A., 1999. Individual-based models and the individual-based approach to population ecology. Ecological Modelling 115 (2-3), 191–198.

Longhurst, A., 1998. Cod: perhaps if we all stood back a bit? Fisheries Research 38 (2), 101–108.

Lotka, A., 1925. Elements of physical biology. Williams & Wilkins.

Lotka, A., 1939. On an integral equation in population analysis. The Annals of Mathematical Statistics 10 (2), 144–161.

MacArthur, R., 1955. Fluctuations of animal populations and a measure of community stability. Ecology 36 (3), 533–536.

Mari, X., Burd, A., 1998. Seasonal size spectra of transparent exoploymeric particles (tep) in a coastal sea and comparison eith those predicted using coagulation theory. Marine Ecology Progress Series 163, 63–76.

Marquet, P. A., Quiñones, R. A., Abades, S., Labra, F., Tognelli, M., Arim, M., Rivadeneira, M., 2005. Scaling and power-laws in ecological systems. Journal of Experimental Biology 208, 1749–1769.

Maury, O., Faugeras, B., Shin, Y.-J., Poggiale, C., Ari, T. B., Marsac, F., 2007a. Modelling environmental effects on the size-structured energy flow through marine ecosystems. Part 1: the model. Progress in Oceanography 74, 479–499.

Maury, O., Shin, Y., Faugeras, B., Ben Ari, T., Marsac, F., 2007b. Modeling environmental effects on the size-structured energy flow through marine ecosystems. Part 2: simulations. Progress in Oceanography 74 (4), 500–514.

May, R., 1972. Will a large complex system be stable? Nature 238, 413–414.

McCauley, E., Wilson, W., de Roos, A., 1993. Dynamics of age-structured and spatially structured predator-prey interactions: individual-based models and population-level formulations. American Naturalist, 412–442.

McKane, A. J., Newman, T. J., 2005. Predator-prey cycles from resonant amplification of demographic stochasticity. Phys. Rev. Lett. 94, 218102.

McKendrick, A. G., 1926. Applications of mathematics to medical problems. Proceedings of the Edinburgh Mathematical Society 40, 98–130.

Meekan, M., Carleton, J., McKinnon, A., Flynn, K., Furnas, M., 2003. What determines the growth of tropical reef fish larvae in the plankton: food or temperature? Marine Ecology Progress Series 256, 193–204.

Meekan, M., Fortier, L., 1996. Selection for fast growth during the larval life of Atlantic cod *Gadus morhua* on the Scotian Shelf. Marine Ecology Progress Series 137 (1), 25–37.

Menzel, D. W., Ryther, J. H., 1960. The annual cycle of primary production in the Sargasso Sea off Bermuda. Deep Sea Research 6, 351–367.

Mertz, G., Myers, R. A., 1994. Match/mismatch predictions of spawning duration versus recruitment variability. Fisheries Oceanography 3 (4), 236–245.

Moloney, C. L., Field, J. G., 1991. The size-based dynamics of plankton food webs. I. A simulation model of carbon and nitrogen flows. Journal of Plankton Research 13(5), 1003–1038.

Montoya, J., Pimm, S., Solé, R., 2006. Ecological networks and their fragility. Nature 442 (7100), 259–264.

Mullon, C., Fréon, P., Cury, P., 2005. The dynamics of collapse in world fisheries. Fish and Fisheries 6 (2), 111–120.

Murray, J. D., 2002. Mathematical biology, I: An introduction, 3rd Edition. Springer-Verlag, Berlin.

Myers, R., Hutchings, J., Barrowman, N., 1997. Why do fish stocks collapse? the example of cod in Atlantic Canada. Ecological Applications 7 (1), 91–106.

Navarro, J. M., Thompson, R. J., 1995. Seasonal fluctuations in the size spectra, biochemical composition and nutritive value of the seston available to a suspension-feeding bivalve in a subarctic environment. Marine Ecology Progress Series 125, 95–106.

Nee, S., Read, A., Greenwood, J., Harvey, P., 1991. The relationship between abundance and body size in british birds. Nature 351 (6324), 312–313.

Nisbet, R., Gurney, W., 1983. The systematic formulation of population models for insects with dynamically varying instar duration. Theoretical Population Biology 23, 114–135.

Nisbet, R., Gurney, W., Murdoch, W., McCauley, E., 1989. Structured population models: a tool for linking effects at individual and population level. Biological Journal of the Linnean Society 37 (1-2), 79–99.

Okubo, A., 1980. Diffusion and ecological problems: Mathematical models. Biomathematics, vol. 10. Springer, Berlin.

Okubo, A., Levin, S. A., 2001. Diffusion and ecological problems, 2nd Edition. Springer, New York.

Paine, R., 1966. Food web complexity and species diversity. The American Naturalist 100 (910), 65–75.

Paloheimo, J. E., Dickie, L. M., 1966. Food and growth of fishes. III. Relations among food, body size, and growth efficiency. Journal of the Fisheries Research Board of Canada 23, 1209–1248.

Pannella, G., 1971. Fish otoliths: daily growth layers and periodical patterns. Science 173 (4002), 1124.

Pauly, D., Christensen, V., Guénette, S., Pitcher, T., Sumaila, U., Walters, C., Watson, R., Zeller, D., 2002. Towards sustainability in world fisheries. Nature 418 (6898), 689–695.

Persson, L., Leonardsson, K., de Roos, A., Gyllenberg, M., Christensen, B., 1998. Ontogenetic scaling of foraging rates and the dynamics of a size-structured consumer-resource model. Theoretical Population Biology 54 (3), 270–293.

Petchey, O., Beckerman, A., Riede, J., Warren, P., 2008. Size, foraging, and food web structure. Proceedings of the National Academy of Sciences 105 (11), 4191.

Petchey, O., Downing, A., Mittelbach, G., Persson, L., Steiner, C., Warren, P., Woodward, G., 2004. Species loss and the structure and functioning of multitrophic aquatic systems. Oikos 104 (3), 467–478.

Peters, R., 1986. The ecological implications of body size. Cambridge Univ Press.

Peters, R., Wassenberg, K., 1983. The effect of body size on animal abundance. Oecologia 60 (1), 89–96.

Pfister, C. A., Stevens, F. R., 2002. The genesis of size variability in plants and animals. Ecology 83, 59–72.

Pimm, S., 1977. Number of trophic levels in ecological communities. Nature 268, 329–331.

Pimm, S., 1979. Complexity and stability: another look at MacArthur's original hypothesis. Oikos 33 (3), 351–357.

Pimm, S., 1984. The complexity and stability of ecosystems. Nature 307 (5949), 321–326.

Pimm, S., Lawton, J., Cohen, J., 1991. Food web patterns and their consequences. Nature 350 (6320), 669–674.

Pitchford, J., James, A., Brindley, J., 2005. Quantifying the effects of individual and environmental variability in fish recruitment. Fisheries Oceanography 14 (2), 156–160.

Plank, M., Law, R., 2011. On balanced exploitation of marine ecosystems: results from dynamic size spectra. (submitted).

Platt, T., Denman, K., 1977. Organisation in the pelagic ecosystem. Helgoland Marine Research 30 (1), 575–581.

Platt, T., Denman, K., 1978. The structure of pelagic marine ecosystems. Rapports et Procs-Verbaux Des Runions, Conseil International Pour l'Exploration de la Mer 173, 60–65.

Platt, T., Fuentes-Yaco, C., Frank, K., 2003. Marine ecology: Spring algal bloom and larval fish survival. Nature 423 (6938), 398–399.

Pope, J., Rice, J., Daan, N., Jennings, S., Gislason, H., 2006. Modelling an exploited marine fish community with 15 parameters - results from a simple size-based model. ICES Journal of Marine Science 63 (6), 1029.

Pope, J. G., Shepherd, J. G., Webb, J., Stebbing, A. R. D., Mangel, M., 1994. Successful surf-riding on size spectra: The secret of survival in the sea [and discussion]. Philosophical Transactions: Biological Sciences 343(1403), 41–49.

Post, W., Pimm, S., 1983. Community assembly and food web stability. Mathematical Biosciences 64 (2), 169–192.

Press, W. H., Teukolsky, S. A., Vetterling, W. T., Flannery, B. P., 1992. Numerical Recipes in C, 2nd Edition. Cambridge University Press, Cambridge.

Puvanendran, V., Brown, J., 1999. Foraging, growth and survival of Atlantic cod larvae reared in different prey concentrations. Aquaculture 175 (1-2), 77–92.

Quéro, J., 1984. Les poissons de mer des pêches françaises. J. Grancher.
URL http://books.google.co.uk/books?id=448WAQAAIAAJ

Reul, A., Rodríguez, V., Jiménez-Gómez, F., Blanco, J., Bautista, B., Sarhan, T., Guerrero, F., Ruiz, J., Garcia-Lafuente, J., 2005. Variability in the spatio-temporal distribution and size-structure of phytoplankton across an upwelling area in the NW-Alboran Sea, (W-Mediterranean). Continental Shelf Research 25 (5-6), 589–608.

Reuman, D., Cohen, J., 2004. Trophic links length and slope in the Tuesday Lake food web with species body mass and numerical abundance. Journal of Animal Ecology 73 (5), 852–866.

Rice, J., Miller, T., Rose, K., Crowder, L., Marschall, E., Trebitz, A., DeAngelis, D., 1993. Growth rate variation and larval survival: inferences from an individual-based size-dependent predation model. Canadian Journal of Fisheries and Aquatic Sciences 50 (1), 133–142.

Rochet, M., Benoît, E., 2011. Fishing destabilizes the biomass flow in the marine size spectrum. Proceedings of the Royal Society B: Biological Sciences.

Rooney, N., McCann, K., Gellner, G., Moore, J. C., 2006. Structural asymmetry and the stability of diverse food webs. Nature 442, 265–269.

Rosenberg, A., Haugen, A., 1982. Individual growth and size-selective mortality of larval turbot (*Scophthalmus maximus*) reared in enclosures. Marine Biology 72 (1), 73–77.

Rossberg, A., 2011. A complete analytic theory for structure and dynamics of populations and communities spanning wide ranges in size. Advances in Ecological Research.

Roy, S., Platt, T., Sathyendranath, S., 2011. Modelling the time-evolution of phytoplankton size spectra from satellite remote sensing. ICES Journal of Marine Science 68 (4), 719.

Salomon, A., Shears, N., Langlois, T., Babcock, R., 2008. Cascading effects of fishing can alter carbon flow through a temperate coastal ecosystem. Ecological Applications 18 (8), 1874–1887.

San Martin, E., Irigoien, X., Harris, R. P., López-Arrutia, A., Zubkov, M. V., Heywood, J. L., 2006. Variation in the transfer of energy in marine plankton along a productivity gradient in the Atlantic Ocean. Limnology and Oceanography 51(5), 2084–2091.

Sarukhan, J., Gadgil, M., 1974. Studies on plant demography: *Ranunculus repens* L., *R. bulbosus* L. and *R. acris* L.: III. A mathematical model incorporating multiple modes of reproduction. Journal of Ecology 62 (3), 921–936.

Schartau, M., Landry, M., Armstrong, R., 2010. Density estimation of plankton size spectra: a reanalysis of IronEx II data. Journal of Plankton Research 32 (8), 1167.

Schnakenberg, J., 1976. Network theory of microscopic and macroscopic behavior of master equation systems. Reviews of Modern Physics 48 (4), 571.

Searcy, S., Sponaugle, S., 2000. Variable larval growth in a coral reef fish. Marine Ecology Progress Series 206, 213–226.

Sheldon, R., Parsons, T., 1967. A continuous size spectrum for particulate matter in the sea. Journal of the Fisheries Research Board of Canada 24(5), 909–915.

Sheldon, R. W., Prakash, A., Sutcliffe Jr., W. H., 1972. The size distribution of particles in the ocean. Limnology and Oceanography 17(3), 327–340.

Sheldon, R. W., Sutcliffe, W. H., Paranjape, M. A., 1977. Structure of pelagic food chain and relationship between plankton and fish production. Journal of the Fisheries Research Board Canada 34, 2344–2353.

Shin, Y., Cury, P., 2004. Using an individual-based model of fish assemblages to study the response of size spectra to changes in fishing. Canadian Journal of Fisheries and Aquatic Sciences 61 (3), 414–431.

Shin, Y., Rochet, M., Jennings, S., Field, J., Gislason, H., 2005. Using size-based indicators to evaluate the ecosystem effects of fishing. ICES Journal of Marine Science 62 (3), 384.

Silva, J., Hallam, T., 1993. Effects of delay, truncations and density dependence in reproduction schedules on stability of nonlinear Leslie matrix models. Journal of Mathematical Biology 31 (4), 367–395.

Silvert, W., 1980. Dynamic energy-flow model of the particle size distribution in pelagic ecosystems. In: Kerfoot, W. (Ed.), Evolution and ecology of zooplankton communities. University Press of New England, Hanover, New Hampshire and London, England, pp. 754–763.

Silvert, W., Platt, T., 1978. Energy flux in the pelagic ecosystem: a time-dependent equation. Limnology and Oceanography 23(4), 813–816.

Sinclair, M., 1988. Marine populations: an essay on population regulation and speciation. Books in Recruitment Fishery Oceanography.

Smoluchowski, M., 1916. Drei Vorträge über Diffusion, Brownsche Bewegung und Koagulation von Kolloidteilchen. Phys Z. 17, 557–585.

Stock, C., Powell, T., Levin, S., 2008. Bottom-up and top-down forcing in a simple size-structured plankton dynamics model. Journal of Marine Systems 74 (1-2), 134–152.

Strickland, J., 1968. A comparison of profiles of nutrient and chlorophyll concentrations taken from discrete depths and by continuous recording. Limnology and Oceanography 13 (2), 388–391.

Truscott, J., Brindley, J., 1994. Ocean plankton populations as excitable media. Bulletin of Mathematical Biology 56 (5), 981–998.

Truscott, J. E., 1995. Environmental forcing of simple plankton models. Journal of Plankton Research 17(12), 2207–2232.

Uchida, S., Drossel, B., Brose, U., 2007. The structure of food webs with adaptive behaviour. Ecological Modelling 206 (3-4), 263–276.

Uchmaski, J., Grimm, V., 1996. Individual-based modelling in ecology: what makes the difference? Trends in Ecology & Evolution 11 (10), 437–441.

Ursin, E., 1973. On the prey sizes of cod and dab. Meddr Danm. Fisk.- og Havunders 7, 85–98.

van der Veer, H., Kooijman, S., van der Meer, J., 2001. Intra-and interspecies comparison of energy flow in North Atlantic flatfish species by means of dynamic energy budgets. Journal of Sea Research 45 (3-4), 303–320.

van Kampen, N. G., 1992. Stochastic processes in physics and chemistry. Elsevier, Amsterdam.

Vlado, 2011. Image of grass carp. FreeDigitalPhotos.net.

Volterra, V., 1926. Fluctuations in the abundance of a species considered mathematically. Nature 118 (2972), 558–560.

von Bertalanffy, L., 1957. Quantitative laws in metabolism and growth. The Quarterly Review of Biology 32 (3), 217–231.
URL http://www.jstor.org/stable/2815257

von Foerster, H., 1959. Some remarks on changing populations. In: Stohlman, J. F. (Ed.), The Kinetics of Cellular Proliferation. Grune and Stratton, New York, pp. 382–407.

Wang, Z., Qi, Y., Chen, J., Xu, N., Yang, Y., 2006. Phytoplankton abundance, community structure and nutrients in cultural areas of Daya Bay, South China Sea. Journal of Marine Systems 62 (1-2), 85–94.

Ware, D. M., 1975. Relation between egg size, growth, and natural mortality of larval fish. Journal of the Fisheries Research Board of Canada 32, 2503–2512.

Ware, D. M., 1978. Bioenergetics of pelagic fish: theoretical change in swimming speed and ration with body size. Journal of the Fisheries Research Board of Canada 35, 220–228.

Warren, P., Lawton, J., 1987. Invertebrate predator-prey body size relationships: an explanation for upper triangular food webs and patterns in food web structure? Oecologia 74 (2), 231–235.

Werner, E., Gilliam, J., 1984. The ontogenetic niche and species interactions in size-structured populations. Annual Review of Ecology and Systematics, 393–425.

Werner, F., Quinlan, J., Lough, R., Lynch, D., 2001. Spatially-explicit individual based modeling of marine populations: a review of the advances in the 1990s. SARSIA-BERGEN 86 (6), 411–422.

White, E., Ernest, S., Kerkhoff, A., Enquist, B., 2007. Relationships between body size and abundance in ecology. Trends in Ecology & Evolution 22 (6), 323–330.

Williams, R., Berlow, E., Dunne, J., Barabási, A., Martinez, N., 2002. Two degrees of separation in complex food webs. Proceedings of the National Academy of Sciences 99 (20), 12913.

Woodward, G., Blanchard, J., Lauridsen, R., Edwards, F., Jones, J., Figueroa, D., Warren, P., Petchey, O., 2010. Individual-based food webs: Species identity, body size and sampling effects. In: Woodward, G. (Ed.), Advances in Ecological Research: Integrative Ecology. Academic Press, U.K., pp. 211–260.

Woodward, G., Ebenman, B., Emmerson, M., Montoya, J., Olesen, J., Valido, A., Warren, P., 2005a. Body size in ecological networks. Trends in Ecology & Evolution 20 (7), 402–409.

Woodward, G., Jones, J., Hildrew, A., 2002. Community persistence in Broadstone Stream (U.K.) over three decades. Freshwater Biology 47 (8), 1419–1435.

Woodward, G., Speirs, D., Hildrew, A., 2005b. Quantification and resolution of a complex, size-structured food web. Advances in Ecological Research 36, 85–135.

Wootton, R., 1977. Effect of food limitation during the breeding season on the size, body components and egg production of female sticklebacks (*Gasterosteus aculeatus*). Journal of Animal Ecology 46 (3), 823–834.

Wright, P., Bailey, M., 1996. Timing of hatching in *Ammodytes marinus* from shetland waters and its significance to early growth and survivorship. Marine Biology 126 (1), 143–152.

Yodzis, P., Innes, S., 1992. Body size and consumer-resource dynamics. The American Naturalist 139 (6), 1151–1175.

Zarauz, L., Irigoien, X., Fernandes, J. A., 2009. Changes in plankton size structure and composition, during the generation of a phytoplankton bloom, in the central Cantabrian sea. Journal of Plankton Research 31(2), 193–207.

Zhou, M., 2006. What determines the slope of a plankton biomass spectrum? Journal of Plankton Research 28 (5), 437.

Zhou, M., Carlotti, F., Zhu, Y., 2010. A size-spectrum zooplankton closure model for ecosystem modelling. Journal of Plankton Research 32(8), 1147–1165.

Zhou, M., Tande, K. S., Zhu, Y., Suñnje Basedow, 2009. Productivity, trophic levels and size spectra of zooplankton in northern Norwegian shelf regions. Deep Sea Research II 56, 1934–1944.